Assessing Participants' Feedback to Dental Screenings and Hygiene Care Provided by City Tech's Dental Hygiene Students

Alona Abdullaieva, Wen Wen Dong, Yujing Mei and Professor Susan Davide RDH, MS, MSEd and Professor Audra Haynes RDH, MPH (Mentors)

Dental Hygiene Department

Purpose

This study is a continuum of the initial dental screenings provided at the CUNY Graduate Center's Wellness Fair in spring 2018. A new cohort of dental hygiene students provided this second annual dental screenings in April 2019. In addition to the dental screenings, each participant was asked questions related to their oral hygiene and dental hygiene students conducted an intra-oral inspection.

Following the dental screening those participants who made an appointment received complimentary care at NYCCT's Department of Dental Hygiene Clinic. This study will further continue to allow Dental Hygiene faculty and students to improve accessibility and strategies to increase public awareness of services, access to care and patient recruitment opportunities. CUNY Human Subject Research Exempt Status granted by the University Integrated Institutional Review Board (IRB); file #2018-1000.

Materials & Methods

Dental hygiene students and faculty performed in excess of 62 dental screenings. Participants filled out a consent form prior to being screened that included information such as name, date of birth, phone number, address, email address and some general questions pertaining to their most recent dental exam, their current oral home care and whether they have dental insurance. Following IRB approval, this data was analyzed to determine the participants' demographics, oral healthcare history and intra-oral inspection.

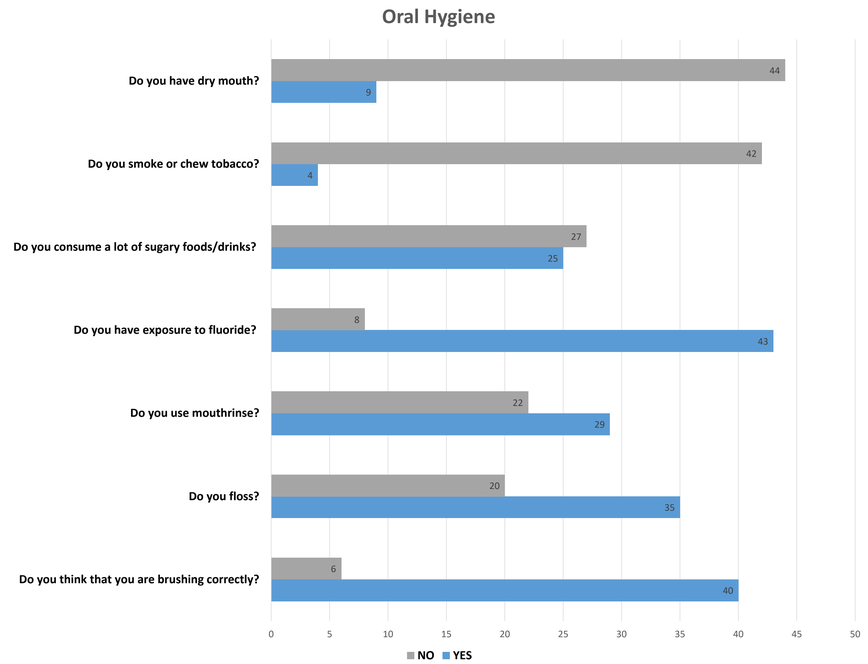

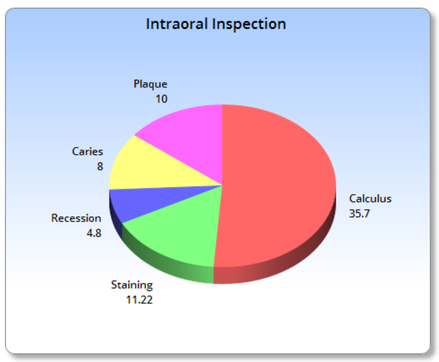

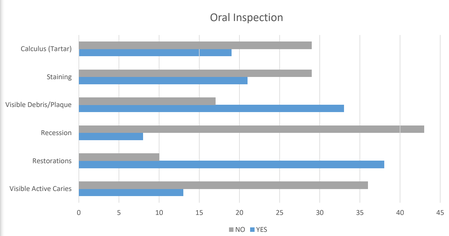

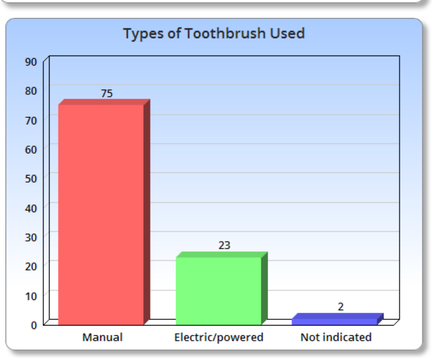

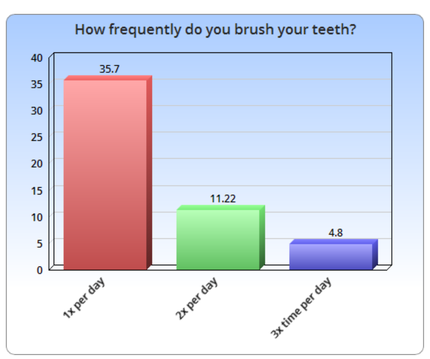

Fall 2019

Of the four participants surveyed who completed their dental treatment, 100% stated that they were satisfied with the services that they received, would return to the clinic in the future and would recommend NYCCT's Dental Hygiene program's clinic to their friends and family. All surveyed respondents stated that they made their dental hygiene appointment as a result of attending the free dental screening at the CUNY Wellness Festival.

According to the information collected at the Wellness Fair, most of the participants were between ages 30 and 39, which is 52% out of the total amount of participants. 34% were age 20 to 29, and 23% were age 40 to 49, the rest were 50+ years old.

78% of the participants are insured.

43% of participants had their most recent dental visit within the past year (2018), 25% this year and 24% prior to 2017.

According to the research most of the participants brush twice a day and believe that they brush correctly. However, during Phase II of the research, it was evident that all the 4 participants received an adult referral form for the treatment of more than 3 caries lesions. It made us come to the realization that patients' perception is not the same as the patients' reality. And we must devote more time to patients' education during dental hygiene visits.

Conclusions

The remaining participants from the CUNY Wellness Festival Dental Screening were contacted and offered complimentary dental hygiene services at NYCCT's dental hygiene clinic. Patients will be treated over the remainder of the Fall 2019 Semester and throughout the Spring 2020 semester. As part of our ongoing research, we have determined that many of the dental screening participants have dental insurance coverage. However, the greater part of the population does not practice routine dental prophylaxis which is recommended at 6 month intervals. Therefore we are considering to host a dental screening and a tooth brush sale at NYCCT in January/February of 2020. It is essential to increase awareness among NYCCT students, faculty and staff, to free dental hygiene care. As dental health professionals, we strive to improve patients' understanding of dental hygiene care importance. We believe that our research will contribute to patients' oral health education.

Acknowledgements:

Thanks to the senior dental hygiene students who attended and assisted at the Spring 2019 Wellness Festival:

Roseanna Torres, Student Research Assistant 2018-2019

Dirien Santos, Student Research Assistant 2018-2019

What are The Most Influencing Factors for The Crime Rates

Mentor: Professor Nan Li

Afsana Mimi, Dung Mai, Fabliha Afia, Shubha Shrestha

New York City College Of Technology

Abstract

This project is conducted to see the top factors that influence the Violence Per Population using *Communities and Crime Unnormalized Data Set* collected in 1995. The method we used is Lasso Regression. Linear regression is not used in this project since it is not able to select the variables and answer the proposed question . All the required calculations and graphical displays are performed using the R software for statistical computing.

Introduction

Lasso stands for Least Absolute Shrinkage and Selection Operators. It performs both variable selection and regularization to enhances the prediction accuracy and model interpretability. Variable selection is to select the most influential subset from the data model which these variable will give more accurate result for the calculation. The coefficients which tend to be zero are less significant therefore we will eliminate it. The coefficient of variables in lasso regression follows from the equation given below:

$$\hat{\beta}^{lasso} = \underset{\beta \epsilon \mathbb{R}^p}{argmin} \|y - X\beta\|_2^2 + \lambda \sum_{j=1}^{p} |\beta_j|$$

$$= \underset{\beta \epsilon \mathbb{R}^p}{argmin} \underbrace{\|y - X\beta\|_2^2}_{\text{Loss}} + \lambda \underbrace{\|\beta\|_1}_{\text{Penalty}}$$

In this equation, y is a response vector , and X represents the predictor variables. (lambda) is the tuning parameter that controls the strength of the penalty and is the coefficient of predictor variables.

Method

The first of step of this project was using excel to clean up the missing data. After the data was sorted, it was transferred in .csv(comma separated value) file. In Rmarkdown, data was imported, then we performed Lasso Regression to execute variable selection. We separated the dataset into training (used to adjust the parameters of the model) and testing data(used to provide an unbiased evaluation from the training model) to compare their errors with each other. After examining the Average Errors, we were able to select the best lambda that yielded the minimal error for the testing data set. For such a lambda, the variables with non-zero coefficients are supposed to be most influencing factors.

Result

The following graph exhibits the global image of the average testing and training errors obtained from lasso regression.

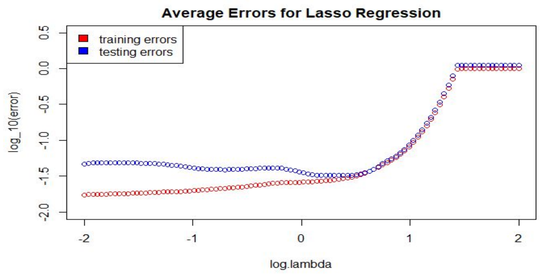

There is a overfitting whenever the testing errors is larger than the training errors, meaning that the classifier learn on the training set is too specific and cannot be used to accurately conclude anything about the testing data. When training and testing errors come close, the model is more reasonable. In particular, the model is optimally tuned when the testing errors come close to training errors and both approach zero.

The below graph is zoomed from the global image graph.

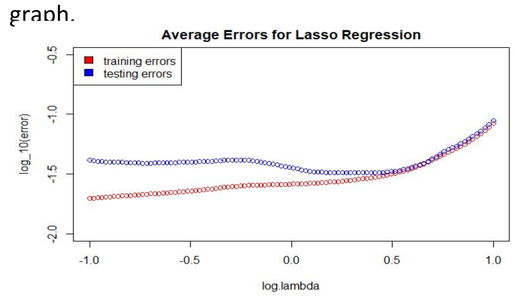

Based on the graph, the best lambda lies in the interval [0,0.5] when the testing error is at its minimal. By observing the plot above, we can see that lambda at the value 0.4 gives the smallest error. Thus we choose our optimal lambda to be 10^4 since we initially define log lambda of 0.4 to be 10^4.
We picked lambda = 0.4 as it already gives us 6 variables with non-zero coefficients. In future work, we will perform more precise analysis.

The table below demonstrates the variables that survive after performing Lasso Regression at Lambda equals to 10^0.4. The larger the coefficients, the more significant the variables take role in the model.

Variable Names	Coefficients
Percentage of kids born to never married	0.460599439
Percentage of males who are divorced	0.120516295
Race Black (percentage of population that is Black.	0.094210183
Percent of persons in dense housing (more than 1 person per room)	0.087571993
Number of vacant households	0.065006117
Percentage of households with public assistance income	0.064268353

Conclusion

· Lasso regression can set less influencing variables to zero as lambda approaches infinity, thus performing variable selection.

· Based on the result from Lasso Regression, the most important variable that gives the most effect in Violence per Population is the percentage of kids born to never married.

Future Study

In the future, we will try to use Lasso Regression to predict the influencing factors in broader fields such as:

- **Finance or economic related** (predict the variable has more contribution in the economy)
- **Education** (select the variable which causes student to drop the college)
- **Medical field** (predict the cause of some specific disease such as diabetes, or cardiovascular related to health problems)

We will also do more detailed analysis and compare the Lasso Regression with Ridge Regression, which functions similarly but has different tuning parameters.

Citation

1 UCI Machine Learning Repository, *Communities and Crime Unnormalize Data set,* 1995 FBI UCR https://archive.ics.uci.edu/ml/datasets/Communities+and+Crime+Unnormalized
2. Trevor Hastie, Robert Tibshirani, Martin Wainwright, Statistical Learning with Sparsity The Lasso and Generalizations https://web.stanford.edu/~hastie/StatLearnSparsity_files/SLS_corrected_1.4.16.pdf
3. Statistics Knowledge Portal, Statistical Discovery from SAS, What is Variable Selection.

Acknowledgement

We would like to thank Professor Nan Li for his valuable advices and teachings for this Lasso Regression project and his tremendous help in creating this presentation possible. We would also like to thank Undergraduate Research to publish our poster presentation.

High Performance Facade Metrics, Closed Cavity Systems and Incentives in Context of Net-Zero Building

High Performance Facade Systems

Laurin Moseley, Tasfia Amir, Rafia Amin, & Taylor Hernandez with Professor John Neary, AIA, LEED, AP

Special thanks to Professor Victoria Ereskina, Elliot Glassman & Davit Khomasuridze

ABSTRACT

Curtain Wall facades -- modular enclosures of aluminum framing and with vision glass and opaque spandrel infill -- have come under attack recently as inefficient in terms of insulating performance and as a principal contributor to the problem of greenhouse gas emissions related to buildings. But they are ubiquitous and the reasons for that are not changing overnight. We need to understand how the curtain wall performs and how it can improve to make buildings, especially tall urban buildings, more sustainable in the future. We investigated the strengths and weaknesses of the curtain wall, especially the recent emerging technology of Closed Cavity Facades with integral automated shades and photovoltaic screening. These technologies control heat gain (which is the principal environmental problem with the glass building) while reducing the need for artificial lighting, and generating electricity.

In our research, we compared the U values and Solar Heat Gain Coefficient of the conventional high-performance curtain wall enclosure with the Closed Cavity curtain wall. We have also documented code performance requirements for façade insulation and Solar Heat Gain, as well as targets set forth in incentive programs such as New York's Zone Green FAR Bonus program and the recently announced Climate Mobilization Act (Local Law 97). Next, we evaluated the impact of the façade, specifically the Closed Cavity Façade, on the metrics of the Net-Zero energy consumption commercial building. This puts the relative importance of the façade system performance in context for evaluating the life-cycle cost and benefit of the premium represented by the high-performance curtain wall.

The Closed Cavity Facade can result in a 15% energy savings in annual energy use compared to a conventional curtain wall. This significant energy reduction proves that improving facade performance contributes to lowering a building's carbon emission and helps to reach Net-Zero. Achieving Net-Zero should mean compliance with new energy laws of NYC, as well as creating more sustainable buildings beneficial for the world we live in.

New York City - South facing office room

				FAÇADE 1	FAÇADE 2	FAÇADE 3	FAÇADE 4	FAÇADE 5
INPUT	CAPSOL EXCELLENT (Indicative values For comparison only)			DGU	TGU	AW	IW	mFree-S
	GLAZING TYPE			VNE63	LowE + LowE	LowE	LowE	LowE
OUTPUT (glazing only) Steady state / WIS	NFRC Tin=0.04°F / Tin=68.8°F Ta=0	U [Btu/hr.ft²F]	no blinds	0.28	0.16	0.13	0.18	0.18
			blinds	0.22	0.14	0.11	0.15	0.15
	NFRC Tin=89.6°F / Tin=75.2°F Ia=248.2Btu/hr.ft²	SHGC [-]	no blinds	0.32	0.48	0.52	0.52	0.53
			blinds	0.22	0.38	0.29	0.12	0.13
		VT [-]	no blinds	0.63	0.69	0.70	0.70	0.70
			blinds	0.03	0.03	0.03	0.03	0.03

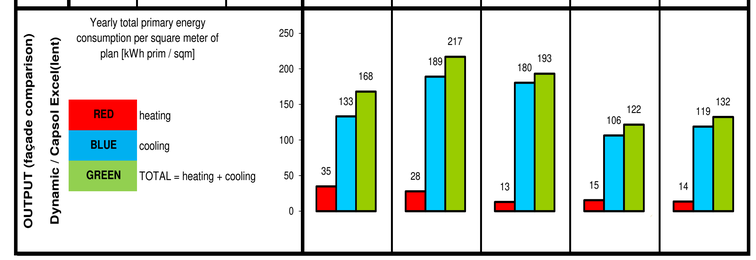

Source: A compact, unitized double skin facade by Alex Cox, LEED AP, James Hock, LEED AP BD+C, Laura Ziegler Permasteelisa North America, and Karin Lamberts Scheldebouw B.V.

Double-Glazed Unit (DGU) - A double-glazed unit (DGU) with internal blinds in the room and a high performance low- E coating on surface #2. This is considered standard practice in most US cities today and serves as a baseline.
Triple-Glazed Unit (TGU) - A triple-glazed unit (TGU) with internal blinds in the room and low-E coatings on surface.
Active Wall® (AW) - A DSF consisting of a DGU on the outside and single glazing on the inside, creating a ventilated cavity where blinds can be integrated and indoor return air passing through the cavity of the DSF is ducted to the mechanical system.
Interactive Wall® (IW) - A DSF consisting of single glazing on the outside and a DGU on the inside, creating a ventilated cavity where blinds can be integrated and air flowing from outdoors through the cavity returning back to the outdoors via stack and/or wind effects.
Permasteelisa moisture-maintenance free Sustainability Closed Cavity Facade (mfree-SCCF) - a fully sealed cavity with the same glazing and blind configuration as IW, with a very low volume of clean, dry air supplied to the cavity to prevent condensation and dust with the cavity at all times. A detailed analysis software tool, called DSCAT, was developed to design the air supply system in order to optimally condition the cavity.

U-Value - The rate of transfer of heat through a building part.
Solar Heat Gain Coefficient (SHGC) - The fraction of solar radiation admitted through a window, directly transmitted or absorbed, and subsequently released inside the home. The value is between 0 and 1. The more solar heat is gained, the more value it has.
Visible Transmittance (VT) - The amount of light in the visible portion of the spectrum that is transmitted through a window. The more daylight is there in a space, the higher the VT.

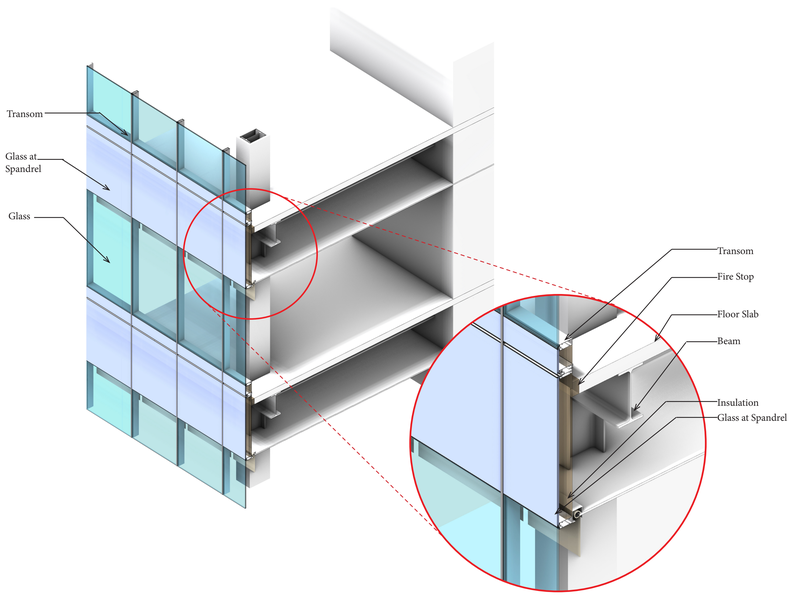

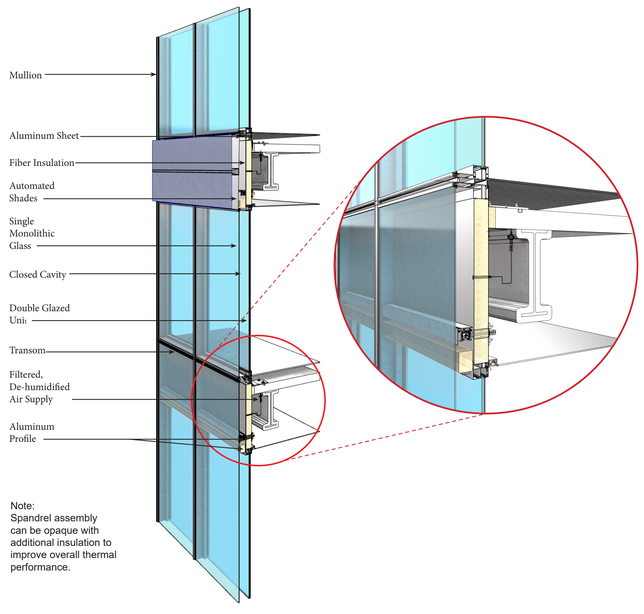

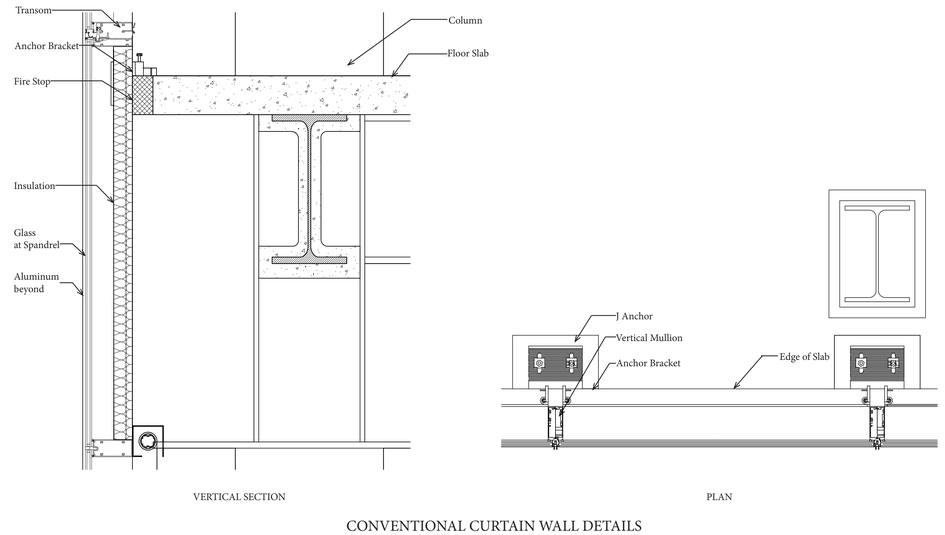

VERTICAL SECTION PLAN

CONVENTIONAL CURTAIN WALL DETAILS

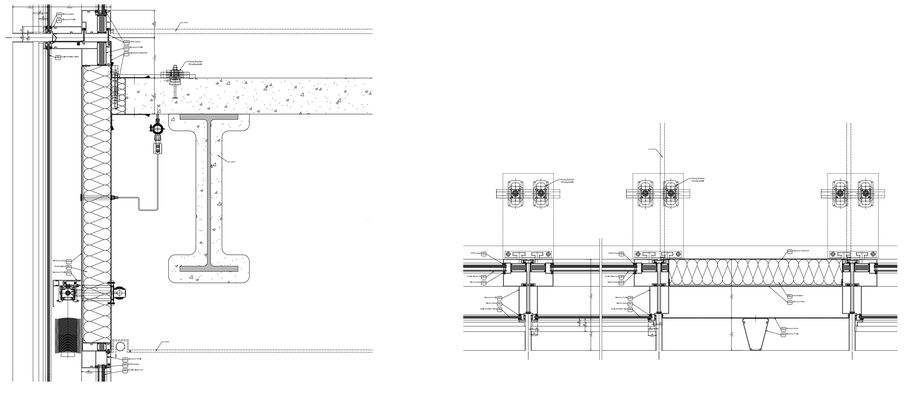

VERTICAL SECTION PLAN

CLOSED CAVITY FACADE DETAILS

CONVENTIONAL UNITIZED WALL PROS AND CONS

Pros:
- Can be installed quicker and easier because they are pre-assembled and glazed in factory
- Cheaper labor cost in site
- Availability of various materials for the spandrel systems (glass, metal panels, stone, terra cotta, etc.)
- High performance systems (thermal, air, water, dynamics)
- Minimizes site operations
- The fabrication process for unitized systems is more consistent

Cons:
- Can be expensive for low to mid-rise buildings
- Requires a highly skilled and experienced contractor to properly erect this system

CLOSED CAVITY FACADE PROS AND CONS

Pros:
- Blinds are protected in the cavity, and a low-pressure supply of dry, clean air prevents condensation and dust
- The most significant benefits of closed-cavity facade (CCF) are the potential energy savings due to the extremely low U-value and solar heat gain
- Provides the thermal advantage of an exterior operable shading device without the high maintenance costs
- The facade prioritizes occupant comfort and reduces the energy demand and carbon emissions of the building
- It can be installed in the same manner as SSF

Cons:
- Expensive compared to other curtain walls

References:
1. A compact, unitized double skin facade by Alex Cox, LEED AP, James Hock, LEED AP BD+C, Laura Ziegler Permasteelisa North America, and Karin Lamberts Scheldebouw B.V.,
2. Closed Cavity Facade details by Gartner/ Permasteelisa,
3. Conventional Unitized Curtain Wall Details by Victoria Ereskina, HOK;
4. Arjun,N. Types of Curtain Wall System – its Details, Functions and Advantages. Retrieved from https://theconstructor.org/building/curtain-wall-system-types-details/13676/

REDEFINING GENDER CULTURE: A NEW PERSPECTIVE ON DRESS AND IDENTITY

Arsha Attique, Chayange Davis-Levy and Dr. Alyssa Dana Adomaitis
Business & Technology of Fashion, New York City College of Technology

Introduction

Recently, social and cultural changes have influenced the way individuals think, whether it is culture itself, fashion, technology, or even gender. The impact of this change, as well as future changes, helping one be more aware of what is allowed and appropriate in conversations regarding a current shift, gender identity and expression. Many no longer identify with "he" or "she," or "male" or "female" as their preferred pronouns. In New York City alone, 31 separate categories have been identified by the New York City Commission on Human Rights, and if one does not adjust to or incorrectly identifies and individual's gender, they will be fined. The purpose of this research is for us, as a society, to understand more about the various types of gender identities, how individuals preferred to be addressed, and the appropriate identifications. With the prior knowledge of how dress and appearance cues were a way to help represent a gender, how can that be used to help others be respectfully addressed or identified?

Method

In regards to gender and dress, individuals all have different ways of thinking, whether it is about what ones preferred pronoun is, one's appearance cues, how one dresses and/or should dress, or even look. To get a better understanding, phenomenology was used which consists of 2-3 hr interviews with participants, who will remain anonymous, but their responses to open-ended questions will be labeled as a number (i.e. 001, 002, 003), without any further personal information attached. Each response given from the participants' is being read, as data analyses was collected with the use of Van Manen's (1990) line-by-line method to help identify major concepts. Similar responses are grouped together, which is being calculated following the *inter-coder reliability* formula.

Conclusion

Prior to the realization and ability to self-express through dress, regardless of gender, sumptuary laws had created barriers for individuals, as it prevented one to stay within their social, political, and possibly religious hierarchy (Stone, 2013, p. 70). In recent times, each person has the ability to dress and present themselves they see fit, allowing them to self-express, as well as show individuality, no longer following the stereotypes created by society. After the approval from IRB, and following Van Manen's (1990) method to gather major concepts from the interviews, this on-going research shows how each person's cognitive thinking on dress and identity is different.

Literature Review

To understand the barriers of effective gender identification for those who tend to stray from heteronormative labels, one can look to the words of Stoller and Oakley (1968 & 1970), "The theoretical construct appeared to escape the essentialism of 'sex' capturing the way in which different patterns of behavior (and indeed bodies) as socially constructed, rather than innate" (p.). A common thought process shared also by Haslanger (1995, p.98) "They are casually constructed". Which is to say while widely understood as a defining factor of one's identity, society is who has imposed the labels of who one is sexually through only the look of one's body, which is not in any way a complete look into an individual. This thought process of society has increased the binary and many instances abusive treatment of individuals who cannot conform to gender norms and stereotypes, such as transgender, gender non-conforming, and gender non-binary individuals.

When looking at gender identity through the scope of fashion, one can see that many contributions to fashion have been made through bending heteronormativity, like the use of broadening shoulder pads in women's suits beginning in the 1980's, to the recent popularization of young men wearing skirts, like Jaden smith for Louis Vuitton "Series 4" Spring 2016 collection. The increasing of breaking down the barriers of dress for gender expression have been continuous for many decades, and keep consistent with the notion that fashion is the way to show one's inside feelings to the world, one outfit at a time. In Mary Ellen Roach-Higgins and Joanne B. Eicher's work *Dress and Identity*, they explain the use of symbolic interaction perspective of dress as it relates to identity, including writings by "Stone (1962), Goffman (1963, 1971), Stryker (1980), and Weigert, Teitge and Teitge (1986)" that also fit into the category of concepts. In relation to dress and expression of one's self, it is conveyed, "From the perspective of symbolic interaction theory, individuals acquire identities through social interaction in various social physical and biological settings. So conceptualized, identities are communicated by dress as it announces social positions of wearer to both wearer and observers within a particular interaction situation."

This can be broken down to mean that as one makes dress choices, they are not only for the one who wears but the one who admires from afar or stares as the wearer passes on the street. The social interaction of dress happens in multiple forms and overall, the wearer has identities that are non-verbally communicated in each piece worn, such as gender. Explaining the concept further, Roach-Higgins and Eicher wrote, "The identities for any one person, including those communicated by dress are uniquely personal. They are at the same time completely social because they are socially acquired "selections" from socially constructed ways of attributing identities on the basis of social positions individuals fill."

Theoretical Framework

Stone's highly-influential 1962 "Appearance and the Self" which first printed in *Human Behavior and the Social Processes: An Interactionist Approach* outlined a process that explains the role of dress in forming identities. The process entails four parts. The first is labeled ***program,*** wherein people adopt dress intended to announce their individual identity, both to themselves and to others. The individual then responds to the adopted dress for its effectiveness in communicating the desired identity. The second part is ***review***, where the presented appearance is reviewed by others, who either validate or challenge the program identity. ***Validation*** entails others attributing the desired identity to the individual, while ***challenge*** entails others questioning whether the individual can actually claim the desired identity. Thus, dress impacts the ability of an individual to lay claim to an identity that, in turn, can impact an individual's ability to perform roles in society.

References

Adomaitis, A. D., & Johnson P., K. K. (2005). Casual Versus Formal Uniforms: Flight Attendants' Self-perceptions and Perceived Appraisals by Others. *Clothing and Textiles Research Journal*, *23*(2), 88–101. https://doi.org/10.1177/0887302X0502300203

Celebratory Pride Fashion Collections inclusive fashion. (2018, June 5). Retrieved from https://www.trendhunter.com/trends/inclusive-fashion1.

Eicher, J. B. (n.d.). Introduction: Dress as Expression of Ethic Identity. Ethnicity and Identity Series Dress and Ethnicity. doi: 10.2752/9781847881342/dressethn0005

Francis, B., & Paechter, C. (2015). The problem of gender categorisation: addressing dilemmas past and present in gender and education research. Gender and Education, 27(7), 776–790. doi: 10.1080/09540253.2015.1092503

NYC Commission on Human Rights. Gender Identity/Gender Expression: Legal Enforcement Guidance. http://www1.nyc.gov/site/cchr/law/legal-guidances-gender-identity-expression.page (2018).

Roach-Higgins, Mary Ellen. and Joanne B. Eicher. "Dress and Identity," *Clothing and Textiles Research Journal,* 10.4 (1992):1-8.

Stone, E. (2013). The Dynamics of Fashion (4th ed.). New York: Fairchild Books. Bloomsbury Publishing Inc. (p.70).

The Evolution Of Androgynous Fashion. (n.d.). Retrieved from https://www.bustle.com/articles/149928-the-evolution-of-androgynous-fashion-throughout-the-20th-century-photos.

Long-Term Effect Of Very High Fat Diet To Study The Synergism In Hormonal And Cellular Changes in Male Mice

Department of Biological Sciences, New York City College of Technology/CUNY, New York
Students: Ilhom Bakiyev, Bushra Miah, and Brian Holliday
Faculty Mentor: Dr. Sanjoy Chakraborty

ABSTRACT

Long term intake of very high fat diet (VHFD) leads to the hormonal changes causing simultaneous changes in the islets of Langerhans and adipocyte cell size. The role of a High Fat Diet (HFD) and its direct correlation with regards to health has become one of the most important subjects of our time. The aim of this study is to analyze the effect of high fat induced obesity in the male mice model by feeding some of them a normal chow diet (ND, n=15) and the others with a VHFD (n=30) for 2, 12, and 24 weeks. Body weight, food intake, caloric intake [fat (saturated and unsaturated), protein, and carbohydrate], hormone levels (leptin and insulin), and islet of Langerhans/adipocyte size were quantitatively recorded. In VHFD-fed animals, body weight (as well as leptin and insulin levels, along with growth in islet and adipocyte size) significantly increased within the first 12 weeks and then plateaued with time. VHFD-fed animals consumed significantly less food than ND-fed animals at all time periods indicating that it was the quality of food, and not the quantity, which caused the increase in body weight. The increases in islet and adipocyte size in VHFD-fed animals were similar to the analogous increases in hormonal levels (at 2 vs 12 vs 24 weeks). These results, therefore, suggest that in diet-induced obesity changes, shifts in hormonal levels works hand in hand with metabolic adjustments at the cellular level to combat the effect of fat. Thus, mechanisms like hormonal resistance, changes in adiposity, islet size and caloric intake with prolonged exposure to high fat are probably defensive mechanisms employed to protect against diabetes. In order to understand these complicated and nuanced effects of high fat and to comprehend the underlying mechanism associated with it, it is important to focus on long-term studies that emphasize the synergy between cellular and hormonal changes in addition to an analysis of individual components.

MATERIAL AND METHODS

Animals

WT mice (n=45) of genetic background (C57BL/6J) were housed in a colony room, with a partially revised light cycle of 14:10 (lights on 2300h and off at 1300h). Food and water were available ad libitum. Animals were 12-14 weeks of age at the time of experimentation. All animals studies were conducted in accordance with Guide for the Care and Use of the Laboratory Animals, using protocols approved by the Institutional Animal Care and Use Committee at Adelphi University.

Food consumption

A quantified amount of food (ND and VHFD) was given on a particular day of the week and the remaining food was weighed every week. The amount of food consumption was calculated by subtracting the amount of food given and amount of food remaining in the cage. Caloric intake was calculated using the values provided by the supplier (ND, kcal/gm= 3.07, VHFD, kcal/gm= 5.24). Physiological fuel value (kcal/gm)= Sum of decimal fractions of fat, protein and carbohydrate multiplied by 9, 4 and 4 kcal/gm respectively.

Leptin and insulin Assay

Blood samples were then allowed to clot, centrifuged, and the serum stored at -20 C for leptin and insulin assay. Serum leptin was assayed by Enzyme Immuno Assay (Enzo Life Science) and insulin with Radioimmuno Assay using RIA assay kit (Millipore, LIPCO). The Inter-assay precision% for leptin was 3.7-6.1 and insulin was 8.5-9.4 and intra-assay precision % 1.9-5.9 for leptin and 1.4-4.6 for insulin.

Biopsy of different organs

Tissue of appropriate size was dissected out and wrapped in lens paper, marked with a pencil and placed in formalin overnight. Next day tissues were placed in cassettes and dipped again in formalin and then send to Cross Island Laboratories for biopsy.

Statistical Analysis

Statistical analysis was done to compare levels of hormones, glucose, body weight, food consumed, caloric intake and pancreatic islet's area among ND and VHFD fed animals using ANOVA, JMP software, version 7, SAS Institute Inc., Cary, NC. Effects were considered significant at $p < 0.05$.

NORMAL DIET VS. VERY HIGH FAT DIET

Normal Chou Diet

Wild Type on Normal Chou Diet

Very High Fat Diet

Wild Type on Very High Fat Diet

What do the Findings of this Research Say About Humans?

- Scientists and researchers find the mice model to be a convenient, important and relevant model in studies because their genetic, biological, and behavioral characteristics very closely resemble those of humans.
- The results taken from experiments and research like these can be used to mimic what happens in humans and better understand human obesity and propose solutions to obesity, diet or nutrition related issues or diseases.
- VHFD-fed organisms are obese compared to those that are not on the VHFD. The impacts on glucose homeostasis and insulin resistance increase with the increasing fat content that is fed to them.
- VHFD feeding not only caused a significant increase in size, but also in the production of blood glucose at all times. This effects how insulin removes glucose from the blood and into the cell for later energy and storage.

LEPTIN

INSULIN

Changes in the leptin and insulin levels in ND and VHFD fed mouse at various time points. Serum leptin (ng/ml) and insulin (ng/ml) were obtained by RIA. The values are expressed as absolute numbers. The VHFD fed mouse showed significantly higher levels of insulin ($p<0.0001$) than ND.

BODY WEIGHTS

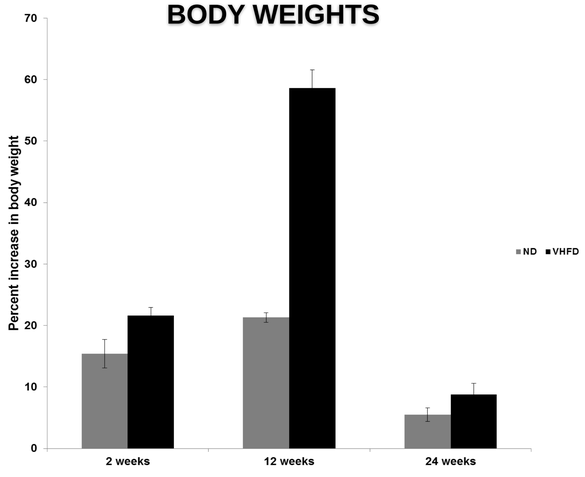

Body Weights changes over 6 months in animals fed in ND and VHFD. There was an increase in body weight in both ND and VHFD. But the increase in weight was significantly higher in VHFD than ND ($p < 0.001$).

MICROPHOTOGRAPHS OF PANCREATIC ISLETS AND ADIPOSE TISSUE

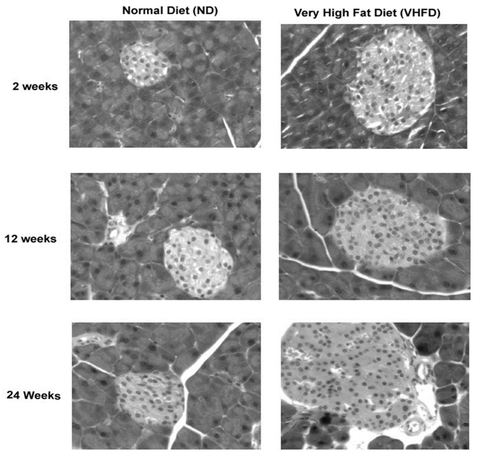

Pancreatic islets stained with hematoxylin-eosin stain: Representative pancreatic islets from VHFD and ND at A) 2 weeks, and B) 24 weeks. Note the increase in size of the islets which increases in time.

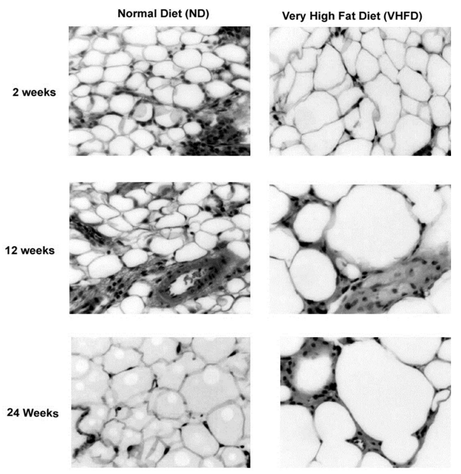

Adipocytes stained with hematoxylin-eosin stain: Representative adipocytes from VHFD and ND at A) 2 weeks, B) 24 weeks. Note the increase in size of adipocytes which increases in time

SUMMARY AND CONCLUSIONS

1. There is a steep rise in body weight in animals fed on VHFD for 12 weeks . The increase in body weight then plateaued (% increase in body weight). Food intake was lower for VHFD animals than HFD although the caloric intake was higher.

2. The increase in glucose, leptin and insulin levels increased in VHFD till 12 weeks and then plateaued. However, in ND there was only a slight increase over the time period studied. The increase in glucose level was much controlled in the first 2 weeks in VHFD animals due to the sharp increase in insulin and leptin levels. Animals in VFHD diet were not diabetic (below 240mg/dl). With time, animals developed hyperinsulinemia and hyperleptinemia resulting in diabetes and probably became insulin and leptin resistant..

3. There was an increase in size of the islets of Langerhans and adipose tissue throughout the time period in VHFD not for ND. The increase could be due to hypertrophy, hyperplasia, cell replication. The increase in the islet size was probably a compensatory mechanism to combat insulin deficiency. Glucose acts on the islets growth (beta cell) which secretes insulin. Insulin in turn causes increases in the islets mass. Therefore, the two major factors that affect the islet size are glucose and insulin. The cumulative effect of glucose and insulin shows a drastic increase in the islet size although glucose and insulin do not rise proportionally.

ACKNOWLEDGEMENT

Dean: Justine Vasquez-Poritz; Director of Undergraduate Research: Hamid Norouzi, PhD, P.E.
Coordinator of Honors Scholars Program: Laura Yuen-Lau;
Chairman of the Biology Department: Dr. Andleeb Zameer

Hybrid Green Technology Systems for New York City Roof Tops:

Green Roofs and Solar Energy

Ilana Berger, Faculty Mentor: Ivan L. Guzman

Department of Construction Management and Civil Engineering Technology

Abstract

Climate change is a reality which we can no longer ignore. As a response New York City has set some of the most stringent energy code regulations in the nation. In 2019 the Mayor's office of Sustainability released an initiative to reduce carbon emissions by 80% by 2050. In order to meet this goal, the new building codes stipulate that all new buildings must include green technology. The issue however is how can we maximize the limited space we have available within the urban environment and how can designers and builders develop feasible solutions for developers and owners. I intend to explore the possibilities of maximizing rooftop space by creating hybrid green technology solutions for New York City rooftops. Green roofs and solar energy are both proven to be efficient and sustainable solutions. The issue however is that both technologies occupy the same space and therefore in conventional practice, are mutually exclusive. The challenge is how to make these and other technologies work in unison within the same roof real estate. With the development of new fully translucent solar cell technology, components of natural light that are not used for the generation of electricity can now be harvested for other purposes. By installing these types of solar panels on a canopy system which are mounted above a roof's surface, the roof can then be used perhaps for a green roof. With the combination of solar electric onsite generation and the thermal insulating benefits of green roofs, homes, buildings, and factories can significantly reduce their energy consumption and therefore decrease their dependency on fossil fuels. With the successful combination of solar energy and green roof technology, buildings can now move closer to meeting the new energy code requirements while also reducing their carbon footprint.

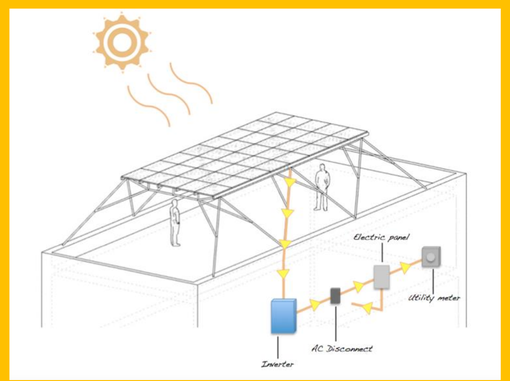

What is Solar Electric?

- Solar panels are used to transform sunlight into electricity
- Solar cells convert the energy From photons into electricity
- An inverter is used to change The DC power into AC power

What is a Solar Canopy?

- It is a racking system used to mount solar panels above the roof's surface
- Allows the roof's surface to remain usable while still harvesting power from the sun

Clear Solar Cells

- Solar panels that are translucent and allow light to pass though while still generating electricity.
- A new technology called transparent luminescent solar concentrator (TLSC) which are made with organic salts absorb non-visible ultraviolet and infrared light.
- Sunlight is guided to the edge of the panels where conventional solar cell technology is used to then convert it into electricity

What is a Green Roof?

A roof which is either Partially or fully covered In vegetation

What are the benefits of A green roof?

- Adds an extra layer of Insulation to the roof
- In the summer it acts as a heat barrier reducing heat transfer by up to 72%
- In the winter it prevents heat from escaping a building, reducing heat loss by up to 33%

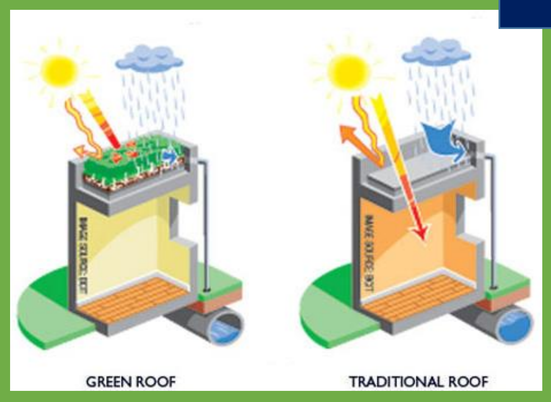

Green Roof Plants

Semi shade tolerant green roof plants can thrive underneath a solar canopy. Clear panels provide an added benefit by blocking ultraviolet and infrared light which can be harmful to plants.


Four-nerve Daisy

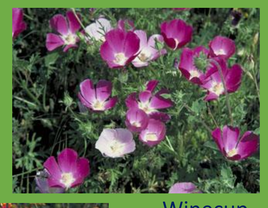
Winecup

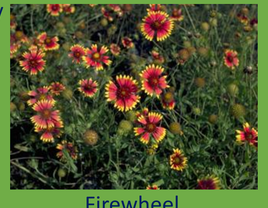
Firewheel

Real World Scenario

- 6 family home
- 2,500 square feet of roof top
- Average electrical consumption per family = 10,972 kWh

Using Only Solar Energy

A 40 kW solar system will take up 2,000 sq. ft. of roof space and produce 54,900 kWh annually covering 83% of the building's electrical usage. Thereby reducing the building's power needs from the grid by 83%.

Using Solar Energy Plus a Green Roof

The solar system will cover 83% of the building's electricity plus the green roof will reduce the building's heating and cooling usage by up to 33%.

Selected References

Mahmoud, et al. "Energy and Economic Evaluation of Green Roofs for Residential Buildings in Hot-Humid Climates." *Buildings*, Vol. 7, no. 2, 2017, p. 30.

Zhao, Yimu, et al. "Near-Infrared Harvesting Transparent Luminescent Solar Concentrators." *Advanced Optical Materials*, vol. 2, no. 7, 2014, pp. 606–611., doi:10.1002/adom.201400103.

"Plant Database." *Lady Bird Johnson Wildflower Center - The University of Texas at Austin*, www.wildflower.org/plants/result.php?id_plant=CAIN2.

"PVWatts." *PVWatts Calculator*, pvwatts.nrel.gov/pvwatts.php.

Acknowledgments

Brooklyn Grange
Emerging Scholar Program

The Psychology of Hurricane Warnings: Why They Are Sometimes Ignored

Department of Social Science, New York City College of Technology/CUNY, New York

Students: Christina Bhawanidin and Jeevanie Liliah
Faculty Mentors: Dr. Howard Sisco and Ann Ngana Mundeke

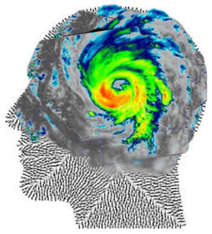

Abstract

Why do some people heed evacuation orders given before an impending major disaster such as a hurricane, while others do not? Failure to comply with departure instructions puts the individual at personal peril, as well as the first responders responsible for rescue and evacuation during those dangerous times. For example, during Hurricane Sandy in New Jersey, 72% of people refused to evacuate their homes, whereas during Hurricane Rita in the Gulf of Mexico, 53% of people disobeyed orders to evacuate. The purpose of this research is to begin the process of investigating the psychological factors that contribute to individual differences in disregarding evacuation orders. A hurricane preparedness questionnaire was developed using rational methods to assess the psychological reasoning behind why people overlook precautious warning. When completed, the survey will be administered in person to future hurricane victims at disaster response centers.

Methods

Survey Development-Phase 1

Development of the questionnaire began by reviewing relevant media reports regarding past hurricane evacuations. The questionnaire was developed by generating and linking potential survey questions to explanations and rationale given from interviews of disaster victims who chose to stay and those that choose to leave. Several types of questions were included in the questionnaire. The types of questions included were dichotomous questions, open-ended questions, multiple choice questions, rank-order questions and rating scale questions. These initial questions were reviewed and edited to be clear, concise, and direct.

Survey Implementation-Phase 2

Professors and students involved with this project will visit the sites hit by natural disasters to conduct interviews to assess various factors that prevent or discourage people from evacuations. The study will include observation, participant observation and face-to-face interviews on sites.

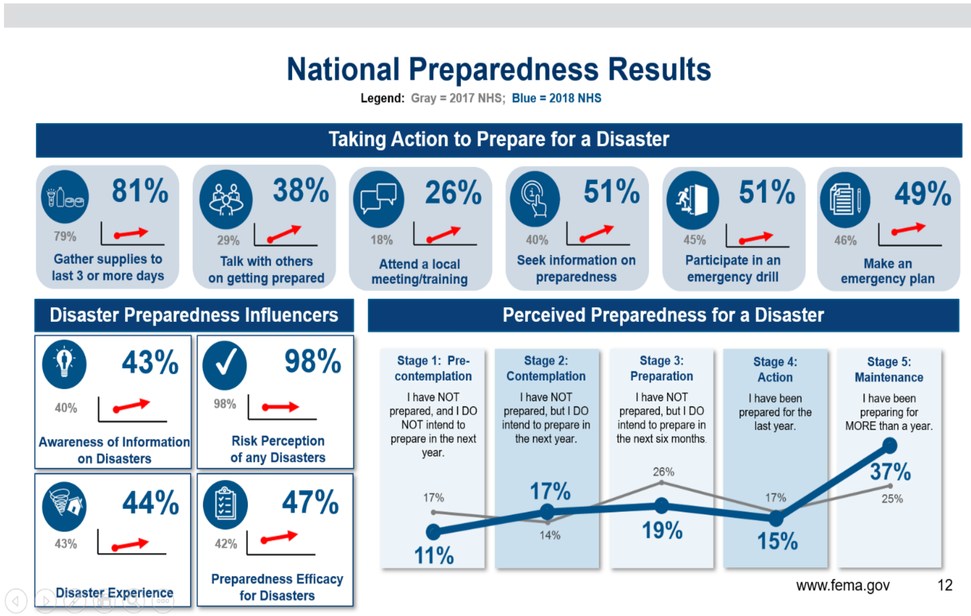

Hurricane Preparedness Survey

1. Before this hurricane, approximately how many hurricanes have you experienced?
   a. 0
   b. 1 - 4 hurricanes
   c. 5 - 10 hurricanes
   d. More than 10 hurricanes

2. Were you aware of hurricane warnings before the storm?

   Yes No

3. Were you informed of the evacuation level for hurricane storm surge?

   Yes No

4. Did you have a plan in place if an evacuation was ordered in your area?

   Yes No

5. Did you have the following supplies ready for use in case of a hurricane?
   A. 3 day supply of water Yes No
   B. 3 day supply of canned / non perishable food Yes No
   C. 3 day supply of medicine / first aid kit Yes No
   D. 3 day supply of warm / extra clothing Yes No
   E. Battery operated flashlight Yes No
   F. Battery operated radio Yes No
   G. Extra batteries Yes No

6. Does your home have storm proof windows or hurricane shutters?

   Yes No

7. Did you lose power after the hurricane?

   Yes No

8. Do you have a built in or portable generator in case of a black-out?

   Yes No

9.. How severe was the damage to your home from the hurricane?

1	2	3	4	5
No damage	*Very little damage*	*Damaged*	*Very damaged*	*Extremely damaged*

10. Did you have to evacuate your home because of the storm?

    Yes No

11. Circle all of the following ways you used to learn about the hurricane.
    a. TV
    b. Radio
    c. Newspaper
    d. Hearing from other people
    e. The internet
    f. Social media
    g. Other methods

12. Did you planned multiple evaluation routes and plans?

    Yes No

13. Did you have an emergency evacuation plan for staying in touch or getting messages to family and friends?

    Yes No

14. Is your homeowner's and flood insurance up-to-date?

    Yes No

15. Is your homeowner's and flood insurance sufficient to replace your home and belongings if they are damaged or destroyed?

    Yes No

16. Have an inventoried your property and belongings?

    Yes No

17. Do you have copies of your insurance policies, household inventory, and other important papers as well as other valuables in a safe place-- one that's waterproof and fireproof?

    Yes No

18. . Do you know how to turn off your utilities (electricity, gas and water)?

    Yes No

Overview of Student Needs & Readiness in Working with Persons with Substance Abuse Issues at Professional Internship Sites

By: Joya Biswas & Nashrin Akter Faculty Mentor: Professor Charisse Marshall, *PhD*

Human Services Department

New York City College of Technology, CUNY

300 Jay St, Brooklyn, NY 11201

ABSTRACT

A quantitative survey study of a cohort of 12 Human Service (HUS) Department Interns is proposed to assess the readiness and needs of HUS students during their internship semester. The data yielded from this study will help the HUS Department-specifically students and instructors from the HUS 1203 Human Seminar Course-understand what skills and abilities are needed to prepare HUS Students for professional internships dealing with persons coping with substance abuse and addiction.

INTRODUCTION

Substance abuse and addiction are major social issues that afflict millions of people and interrupts the lives of their families and friends. The definition of addiction and improvement varies from person to person. An individual's viewpoint on addiction comes from their experiences, environment, family history and more. Substance abuse and addiction occur everywhere. Through professional internship sites to work with persons with substance abuse issues will give the interns the opportunity to obtain the knowledge and their attitudes regarding working with this population. Student interns will acknowledge the perception of a world where using and abusing substances have critical consequences and allow them to explore the various techniques and methods of each therapist. Another main reason is student interns experience including learning to be in the professional world and conduct themselves properly in a professional setting. In order to gain all these crucial knowledge Human Services Department students at City Tech needs to have substantial skills and abilities to prepare themselves to work at professional internship sites. By conducting this research, we will be able to learn and comprehend the essential skills needed for student interns to prepare to work with this population in the fields. This research has approved by the Human Services Department chairperson of the college at New York City College of Technology.

METHODOLOGY

This study was conducted by a quantitative survey for the Human Services Seminar- HUS 1203 students. A total of 12 students completed the survey, representing a response rate of 90% of the HUS 1203 students. This survey was taken to find out their responses to certain essential questions for the preparedness to be an intern to work with substance abuse & addiction clients and to distinguish the differences in their exposure to educational, vocational, and personal opportunities to learn about this population.

- The questionnaires, which required about 10-15 minutes to finish, included scales measuring the students' understanding and opinions toward working with substance- abusing clients.
- At the beginning of the survey, students were instructed to read a statement that emphasized, "the voluntary nature of the study and that participation or nonparticipation in the survey would not affect their grades or class standing." (Senreich, 2012, p. 108)
- Participation in the study was voluntary, this study was conducted through Google Survey Form that was created by one of the researchers, Joya Biswas and with the help of the mentor and another researcher Nashrin Akter.
- The survey form was emailed to students. Students' names were not required anywhere in the survey. The survey was anonymous.

RESULTS

Quantitative Survey:

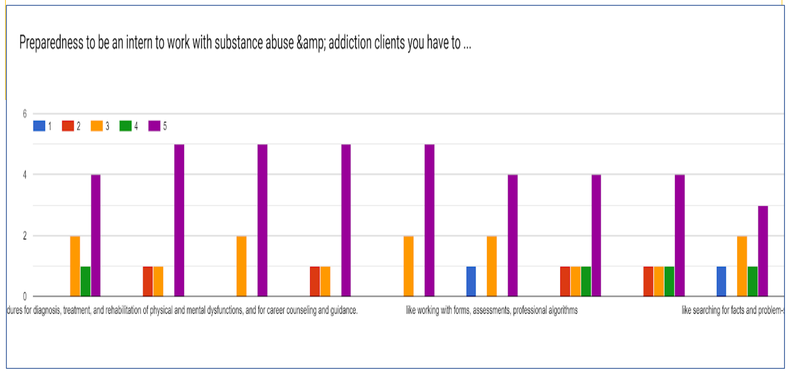

Based on the results, most of the participants considered it is important to have the skills to work with people, counsel people with patience, do an assessment which is an essential part of the procedure.

DISCUSSIONS

The results reveal that participants considered it vital to have the efficient skills to work the Substance Abuse individuals. Filing and documentation is important which was considered by most of the participants.

- ❑ Documenting data, the progress of the treatment provide excellent outcomes. It is also a significant skill based on the results, to counsel and assist the clients to adjust crucial situations of life.
- ❑ Interest of communication with people is also essential to work with this population. Participants also answered it's an important skill to support people with proper services.
- ❑ Self-expression and rules are crucial for working with this population, to set boundaries.

Critical thinking and time are mandatory for the counseling session. Research and facts also necessary to achieve the goals of the clients.

ACKNOWLEDGEMENT

This research was supported by the Honor Scholars Program and Emerging Scholars Program, and we acknowledge the supports from the Human Services Department to conduct this research. We would like to thank Professor. Marshall for the support and guidance and Human Services Seminar– HUS 1203 students for participating in the anonymous survey for this study.

REFERENCES

Stein, J. (2003). Attitudes of Social Work Students About Substance Abuse: Can a Brief Educational Program Make a Difference? Journal of Social Work Practice in the Addictions, 3(1), 77-90.

Senreich, E., & Straussner, S. (2013). The Effect of MSW Education on Students' Knowledge and Attitudes Regarding Substance Abusing Clients. Journal of Social Work Education, 49(2), 321-336.

Slabbert, I. (2015). REFLECTIVE LEARNING IN SOCIAL WORK EDUCATION IN THE FIELD OF SUBSTANCE ABUSE. Social Work = Maatskaplike Werk, 51(4), 549-591.

The Logical Minimalism Algorithm Applied to First-order Logic Axiom Sets

Aurkaw Biswas

CUNY, New York City College of Technology

Abstract

This poster assumes an acquaintance with some basic knowledge of first-order logic. I describe a recursive process, called the Logical Minimalism Algorithm, on finite axiom sets. This algorithm finds all the minimal subsets of axioms from a given finite set of axioms. A minimal subset of axioms, called a minimal core, is one that has no redundant axioms, where an axiom is redundant if it can be derived from the remaining axioms. Every finite axiom set has at least one minimal core. There is a rooted tree corresponding to the Logical Minimalism Algorithm applied to any finite axiom set. I apply this algorithm to an axiomatization of Boolean Algebras.

Introduction

Let L be a first-order language, and let T be a finite set of axioms in the language L. For any axiom A in T, if $T - \{A\}$ implies A, then A is said to be a *redundant axiom* of T. If A is an axiom of T that is non-redundant, then A is said to be an *independent axiom* of T. A *minimal core* of T is a subset M of T such that M has no redundant axioms and M implies T. It can be easily proven that, since T is finite, it has at leas one minimal core. There is a recursive process, called the **Logical Minimalism Algorithm**, to discover all the minimal cores of a given axiom set T. For each redundant axiom, delete it from T and see which of the remaining axioms of T are still redundant. This process can be repeated in the usual way. In fact, we can form a labeled rooted tree corresponding to T and its minimal cores. Start with a single node, and label it with T. If T has no redundant axioms, stop. If there are n redundant axioms $A_1, \ldots, A_n$ in T, create n nodes and label it with $T - \{A_m\}$, for each $1 \leq m \leq n$. Repeat this process for each of the new nodes. The nodes without children are labeled with precisely the minimal cores of T.

An example

We apply the Logical Minimalism Algorithm to an axiomatization of Boolean Algebras. Our signature of non-logical symbols is {+, *, 0, 1, '}. + and * are binary operations, ' is a unary operation, and 0 and 1 are constants. Following [1], adapted from [2], a Boolean Algebra is a structure $(B, +, *, 0, 1, ')$, where the following axioms, numbered 1 through 9, hold, where x, y, and z are arbitrary elements of B,

1. $0 \neq 1$
2. $x + 0 = x$
3. $x * 1 = x$
4. $x + x' = 1$
5. $x * x' = 0$
6. $x + y = y + x$
7. $x * y = y * x$
8. $x + (y * z) = (x + y) * (x + z)$
9. $x * (y + z) = (x * y) + (x * z)$

Calculations

Due to space constraints, I will only prove that Axiom 2 is redundant from all three of T, $T - \{6\}$, and $T - \{7\}$. First, we prove a lemma:

Lemma: 1+1=1

Proof:

1+1=(1+1)*1	by Axiom 3
(1+1)*1=(1+1)*(1+1')	by Axiom 4
(1+1)*(1+1')=1+(1*1')	by Axiom 8
1+(1*1')=1+0	by Axiom 5
1+0=(1*1)+0	by Axiom 3
(1*1)+0=(1*1)+(1*1')	by Axiom 5
(1*1)+(1*1')=1*(1+1')	by Axiom 9
1*(1+1')=1*1	by Axiom 4
1*1=1	by Axiom 3

Axiom 2: x+0=x

Proof:

x+0=x+(x*x')	by Axiom 5
x+(x*x')=(x+x)*(x+x')	by Axiom 8
(x+x)*(x+x')=(x+x)*1	by Axiom 4
(x+x)*1=x+x	by Axiom 3
x+x=(x*1)+(x*1)	by Axiom 3
(x*1)+(x*1)=x*(1+1)	by Axiom 9
x*(1+1)=x*1	by Lemma
x*1=x	by Axiom 3

Conclusion and Possible Generalizations

The Logical Minimalism Algorithm works with any finite axiom set. In cases with large axiom sets, finding a minimal core is highly desirable.

A possible generalization is working with axiom systems other than first order logic. Another generalization is working with inference rules as well as axioms. A third, very interesting generalization is working with infinite axiom sets. In some cases, there may be no minimal core.

Results

There are four minimal cores of T, each with 7 axioms. By following the Logical Minimalism Algorithm, the minimal cores can be visualized as leaves of a rooted tree. For example, with T being the axiom set described above, the labeled rooted tree corresponding to T is as follows, where the subscripts refer to the numbered axioms that have been deleted from T. So, for instance, Axiom 2 is redundant from T , $T_{\{6\}}$, and $T_{\{7\}}$ and Axiom 6 is redundant from T, $T_{\{2\}}$, and $T_{\{3\}}$, etc.

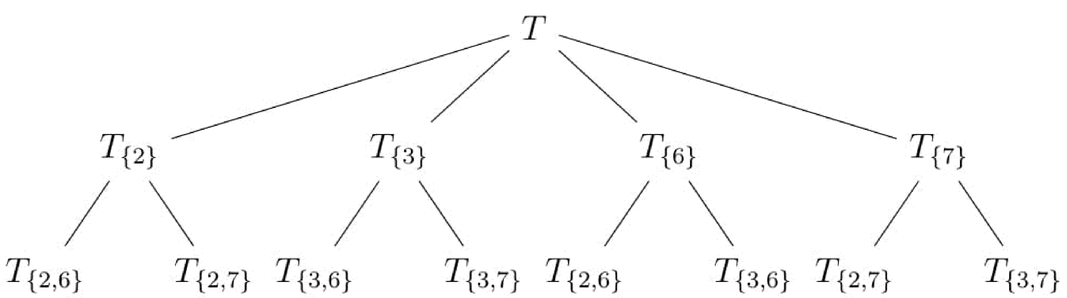

Acknowledgments

I would like to give special thanks to Prof. Isaacson for taking the time to do this project with me. I would also like to thank Profs. Africk and Reitz for providing valuable feedback. I would also like to thank Dean Vazquez-Poritz for taking the time to read my paper.

References

[1] E. Mendelson, *Schaum's Outline of Boolean Algebra and Switching Circuits*, Mc-Graw Hill Education, 1970.

[2] E. V. Huntington, Sets of Independent Postulates For The Algebra of Logic, *Transactions of the American Mathematical Society*, Volume 5, No. 3, 288-309, 1904.

A Study on Building Occupancy Detection with Sensor Data Analysis

Brian Borrerro and Daniel Sampong
Supervisor: Prof. Li Geng
Department of Electrical and Telecommunication Engineering Technology

Abstract

Thermal comfort is a considered factor for building design and innovation. Efficient regulation of thermal comfort can be achieved through incorporation and use of occupancy sensors. However, there are often difficulties in accurate detection of occupants therefore affecting proper auto regulation of occupants' spaces. The sensors often employed are used to gather information regarding possible occupancy. In related work, researchers and investigators employed the use of pre-existing environmental sensors such as CO2, humidity, and temperature sensors. The data collected with those sensors in the tested environment were charted with various software and verified with other instruments such as cameras and logs. This was for the purpose of verifying true occupancy and false ones. For our research, we investigated some of these existing works and endeavored to build our own sensor system to collect temperature and humidity values and then send them to the cloud to be visualized and analyzed remotely. We investigate the feasibility of using these data for occupancy detection. To fulfill this idea, we analyze the time-series data sets, perform the statistical tests and find the significant difference between data sets with and without occupancy. In addition, we observe the change in data sets in using different types of sensors. Due to our limited time and budget, we were unable to create many devices to collect data, but through trial and error, we gained an understanding of the functions of occupancy detection and looked forward to what will come next. Our future work includes building more devices that consist of different sensors in collecting environmental data, using Received Signal Strength of WiFi, and predicting occupancy using machine learning models.

Introduction

- In building design and innovation, thermal comfort is an essential factor. Efficient regulation of thermal comfort can be achieved through incorporation and use of occupancy sensors. However, there are often difficulties in accurate detection of occupants therefore affecting proper auto regulation of occupants' spaces.
- In related work, researchers and investigators employed different types of sensors to gather information regarding possible occupancy, among which, a prevailing trend is the use of pre-existing environmental sensors such as CO_2 , light, humidity, and temperature sensors.
- These sensors are usually preinstalled or existing in modern buildings. Therefore, there's no need to build and deploy extra sensor devices.

Objectives

- Build IoT sensor systems to collect environmental data such as temperature and humidity, send it to the cloud, and analyze it.
- Investigate the feasibility of occupancy detection using different types of sensors.
- Perform statistical tests using a publicly available data sets for occupancy detection.

Methodology

- As part of the practical portion of our research we built sensor systems to log in humidity and temperature measurement of the device. This is still a developing area of tinkering and troubleshooting. Components and platform include:
  - ESP8266 Thing Dev Board
  - RHT03 Temperature and Humidity Sensor
  - ThingSpeak - an open-source Internet of Things application and API
  - Arduino IDE

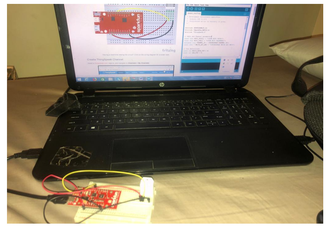

- Due to the time and budget limit, we couldn't gather enough sensor data. Instead, we analyzed publicly available data sets for occupancy detection. In particular we download a public data set from the UCI Machine Learning repository: https://archive.ics.uci.edu/ml/datasets/Occupancy+Detection+
- It is a standard time series data set for "Occupancy Detection" problem. It's a binary classification problem that using environmental factors (temperature, humidity, etc.) to classify whether a room is occupied or unoccupied.
- We use the following Python code to read the data:
  - Language: Python 3.7
  - Software: Jupyter Notebook
  - Python Libraries: Pandas, Numpy, Scipy

```
from pandas import read_csv
from pandas import concat
# load all data
data1 = read_csv('datatest.txt', header=0, index_col=1,
parse_dates=True, squeeze=True)
data2 = read_csv('datatraining.txt', header=0, index_col=1,
parse_dates=True, squeeze=True)
data3 = read_csv('datatest2.txt', header=0, index_col=1,
parse_dates=True, squeeze=True)
# vertically stack and maintain temporal order
data = concat([data1, data2, data3])
data.sort_index(inplace=True)
data.head(2)
```

Results and Further Tests

Table 1. Examples of the data format after preprocessing

	date	Temperature	Humidity	Light	CO2	HumidityRatio	Occupancy
2015 02 02 14:19:00							
2015 02 02 14:19:59							

- We obtain the sensor data for both occupied and unoccupied cases, where we sample the unoccupied data uniformly to get the same size as the occupied data.

```
for col in data.columns.tolist():
    if col == 'date' or col == 'Occupancy':
        continue

    df_yes = data.loc[data.Occupancy==1, [col]]
    df_no = data.loc[data.Occupancy==0, [col]].sample(len(df_yes))
    print("For {}:".format(col))
    print("# occupancy ={}, # non occupancy = {}".format(len(df_yes), len
(df_no)))
```

- We perform basic statistical test to the data sets.

```
print("mean of "+col + ": if occupany = {}; if no occupany = {}".format(ro
und(df_yes[col].mean(), 2), round(df_no[col].mean(), 2) ))
    print("p-value = {}".format(stats.ttest_ind(df_yes[col], df_no[col])
[1]))
    print("")
```

- The results show the mean value of data from different sensors and the p-value of the data set of two different cases (occupied and unoccupied) for each sensor type. The p-values are less than 0.05, which means the data sets from two cases are significantly different.

```
For Temperature:
# occupancy =4750, # non occupancy = 4750
mean of Temperature: if occupany = 21.98; if no occupany = 20.58
p-value = 0.0
For Humidity:
# occupancy =4750, # non occupancy = 4750
mean of Humidity: if occupany = 28.08; if no occupany = 27.57
p-value = 2.5401623755975177e-07
For HumidityRatio:
# occupancy =4750, # non occupancy = 4750
mean of HumidityRatio: if occupany = 0.0; if no occupany = 0.0
p-value = 1.790023208474221e-188
```

- We write the value of different sensors to separate text files for further analysis.

```
    df_yes.to_csv("data_for_student_same_size/" + col + "_occupany.txt", i
ndex=False, header=False)
    df_no.to_csv("data_for_student_same_size/" + col + "_no_occupany.txt",
index=False, header=False)
```

- We then use MATLAB to perform further analysis.

Temperature and Humidity Codes

```
clc
%pkg load statistics %make sure we have the statistics package to use the
test algorithms
%load the temperature data sets
t1=load("Temperature_occupany.txt");
t2=load("Temperature_no_occupany.txt");
s = length(t1); %the total number of the data from each set
% Find its mean and variance
m1 = mean(t1), v1 = var(t1),
m2 = mean(t2), v2 = var(t2),
figure(1),
plot(1:s, t1)
title('Temperature with occupancy')

figure(2),
subplot(2,1,1)
hist(t1, 50) %t100 represents number of bins
title('Temperature with occupancy')
subplot(2,1,2)
hist(t2, 50)
title('Temperature with no occupancy')
```

```
clc
%pkg load statistics %make sure we have the statistics package to use the
test algorithms
%load the temperature data sets
t1=load("Humidity_occupany.txt");
t2=load("Humidity_no_occupany.txt");
s = length(t1); %the total number of the data from each set
% Find its mean and variance
m1 = mean(t1), v1 = var(t1),
m2 = mean(t2), v2 = var(t2),
figure(1),
plot(1:s, t1)
title('Humidity with occupancy')

figure(2),
subplot(2,1,1)
hist(t1, 50) %t100 represents number of bins
title('Humidity with occupancy')
subplot(2,1,2)
hist(t2, 50)
title('Humidity with no occupancy')
```

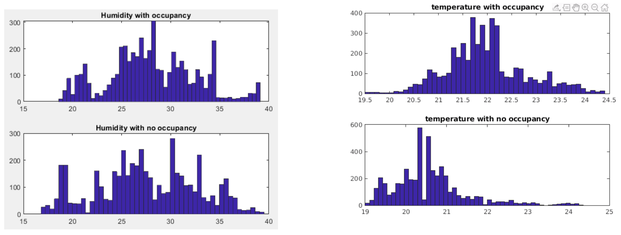

Figure 1. The histograms of the humidity and temperature data in both occupied and unoccupied cases

Conclusions and Future Work

- This preliminary work shows that there is a significant difference between the data sets with and without occupancy. Namely, the feasibility of using these non-traditional occupancy detection sensors is verified.
- Our future work includes building more devices that consist of different sensors in collecting environmental data, using Received Signal Strength of WiFi, and predicting occupancy using machine learning models.

References

[1] Cheng, Z., Jiang, C., Xie L., "Building occupancy estimation and detection: A review" Energy & Buildings, 2018; 2:260-270.
[2] Luis M. Candanedo, VÃ©ronique Feldheim, "Accurate occupancy detection of an office room from light, temperature, humidity and CO2 measurements using statistical learning models." Energy and Buildings, Volume 112, 15 January 2016, Pages 28-39.

Static Analysis of Structural Members

Amani Calderon, Alexis Villalona, & Farhad Alinaghizadeh

Department of Construction Management & Civil Engineering

Abstract

This research is devoted to statics analysis of structural members under mechanical loads. Static analysis of beams under uniform transverse mechanical loads is presented. The beams are supported by simply supported boundary condition at both sides. The equilibrium equation of the beams is obtained and solved using analytical method and numerical method. The numerical method employed in this work is generalized differential quadrature (GDQ) method. The type of differential quadrature method used for numerical solution is the polynomial-based GDQ method. The differential equation is discretized into algebraic equations based on the GDQ technique. The algebraic equations are then solved to obtain the deflections of the beam. The results of GDQ method are compared with the analytical solutions. It is found that the result of GDQ method are in good agreement with those of analytical solution which shows high accuracy of the GDQ method. Effects of material properties, geometrical property (cross section of beam), and mechanical loads on deflection of the beams is investigated.

Introduction

Beams are commonly used in different structures. Skeleton of buildings, body of airplanes, rails of trains, etc. are only few examples for applications of beams. The deflections of beams under external mechanical loads is important. The focus of this research is primarily a static analysis of a beams using numerical and analytical methods to obtain deflections.

The equilibrium equation is first obtained and solved by analytical method and numerical method. The generalized differential quadrature (GDQ) method is to obtain numerical solutions for deflections of the beams.

Background

A simply supported beam under a uniform distributed load, w (per unit of length) is considered as shown in the figure below. The equilibrium equation of the beam is as follows:

$$EI\frac{d^4y}{dx^4} = -w, \qquad (1)$$

Where E is modules of elasticity (for Aluminum is E= 70GPa), I is moment of inertia for a beam ($\frac{1}{12}$b*h^3), and L is length.

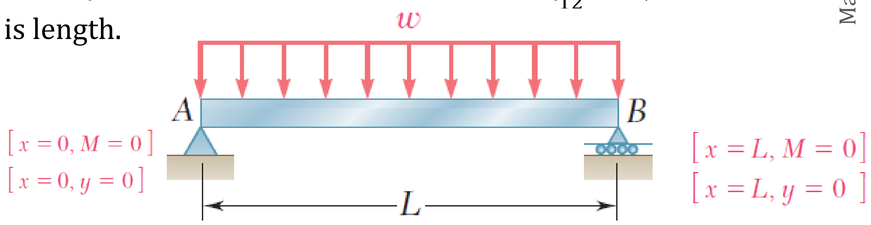

Analytical analysis

To solve the equation analytically, the integral of both sides are written as follows

$$EI\frac{d^3y}{dX^3} = V(X) = -\mathrm{wx} + \mathrm{C}_1 \qquad (2)$$

$$EI\frac{d^2y}{dx^4} = M(x) = -\frac{1}{2}wx^2 + C_1x + C_2 \qquad (3)$$

Carrying the values of C1 & C2 back into equation #3 and integrating twice will result in:

$$EIy = \frac{1}{24}wx^4 + \frac{1}{12}wLx^3 + C_3x + C_4 \qquad (4)$$

The constants C are obtained using the boundary conditions. Carrying the values of C3 &C4 into equation 4, results the equation of the elastic curve:

$$y = \frac{w}{24EI}(-x^4 + 2Lx^3 - L^3x) \qquad (5)$$

The maximum deflection is obtained by setting x= $^L/_2$:

$$|y|_{max} = \frac{5wL^4}{384EI} \qquad (6)$$

Numerical analysis

Based on the generalized differential quadrature (GDQ) method, the m-th order differential of a function can be written as [2] :

$$\left.\frac{d^m f(x)}{dx^m}\right|_{x=x_i} = \sum_{j=1}^{N} C_{ij}^{(m)} f(x_j), \quad i = 1, 2, \ldots, N$$

Where C are weighting coefficients. More information on calculation of the weighting coefficients can be found in Ref. [2].

Data Collections

Results for deflections of beams versus load are obtained and shown in the figures. The results are obtained for beams made of Aluminum E=70 Gpa, length L=1m, b=0.01m, and h=0.05m.

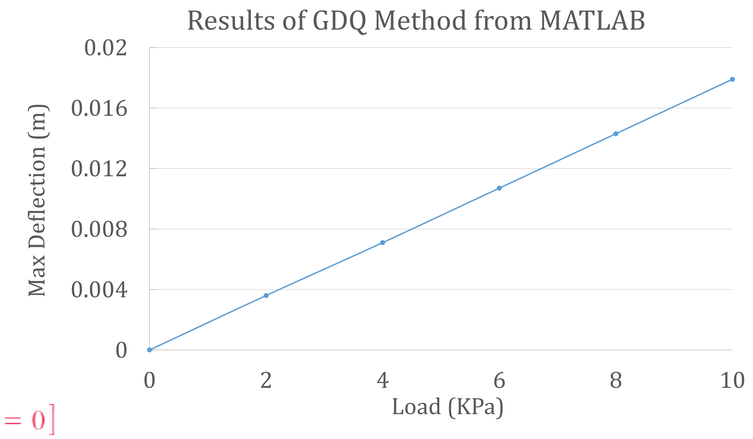

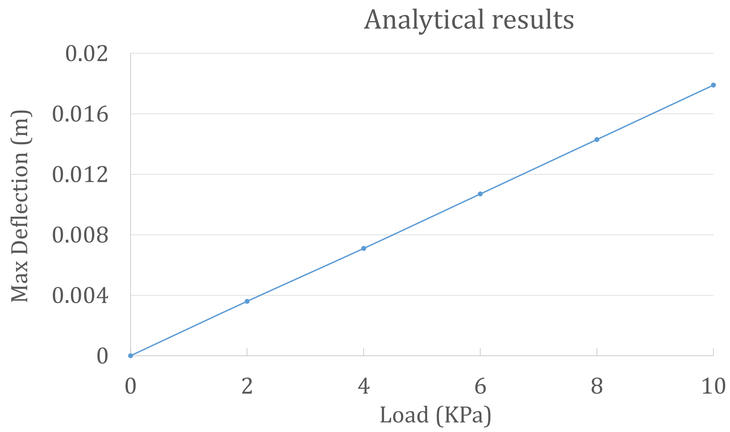

Data Analysis

In analyzing the results of the GDQ method, when compared with the analytical solutions, we found that the result of GDQ method are in close agreement with those of analytical solution. This shows high accuracy of the GDQ method.

Conclusions

The equilibrium equation of beam is obtained as the fourth derivative equation, $EI\frac{d^4y}{dx^4} = -w$. The equation is solved analytically and maximum deflection in the y axis is obtained as $|y|_{max} = \frac{5wL^4}{384EI}$. The equation is also solved used the GQDQ method. The analytical solutions of this equation are in good agreement with the result of GDQ method obtained from MATLAB code.

It is found that the deflection of the beams is depended on different parameters such as loads, material, and cross section of the beam.

References

[1] Beer, Ferdinand P., et al. *Mechanics of Materials*. McGraw-Hill Education, 2020.

[2] Moinuddin, Malik. *Differential Quadrature Method in Computational Mechanics: New Developments and Applications*. 1994.

Characterizing One of Tetrahymena thermophila Calpain Family Member, TTHERM_0047120

Collette Cameron, Prof. Ralph Alcendor, New York City College of Technology

Introduction

Genes and genome sequencing of an organism have knowingly contributed to the knowledge that is accessible on all different kind of species, which are either dead or alive. Tetrahymena *thermophila* genome has been sequenced but there is little evidence on the functionality of these genes, therefore the nucleotide sequences requires additional annotation and gene information.

Tetrahymena *thermophila* is a unicellular eukaryote which is larger than many mammalian cells that lives in fresh water including lakes, ponds and streams, and can be found almost everywhere, in a range of climates. T. *thermophila* consists of two nuclei with different functions. A somatic macronucleus and the diploid micronucleus is the germline. It has various genes and processes that are in common with multicellular organism. Some of the interesting aspect about the organism is that it has features that are precise to multicellular organisms; it exhibit a mouth-like and anus-like structures, a nervous system, and a digestive mechanisms that have a germline and somatic genome. Tetrahymena is a valuable system whose studies have led to valuable discoveries and insights into both conserved and divergent biological processes. The life cycle of Tetrahymena provides the opportunity to study factors important for different cellular processes. It's life cycle comprise of alternating haploid and diploid stages. The sexual stage of its life cycle is during conjugation. Tetrahymena is basically known as an organism that is easy to store alive for 6 months at low temperatures, short generation time (fast growing), cost efficient and very specific inducible promoters can be used for specific genes. Studying this distinctive organism can shed light on important cellular processes found in human beings and other eukaryotes.

Calpains are proteins belonging to the family of calcium-dependent, non-lysosomal cysteine proteases that is expressed in mammals as well as numerous organisms. They are found in several Eukaryotes such as humans, insect, fungus, bacteria, and nematode plant. They are also known as a modulator protease, which mean that it alters the protein substrates and a regulatory protein, which is known as a hybrid of two well-known proteins at the same time, the calcium-regulated signaling protein, calmodium and the cysteine protease of papaya, papain [4]. Hereditary studies show that the shortage of calpains can result in lethality, muscular dystrophies and gasthropathy. Calpains are involved in cell function, it aid with dilate blood vessels, regulating clotting, and skeletal muscle protein breakdown and memory. Human calpains are divided into two categories classical and non-classical. Classical calpains are on the C2L and PEF domains plus the CysPc domain whereas non-classical calpains exclude C2L and/or PEF domains and divide into several sub families. . Classical calpains are preserved in vertebrates and does not essentially reflect functional nor biochemical likenesses in humans. However, non-classical calpains are divided into subcategories for most eukaryotes: PalB, SOL and DEK1 subfamilies.

Objective/Hypothesis

Tetrahymena *thermophila* has about 27 calpains, however only little information is known about the protein. Thherefore, the purpose of this project was to begin characterizing one of T. *thermophila* calpain family member.

Methods and Materials

NCBI BLAST, BLASTP AND SMART BLAST

To identify the domain and conserved regions NCBI BLAST, BLASTP and Smart BLAST was used . Using Blastp from NCBI online, TTHERM_00471200 protein sequence was Blast against the database with parameters such as "protein Database bank" and "human taxid" to find homologs and similar structures from different organism families that can provide information of functional and evolutionary relationship.

Multiple Sequence Alignment Tools

Multiple sequence alignment is the alignment of two or more sequences either protein or nucleotide to find similarity of homology and evolutionary relationships. Alignment tools such as **T-Coffee, MUSCLE,** and **MAFFT** were used to align the full human calpain sequence with TTHERM_00471200 protein sequence. While T-Coffee and MUSCLE construct cladogram, **MEGA, Phylogeny.fr and MAFFT** has been used to construct a phylogenetic tree for evolutionary information. These tools were used to perform multiple sequence alignment and for evolution information.

MUSCLE

MUSCLE algorithm includes fast distance estimation, progressive alignment using a log expectation score and a refinement using tree dependent restriction partitioning. TTHERM_00471200 protein sequence was aligned with 15 human calpains on the online NCBI MUSCLE platform. The results showed that TTHERM_00471200 is closely similar with human calpain 7.

MEGA

MEGA is an integrated tool which is used for conducting sequence alignment, inferring phylogentic trees, and estimating divergentic times. TTHERM_00471200 protein sequence was aligned with 15 human calpains on the online MEGA platform. The results showed a maximum likelihood that TTHERM_00471200 is closely similar with human calpain 7.

Phylogeny.Fr

Phylogenetic tree shows the evolutionary relationship of different kinds of biological species that are believed to be homologous in some way. A phylogenetic tree was constructed using phylogeny.fr to identify the closely related human calpain to TTHERM_00471200. Based on the tree from phylogeny.fr, TTHERM_00471200 is more related to calpain 7.

Results

BLAST Results Using Amino Acid Sequences

Description	Max Score	Total Score	Query Cover	E value	Per. Ident	Accession
calpain 15 isoform X2 [Homo sapiens]	158	158	40%	8.00E-39	31.25%	XP_011520928.1
calpain 15 [Homo sapiens]	158	158	40%	8.00E-39	31.25%	NP_005623.1
calpain 15 isoform X4 [Homo sapiens]	158	158	40%	9.00E-39	31.25%	XP_011520930.1
calpain 15 isoform X1 [Homo sapiens]	158	158	40%	1.00E-38	31.25%	XP_011520922.1
small optic lobes homolog [Homo sapiens]	154	154	35%	1.00E-38	33.33%	AAH21854.1
calpain 15 isoform X3 [Homo sapiens]	158	158	40%	1.00E-38	31.25%	XP_011520929.1
calpain 12, isoform CRA_a [Homo sapiens]	139	139	39%	5.00E-34	32.28%	EAW56813.1
unknown [Homo sapiens]	138	138	43%	6.00E-34	31.27%	AAX82015.1
calpain 13, isoform CRA_b [Homo sapiens]	138	138	43%	6.00E-34	31.27%	EAX00492.1
calpain 13, isoform CRA_c [Homo sapiens]	138	138	43%	6.00E-34	31.27%	EAX00493.1

Table 1: BLAST results showing gene similarities between calpain found in humans and TTHERM_00471200.

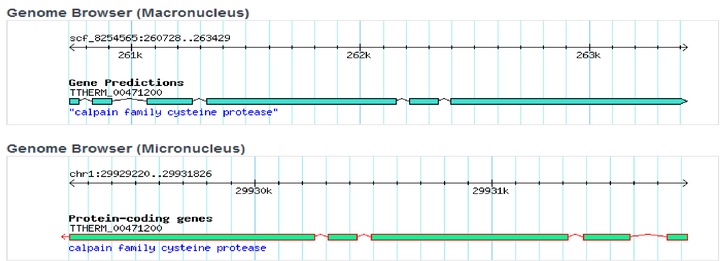

Figure 1. Gene Structure of TTHERM_00471200. Both Macronucleus and Micronucleus has 6 exons and 5 introns(ciliate.org).

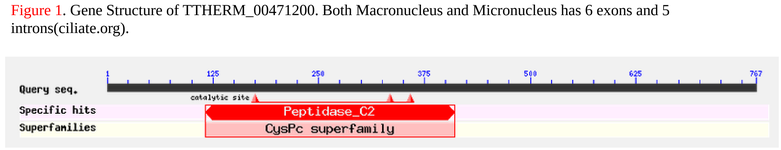

Figure 2. Query sequence and Superfamilies of TTHERM_00471200. Results showed the conserved domains (NCBI BLAST).

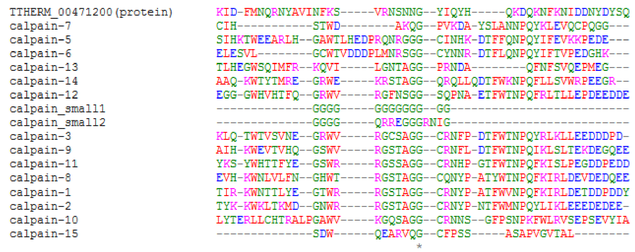

Fig 3. It shows that the G nucleotides in the column are identical in all sequences in the alignment.

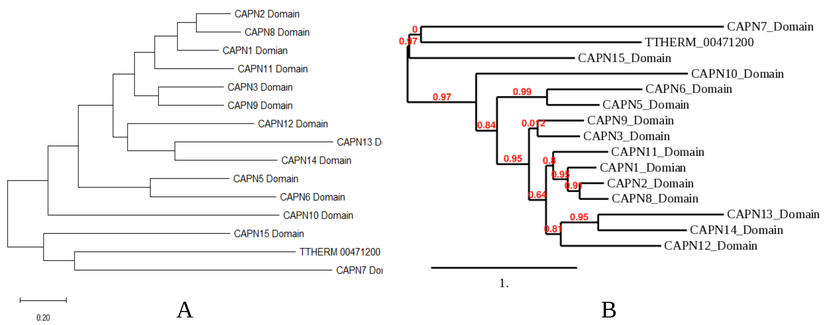

Figure 4: Phylogenic tree analysis. (A) MEGA results showing maximum likelihood, (B) Phylogeny.Fr. In both trees, TTHERM_00471200 is more closely related to human calpain 7

Summary of Results

- BLAST analysis showed TTHERM_00471200 to be more closely related to human calpain 15.
- Both macro and micro nuclei contain 6 exons and 5 introns.
- Like other calpains, TTHERM_00471200 has a CysPc conserve domain. It also contains a Peptidase_C2 domain, which is found in many other calpains.
- Multiple sequence alignment analysis using MUSCLE, T-Coffee and MAFFT showed very close similarity between TTHERM_00471200 and human calpain 15.
- Phylogenic tree analysis using MEGA and Phylogeny.fr show closer relationship to human calpain 7.

Conclusion

Results are inconclusive as to which human calpain TTHERM_00471200 is more closely related to. However, more analysis must be done to identify the human calpain TTHERM_00471200 is more closely related to.

Future Studies

More analysis is needed to identify which calpain is more closely related to TTHERM_00471200, whether it's calpain 15 or calpain 7. Analysis can include localization and protein structure comparison.

References

- Yandell, M., & Ence, D. (2012). A beginner's guide to eukaryotic genome annotation (Vol. 13). Salt Lake City, Utah: Department of Human Genetics, Eccles Institute of Human Genetics, School of Medicine, University of Utah. doi: Macmillan Publishing
- Collins, Kathleen et al. Current Biology , Volume 15 , Issue 9 , R317 - R318
- Ruehle, M.D., Orias, E., & Pearson C.G. (2016, June 01). Tetrahymena as a Unicellular Model Eukaryote: Genetica and Genomic Tools. Retrieved from http://www.genetics.org/content/203/2/649
- Suzuki, KYOKO. "Calpain Research Portal: Calpain Structure and Nomenclature." *Calpain Research Portal: Calpain Structure and Nomenclature*, calpain.net/.
- Calpainhttps://en.wikipedia.org/wiki/Calpain
- Calpains an Elaborate Proteolytic System
  In-text: (Calpains — An elaborate proteolytic system, 2017)
  Your Bibliography: Calpains — An elaborate proteolytic system. (2017).
- Huang, J., & Forsberg, N.E. (1998). Role of calpain in skeletal-muscle protein degradation. Proceedings of the National Academy of Sciences, 95(21), 12100-12105.
- "TGD |Tetrahymena Genome Database Wiki." *TGD* | Tetrahymena Genome Database Wiki, ciliate.org/

Acknowlegement

Special thanks to the Emerging Scholars program and the Office of Undergraduate Research at New York City College of Technolgy, and to my mentor Professor Ralph Alcendor.

Ball Catching with Omni-directional Wheeled Robot Utilizing Computer Vision and Neural Network

Mason Chen, Eric Martinez, Prof. Ali Harb

Department of Mechanical Engineering Technology

Abstract

The purpose of this experiment is to test the hypothetical efficiency and implementation of a computer-vision driven robotic system in order to recognize color coded object and autonomously catch them. This system will feature a PIXY2 camera, a derivative of the CMUCAM5 camera, which will detect objects of fairy uniform color distribution and shape. Utilizing an algorithm which will map out the Cartesian coordinates of the object in relation to the "center" of the camera, the robot will drive to the object. The algorithm was first developed on paper then programmed into Arduino IDE. The chassis for the robot was designed in Autodesk Inventor and 3D printed. Further research is required to develop the neural network with MATLAB. We also have plans to switch the PIXY2 camera with a standard webcam and utilize a Raspberry Pi to develop an algorithm that can detect a true ball rather than a round object.

Background

- Use of object recognition cameras have been an ever increasing trend in the journey of perfection for robotic automation.
- This is a relatively simplistic base algorithm but execution requires multidisciplinary skills in programming, mechanical engineering, and electromechanical design.
- Provided a long term project for developing object following computer vision systems.

Literature Cited

- "STRATASYS FORTUS 400mc." *Second Life*, https://www.multistation.com/second-life/product/stratasys-fortus-400mc/.
- "Documentation." *Wiki:v2:Overview [Documentation]*, https://docs.pixycam.com/wiki/doku.php?id=wiki:v2:overview.
- Bonceng. "Bloghaviza." *Bloghaviza*, 1 Jan. 1970, http://havizas.blogspot.com/2011/09/using-omni-wheel-with-servo-motor-this.html.
- Cherian, Aaron; Shanks, Sam. (2019). Optical Tracking and Recognition for Stage Robotics. Retrieved from the University of Minnesota Digital Conservancy, http://hdl.handle.net/11299/208708
- "CMUcam5 Pixy." Wiki - CMUcam5 Pixy - CMUcam: Open Source Programmable Embedded Color Vision Sensors, 2017.
- "Tutorial: Pixy (CMUcam5)." Physical Computing. IDeate, n.d. Web. 27 Apr. 2017.
- Pin, FG, Killough, SM. A new family of omnidirectional and holonomic wheeled platforms for mobile robots. IEEE T Robotic Autom 1994; 10: 480–489
- Jung, ML, Kim, JH. Development of a fault-tolerant omnidirectional wheeled mobile robot using nonholonomic constraints. Int J Robot Res 2002; 21: 527–539.

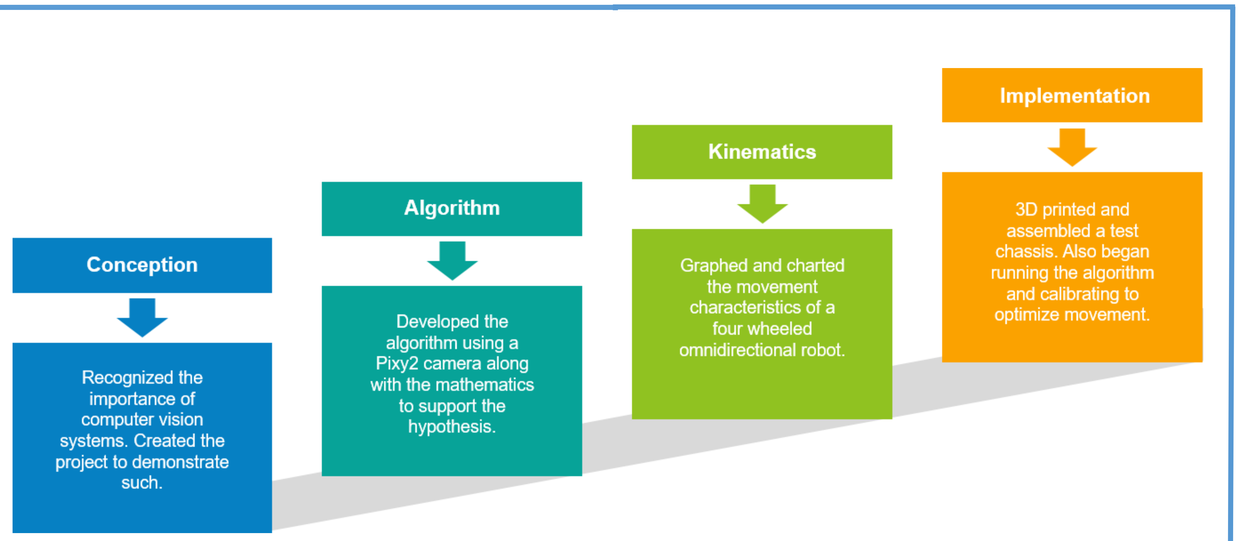

Fortus 400MC printer used

Pixy2 camera

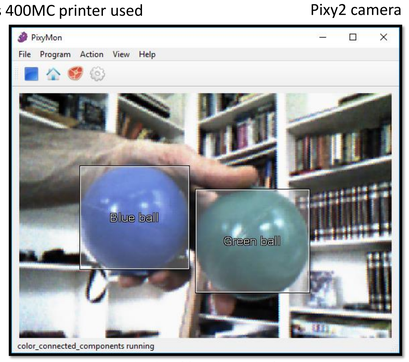

Pixy2 calibration window

```
void getval() {

  pixy.ccc.getBlocks();
  Serial.print(pixy.ccc.getBlocks());
  Serial.print('\t');
  if (pixy.ccc.numBlocks)
  {
    for (int i = 0; i < pixy.ccc.numBlocks; i++)
    {
      if (pixy.ccc.blocks[i].m_signature == 1)
      {
        A = pixy.ccc.blocks[i].m_width * pixy.ccc.blocks[i].m_height;
        sensorvalues[x] = (pixy.ccc.blocks[i].m_x) * (255.0 / 300.0);
        sensorvalues[y] = (pixy.ccc.blocks[i].m_y) * (255.0 / 200.0);

        Serial.print("A:");
        Serial.print(A);
        Serial.print('\t');
        Serial.print("X:");
        Serial.print(sensorvalues[x]);
        Serial.print('\t');
        Serial.print("Y:");
        Serial.print(sensorvalues[y]);
        Serial.print('\t');
        //Serial.print(pixy.ccc.blocks[i].m_signature);
        //Serial.print('\t');
      } else {
        sensorvalues[x] = 127;
        sensorvalues[y] = 127;
        A = 20000;
      }
    }
  }
}
```

Pixy2 sample portion Arduino code for obtaining center and area of object

Results

- The chassis was fully built and the initial object following algorithm correctly drove the robot in all directions until a predetermined area(of the object) was reached, signifying the ball has been caught in the receptacle.
- The robot had to repeatedly correct trajectory along a linear path. This is incumbent of an uncalibrated motor system.

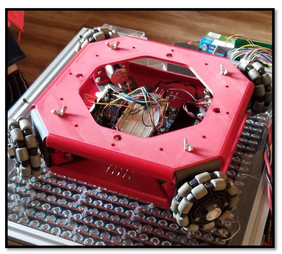

Completed chassis

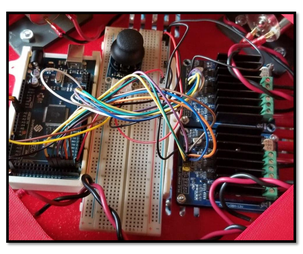

Some of the wiring(subject to change)

Chassis with receptacle

Conclusion

- Robot still requires calibration and the shift to webcam will greatly aid in correct ball detection software.
- Additionally, the motors have a RPM error of 10%, which is extremely difficult to compensate for. Precision DC motors or encoders will be a must for the future.
- Currently, the camera cannot distinguish a flat circular object from a ball.
- A regular webcam will allow the program to add an additional facet of perception- depth, which can be used to see distance topography of a spherical object.
- A chassis made from 5052 aluminum would be more cost and time effective.
- The Omniwheels were a huge success, allowing for all four motors to contribute to locomotion.

Future Research and Applications

- If the autonomous system can be perfected, a more efficient custom PCB board setup could be mass manufactured.
- Adding a second camera system for facial or RFID recognition in addition to a ball hopper/shooter could create a bot that will not only catch stray balls, but also fire them back for ease of use.

Tenniball, an autonomous ball collector

Acknowledgements

- This project supported by Emerging Scholar Program(ESP of NYCCT)
- Special thanks to Professor Andy Zhang, PhD
- Special to NYCCT 3D Printing Labs

Burnside-Pólya Counting Methods

Matthew Edelmann*, Meryem El Baz, Dahiana Jimenez*, Gabrielle Langston*

Mentor: Satyanand Singh Ph.D., Mathematics Department, New York City College of Technology, CUNY

Abstract

We will consider tic-tac-toe, permutation groups, Burnside Lemma, fixed points and stabilizers to perform computations on various sized tic-tac-toe board grids, as well as polygons. Our computations involve rotations, reflections, matrix visualizations, cycle indices and congruence classes. We will ultimately demonstrate that it is preferable to utilize the Burnside Pólya enumeration theory rather than ad hoc methods, because the theory reduces one's chance of error and is applicable for computations that involve large cardinalities, making ad hoc counting impractical.

Introduction

Tic-tac-toe is a beloved worldwide game that tests our strategic and problem-solving skills. In the game, two configurations are considered **congruent** if one can be obtained from the other through a reflection or rotation. This begs the question: what are the various configurations of the board given a fixed number of crosses and naughts (O's)? To help us with this question, we consider **congruence classes**, which are sets of all tic-tac-toe configurations. As a result, we set forth to solve the following problem: what is the number of different congruence classes among configurations with a fixed number of crosses and naughts? This problem is known as the **Congruence-Class Counting Problem (CCCP)**. It is important to note that congruence classes are not the same size, if that were the case, we could simply divide the total number of combinations by the uniform class size. We will demonstrate through various illustrations that the CCCP is not so simple.

Results

For a 3 × 3 tic-tac-toe board with two crosses and seven naughts, we found 2 unique configurations such that the congruence class has cardinality equal to two.

X	O	O
O	O	O
X	O	O

X	O	O
O	O	O
O	O	X

Each of these boards will only have 2 positions no matter how many times they are rotated.

Rotations:

The 3 × 3 board can be rotated by 90◦, 180◦, 270◦ and 360◦. These rotations can be can demonstrated by 2 × 9 matrices.

The 90◦ rotation:

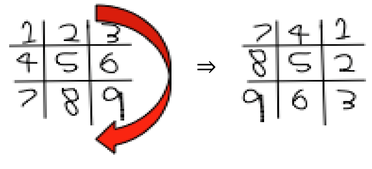

Results (cont.)

In 2 × 9 matrix form: $\begin{pmatrix}1&2&3&4&5&6&7&8&9\\3&6&9&8&5&2&9&6&3\end{pmatrix}$

The top row represents the original board and the bottom row represents the newly rotated board. For example, the top left corner originally had a 1 and after the rotation it had a 7.

For 180◦, 270◦, and 360◦:

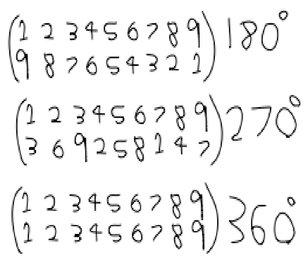

Inverses:

Using a 2 × n matrix, we found that the inverse of the 90◦ rotation of the 2 × 2 tic-tac-toe board is the 270◦ rotation.

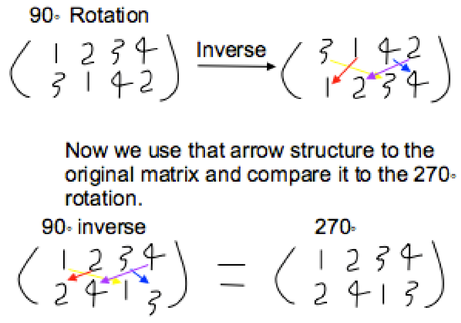

Reflections:

We were able to represent the four reflections on the 3 × 3 tic-tac-toe board by using 2 × 9 matrices.

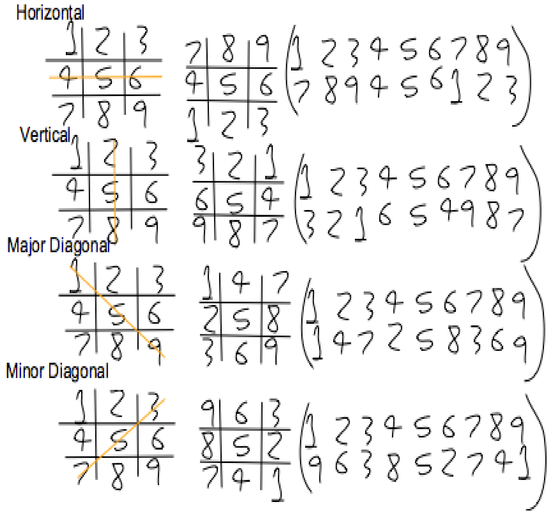

Results (cont.)

Example: Counting Number of Congruence Classes: 3 × 3 Tic-Tac-Toe

Number of possible arrangement of X's and O's: **512**

The **cycle index** is equal to the sum of the cycle structures divided by the group cardinality.

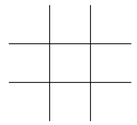

Cycle index: $\frac{1}{8}(t_1^9 + 4t_1^3t_2^3 + t_1t_2^4 + 2t_1t_4^2)$

If the board is filled, there are **102** congruence classes.

Substitute 2 for each t_r, because there are two markers, X and O.

Solving for CCCP:

Substitute $1 + x^r$ into the cycle index for each t_r.

$$\Rightarrow \frac{1}{8}((1+x)^9 + 4(1+x)^3(1+x^2)^3 + (1+x)(1+x^2)^4 + 2(1+x)(1+x^4)^2)$$
$$= 1 + 3x + 8x^2 + 16x^3 + 23x^4 + 23x^5 + 16x^6 + 8x^7 + 3x^8 + x^9$$

The coefficients of x^r are the number of congruence classes with r X's.

X	O	O
O	O	O
O	O	X

The coefficient of x^5 indicates that for a board with 5 X's (and 4 O's), there are **23** congruence classes.

Example: Equilateral Triangle

In the example of a Equilateral Triangle, we have three possible positions for rotations, and three possible reflections about an axis of symmetry:

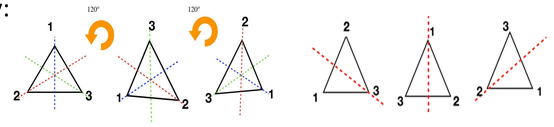

Conclusion

The Burnside-Pólya Counting Method was a method that attempted and succeeded in finding the unique combinations of 5 crosses and 4 naughts on a tic-tac-toe board. Although the answer was found (23) we wanted to expand on the solution. We found that different combinations of rotations and reflections were equivalent to each other as well as the number of unique combinations of new shapes such as the equilateral triangle. Going forward, we could examine other shapes and their properties in relation to this problem.

Acknowledgments

We would like to thank Professor Singh for his ongoing support and advisement. We would also like to thank the Emerging Scholars Program at City Tech for their support.

References

Gross, Jonathan L. "Burnside-Pólya Counting Methods." Applications of Discrete Mathematics, by John G. Michaels and Kenneth H. Rosen, McGraw-Hill, 1991, pp. 203–223.

* Students funded by Emerging Scholars Program

PART I: COMPARATIVE ANALYSIS BETWEEN NATURAL AND CERAMIC TEETH

Ibeth Erazo & Aneeza Hussain

Mentor Professor Daniel Alter

New York City College of Technology, Department of Restorative Dentistry, Honors Scholars Program, ESP, CRSP

ABSTRACT

The aim of this study is to attain a general understanding regarding the developments in the composition and indications of ceramics in dental applications. An in-depth analysis of the evolution this material has undergone during the last century in order to obtain esthetic and functional dental prosthesis that replace natural teeth when they are missing.

MATERIALS AND METHODS

- Selected articles from the PubMed database. Ten scientific articles were selected.
- Key words: natural teeth, dental materials, dental ceramics, ceramic restorations.
- Selection criteria: 2000 to 2019
- Experts consulted: Professor Daniel Alter CDT/MDT, Professor Avis Smith CDT, experienced Ceramists.

INTRODUCTION

Dental Ceramic materials have physical and optical properties that attempt to mimic the properties of natural teeth. The fabrication of ceramic restorations for every case is a complex process due to the particularities that natural teeth exhibit. Dental technicians must work ceramic materials with the purpose of obtaining natural colors aiming to achieve proper esthetics, as well as functionality and durability. Valuable data for ceramic systems is becoming increasingly available and results can be obtained with many commercial materials, providing guidance, regarding proper indications, in order to obtain successful results. However, dental technicians are responsible for processing restorations that meet the particular and desired characteristics for each case, because they are to make the best decision with regards to the use of different ceramic materials.

RESULTS

Natural Teeth

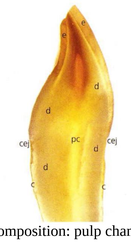

Figure 1. Tooth composition: pulp chamber (pc); enamel (e); dentin (d); cemento-enamel junction (cej); cementum (c)

Mature **enamel** is a **crystalline material**. Mature enamel is by weight **96% inorganic material, 1% organic material, and 3% water**. This crystalline formation consists mainly of **calcium hydroxyapatite/Ca10(PO4)6(OH)2**. CO3, Mg, K, Na, F are present in smaller amounts. The **ribbon-like crystals** of enamel are set at different angles throughout the crown area, each 30% larger than those in dentin. Enamel can endure crushing pressure of around **100,000 pounds per square inch**. Enamel appears **radiopaque (or lighter)**. Enamel alone is various shades of bluish white, which is seen on the incisal ridge of newly erupted incisors, but it turns various shades of yellow-white elsewhere because of the underlying dentin.

Mature **dentin** is a **crystalline material**. Mature dentin is by weight **70% inorganic material, 20% organic material, and 10% water.** This crystalline formation of mature dentin mainly consists of **calcium hydroxyapatite/Ca10(PO4)6(OH)2.** Small amounts of other minerals, such as carbonate and fluoride, are also present. The crystals in dentin are **plate like in shape.** Dentin also has **great tensile strength**, providing an elastic basis for the more brittle enamel. Because of the translucency of overlying enamel, the dentin of the tooth gives the white enamel crown its underlying **yellow hue**, which is a deeper tone in permanent teeth. Dentin appears more **radiolucent (or darker)**.

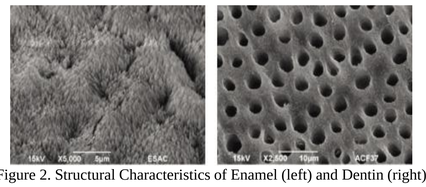

Figure 2. Structural Characteristics of Enamel (left) and Dentin (right)

Ceramic Teeth

Dental ceramics are characterized by their refractory nature, hardness, chemical inertness, biocompatibility and susceptibility to brittle fracture. They are usually referred as nonmetallic, inorganic structures primarily containing compounds of oxygen with one or more metallic or semi-metallic elements like aluminum, calcium, lithium, magnesium, phosphorus, potassium, silicon, sodium, zirconium & titanium.

Physical And Mechanical Properties. Ceramics and glasses are brittle, which means that they display a high compressive strength but low tensile strength and may be fractured under very low strain (0.1%, 0.2%) dental ceramics have disadvantages mostly due to their inability to withstand functional forces that are present in the oral cavity. The structure of porcelain depends upon its composition, surface integrity and presence of voids.

Table 1. Physical and Mechanical Properties of Dental Ceramics

Compressive strength	330 MPa
Diametral tensile strength	34 MPa
Transverse strength	62 - 90 MPa
Shear strength	110 MPa
MOE	69 GPa
Surface hardness	460 KHN
Specific gravity	2.2–2.3 gm/cm^3
Thermal conductivity	0.0030 Cal/Sec/cm^2
Thermal diffusivity	0.64 mm^2/sec
Coefficient of Thermal expansion	12 × 10-6/°C

Classification Of Dental Ceramics. Microstructure and Translucency are the two classifications to consider and focus on. However, dental ceramics classifications interrelate.

Table 1. Physical and Mechanical Properties of Dental Ceramics

CLASSIFICATION OF CERAMIC BASED MATERIALS	
Uses or indications	e.g. anterior, posterior crown, veneer, post and core, fixed prosthesis, ceramic stain, glaze
Composition	ceramics that are predominantly composed of glass, those made of particle-filled glass, and those consisting of polycrystalline
Principal crystal matrix phase	silica glass, leucite-based feldspathic porcelain, leucite-based glass ceramic, lithia disilicate-based glass-ceramic, leucite disilicate-based glass-ceramic, aluminous porcelain, alumina, glass-infused alumina, glass-infused-spinel, glass-infused alumina/zirconia
Processing method	casting, sintering, partial sintering and glass infiltration, slip casting and sintering, hot isostatic pressing, CAD-CAM milling and copy milling
Firing temperature	High-fusing (1,300°C), medium-fusing (1,101°C to 1,300°C), low-fusing (850°C to 1,100°C), and ultra-low-fusing (< 850°C)
Microstructure	**amorphous glass, crystalline, crystalline particles in matrix**
Translucency	**opaque, translucent, transparent**
Fracture resistance	Low, medium, hard
Abrasiveness	Comparison relative to enamel, against tooth enamel

Classification by Microstructure. At the microstructural ceramics are defined by the nature of their composition of glass-to-crystalline ratio. Ceramics can be broadly classified as non-crystalline (Amorphous Solids or glasses) and Crystalline ceramics. They can be broken down into four basic compositional categories, with a few subgroups:

1. Composition category 1 – glass-based systems (mainly silica)
2. Composition category 2 – glass-based systems (mainly silica) with fillers
3. Composition category 3 – crystalline- based systems with glass fillers
4. Composition category 4 – polycrystalline solids (alumina and zirconia)

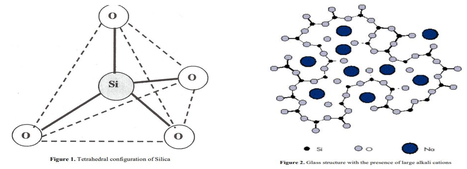

Figure 3. Dental Ceramics Based on Their Microstructure: (1) predominantly glass; (2) particle-filled glass; and (3) fully polycrystalline.

Classification by Translucency. A natural tooth derives most of its color as a result of the light reflectance from dentin that is altered by absorption and scattering by the enamel. Several factors affect the translucency of dental ceramics. Thickness of the material has the greatest effect, but translucency can also be affected by the number of firings, the shade of the substrate, and the type of light source or illuminant. Porcelain translucency is usually measured with the translucency parameter. or the contrast ratio (CR). The chemical nature, size, and number of crystals in a ceramic matrix will determine the amount of light that is absorbed, reflected, and transmitted compared with the wavelength of the source light.

Figure 4. Relation Between Translucency and Opacity

All teeth that are naturally covered by the enamel present opalescence. In ceramic systems, opalescence has been responsible to solve aesthetic problems making possible to produce unnoticeable restorations. The correct reproduction of opalescence involves careful observation of adjacent teeth and the selection and application of opalescent in appropriate locations.

Figure 5. Central Incisors Opalescence. Under Reflected Light (left). Under Transmitted Light (right)

Fluorescence is a luminescence phenomenon. Tooth fluorescence is usually associated with a blue-white chromatic appearance caused by the incidence of the UV wavelength. Under natural light, fluorescence makes teeth more luminous and shinier, giving them an internal luminescence. The incidence of UV wavelengths in a tooth restored with nonfluorescent material causes metameric failure and is responsible for highlighting the restorative material. Fluorescence must be present in restorative materials to obtain natural-looking results.

Figure 6. Central Incisors Fluorescence. Under Daylight (left). Under Black Light (Right)

DISCUSSION

The natural tooth section on the right is 0.55mm thick. From this cross section, it is easy to see the optical complexities of tooth structure. The feldspathic ceramic cross section on the left is 1.5mm thick. This cross section shows the different layers of material that are necessary to mimic natural teeth. The sample in the center is a replica of the left sample. It is made from monolithic zirconia. The zirconia cross section shows the optical challenges the dental technician faces when using this material to match teeth. Light scattering within homogenous monolithic materials makes the replication of teeth very difficult. Monolithic materials have gained in popularity, but present many esthetic challenges.

Figure 7. Natural Tooth Cross Section (Right). Fieldspathic Cross Section (Center). Zirconia Cross Section (right)

A shade value is taken when integrating tooth-colored restorative materials or artificial teeth or crowns within an individual dentition. The goal is to match the color of the patient's surrounding natural teeth as closely as possible. The optical properties of new generation porcelains mimic more closely the interaction of the natural dentition with light. The "illusion of reality" is developed by carefully blending opalescence, fluorescence, and translucency given by the composition of the dental ceramics to be used when fabricating ceramic prosthesis.

CONCLUSION

Dental ceramics is a material group that would continue to play a vital role in dentistry due to their natural esthetics and biocompatibility. However, there will always remain a compromise between esthetics and biomechanical strength. In order to achieve adequate mechanical and optical properties in the final porcelain restoration, the amount of glassy phase and crystalline phase has to be optimized. Good translucency requires a higher content of the glassy phase and good strength requires a higher content of the crystalline phase. For this reason, the two material phases need to be balanced. Success of the ceramic restoration depends on the collaborative work between dental clinicians and technicians and their ability to select the appropriate material to match intraoral conditions and esthetic demands.

REFERENCES

- P. Jithendra Babu, Rama Krishna Alla, Venkata Ramaraju Alluri, Srinivasa Raju Datla, Anusha Konakanchi, and Anusha Konakanchi, "Dental Ceramics: Part I – An Overview of Composition, Structure and Properties." American Journal of Materials Engineering and Technology, vol. 3, no. 1 (2015): 13- 18. doi: 10.12691/materials-3-1-3
- Srinivasa Raju Datla, Rama Krishna Alla, Venkata Ramaraju Alluri, Jithendra Babu P, and Anusha Konakanchi, "Dental Ceramics: Part II – Recent Advances in Dental Ceramics." American Journal of Materials Engineering and Technology, vol. 3, no. 2 (2015): 19-26. doi: 10.12691/materials-3-2-1.
- Fluorescence of natural teeth and restorative materials, methods for analysis and quantification: A literature review. Claudia Angela Maziero Volpato, Mario Rui Cunha Pereira, Filipe Samuel Silva, J Esthet Restor Dent. 2018 Sep; 30(5): 397–407. doi: 10.1111/jerd.12421
- Vaarkamp J., ten Bosch J. J. & Verdonschot E. H. (1995) Propagation of light through human dental enamel and dentine. Caries Research 29 (1) 8-13.
- Johnston W. M. Review of Translucency Determinations and Applications to Dental Materials. Journal of Esthetic and Restorative Dentistry 2014; 26; 217-23.
- Arcus Laboratory. "The Optical Properties of Teeth". 2015. http://www.arcuslab.com/the-optical-properties-of-teeth/
- Gilbert Jorquera, Nicole Merino, Stephanie Walls, Eduardo Mahn and Eduardo Fernández (2016) Simplified Classification for Dental Ceramics. J. Dent. Sci. Ther 1(2): 22-25. doi: https://doi.org/10.24218/jdst.2016.09
- Kelly JR. Dental ceramics: what is this stuff anyway? J Am Dent Assoc. 2008;139(suppl):S4-S7.
- Powers JM, Sakaguichi RL. Craig's Restorative Dental Materials. 12th ed. St. Louis, MO: Mosby Elsevier; 2006:454.
- Denry I, Holloway JA. Ceramics for dental applications: a review. Materials. 2010;3(1):351-368.

Voice Controlled Augmented Reality: A Comparison of Speech-Recognition Tools for AR Applications

Student: Juan Estrella | Advisor: Benito Mendoza

Computer Engineering Technology Department

Abstract

Our research project focuses on exploring the **Integration of Artificial Intelligence (AI) in Augmented Reality (AR) applications.** Specifically on using **Speech Recognition** or Natural Language Processing **for controlling virtual AR objects and enhancing the human-computer interaction**. We present an empirical study that compares currently available alternatives for **creating an AI Bot to implement voice controlled systems**. We selected the alternative that meets the criteria of openness, usability, easy integration, and cost.

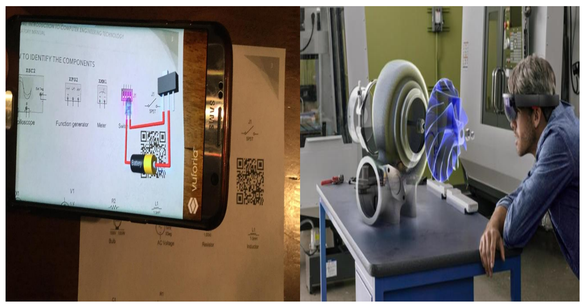

Materials and Methods

To build this app we integrated the following technologies:

- **Unity**: A Video Game Engine to create the virtual elements.
- **Vuforia:** An AR Software Development Kit (SDK) for projecting virtual objects.
- **Wit.ai**: A natural language API and cloud service capable of turning spoken sentences into structured data.

With the combination of these three applications, we can deploy this voice controlled app on Apple iOS, Android, and Windows AR Devices such as the HoloLens.

unity + vuforia

wit.ai

Watson Speech to Text

Google Cloud Speech API

moz://a deep speech

android iOS Windows

Introduction

- **AI** has the potential to benefit society in the realms of manufacturing, medicine, security, entertainment, marketing, and many others.
- A subfield of **AI** is **Natural Language Processing** and **Speech Recognition**; making computers understand what humans say and mean.
- **AR** refers to the technologies that superimpose digital content, generated by computers, over the user's view of the real world.
- AR applications for industrial use such as manufacturing, and equipment maintenance, inspection, and repair are in experimental phase.
- There has not been a **breakthrough** in industrial applications of AR. On one hand, the technology is new, and on the other hand, the software developing tools are limited in scope.
- An AR application could be significantly served by incorporating AI into it.
- However, for developers, it is difficult to find an entryway for incorporating AI into AR apps.

1. A Wit.ai Bot is trained with samples of sentences that will be used as commands.
2. During the training entities, intents, and other elements used to create structured data are identified.

Structured Data
```
intent = weather forecast
when   = April 22, 2019
place  = Palo Alto, CA
```

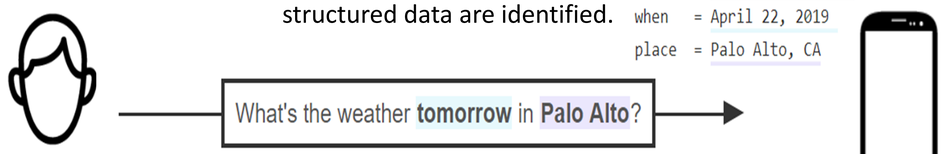

3. Once the Bot reaches high recognition confidence level, it can be used.

wit.ai

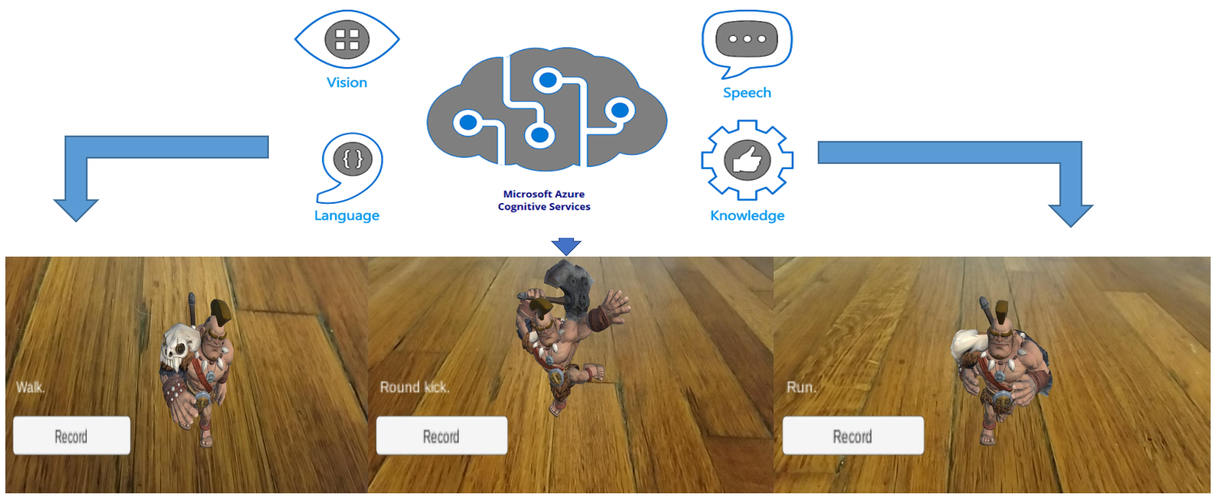

Discussion

- **AI and AR seem ideally suited to one another**. In fact, AR relies on AI to be effective (computer vision is a subfield of AI and AR relies on it).
- AI has a vital role to play in the construction of intelligent **adaptive interfaces**. **Object recognition and tracking, and gestural input**.
- **Eye tracking** and **voice commands** as a means for manipulating the virtual environment, are the **close following steps**.
- Next step, **speech recognition,** including classification and **language translation.**
- **The tread of harnessing AR and big data** to breed new interesting applications **is starting** to have a tangible presence. For example, some apps are incorporating real-world object tagging and advanced data visualization.
- We believe **AI will enable AR interfaces to become truly multidimensional**; this will generate a whole new layer of perception.

Our Work

- We present **an AR application** in which an online **AI Bot process user's commands to control the behavior of a Barbarian character.**
- The technology in this app can be used on a wide range of **Internet Of Things** apps such as monitoring systems, medical, marketing and advertisement, entertainment, etc.
- In manufacturing settings, this technology has the potential to increase work performance; workers could command machines to do several tasks while they work on something else.
- We explored different alternatives for implementing the AI Bot: Googles Cloud Speech to Text, Microsoft Speech Cognitive Service and IBM's Watson Speech API. However, they all come at a high cost to use for the general public.

Results and Conclusions

- Microsoft Azure provides a 12-Month free account with $200 Credit on any of its services for 30 days. The Barbarian currently transitions to certain commands such as "Walk.", "Round Kick." and "Run." Azure is Multi-Platform.
- Watson's and Google's Speech API's start free but is expensive per use overtime. Mozilla DeepSpeech is accurate on transcribing voice to text but its based on Python Language. Unfortunately these services are not currently available to be integrated with Unity.
- Wit.ai is a free and straightforward cloud service owned by Facebook. Wit.ai is integrated with Unity with the use of scripts that trigger specific animations based on the structured data returned by the AI Bot, as a result of converting speech sentences to structured text.

References

- Nahal Norouzi, Gerd Bruder, Brandon Belna, Stefanie Mutter, Damla Turgut, and Greg Welch. "A Systematic Review of the Convergence of Augmented Reality, Intelligent Virtual Agents, and the Internet of Things." Book chapter in Artificial Intelligence in IoT, Fadi Al-Turjman Editor. Springer International Publishing, 2019

Acknowledgements

- Undergraduate Research Program
- CUNY Research Scholars Program
- GRTI 20 Grant, Project 4 "The AREngEd Project: Augmented Reality for Engineering Education"

Summer, 2019

Mechanical Characterization of Nano-material Doped Polydimethylsiloxane (PDMS)

Deldrys Gomez, Ozlem Yasar, Ph.D.

City University of New York, New York City College of Technology, Department of Mechanical Engineering Technology

ABSTRACT

In recent years, Tissue Engineering is utilized as an alternative approach for the organ transplantation. Success rate of tissue regeneration influenced by the biomaterials, cell sources, growth factors and scaffold fabrication. Design and precise fabrication of scaffolds are required to support cells to expand and migrate to 3D environment.

In this project, dog-bone shaped PDMS testers are fabricated at the Research Laboratory SET in the Department of Mechanical Engineering Technology. Tensile tests are performed to investigate the mechanical properties of the PDMS. Similar procedure are also repeated for the nanomaterial doped PDMS to investigate the effects of nanomaterials on the mechanical properties of PDMS.

Our preliminary results indicate that engineered scaffolds' mechanical properties can be improved with nanomaterials.

INTRODUCTION

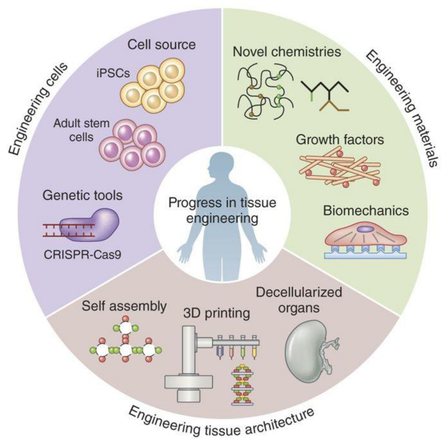

Figure 1. Cell growth on scaffolds

Tissue Engineering is an interdisciplinary field that applies the principles of engineering and life sciences toward the development of biological substitutes that restore, maintain or improve tissue function or whole organ.

This utilizes scaffold matrices to fill the tissue void, to provide structural support and to deliver growth factors and/or cells that have the ability to form tissues within the body upon transplantation.

METHODOLOGY

Molds:

A dog-bone shape mold is designed on Inventor and then 3D printed in order to prepare the testers.

Another alternative we are implementing is to use silicon molds instead of the 3D printed ones in hopes of getting a better surface finish on the specimens created.

Polydimethylsiloxane:

In this research, a thin layer of PDMS solution was prepared by mixing curing agent and base in 10:1 ratio.

Then they were baked in the oven in different temperatures.

Fully solidified PDMS samples will be studied to investigate the toxicity rates. Then, INSTRON Machine will be use to do the compressive tests for PDMS mechanical characterizations.

Fig 2. PDMS Mixing curing agent and Base

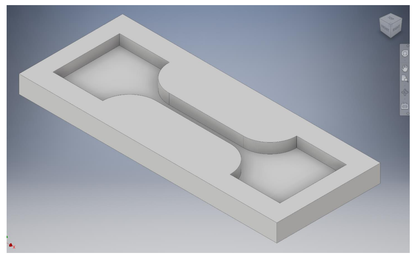

Fig 3. Computer-aided Dog-Bone mold

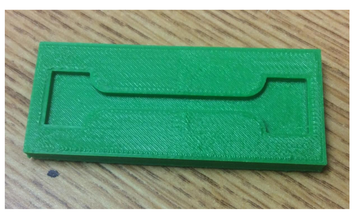

Fig 4. 3D printed Dog-Bone mold

Fig 4. 3D printed Dog-Bone and silicone molds

The silicone mold was made with a 1:1 mixture of Smooth-On Silicone that was poured into the 3D printed mold and left to cure for six hours.

RESULTS

Each sample was placed between two parallel compression platens, attached to a universal materials testing machine (3369, Instron, Canton, MA). Each sample was compressed at a rate of 5 mm/min until failure, which was defined as the catastrophic fracture of the sample.

The preliminary results showed that the specimens doped with nanomaterials were stronger than those composed only of PDMS.

Currently we are working on the improvement of the molds in order to create a sample with better surface finishes than the ones previously obtained.

CONCLUSION

Tissue Engineering has achieved remarkable success. However precise fabrication of tissue scaffolds always has been a challenge. Our preliminary results indicate that engineered scaffolds' mechanical properties can be improved with nanomaterials.

REFERENCES

- Yasar, O and Starly B. "A Lindenmayer System-Based Approach for the Design of Nutrient Delivery Networks in Tissue Constructs.Biofabrication I (2009) 045004

- Suh, J.-K Francis, and Howard W.t Matthew. "Application of Chitosan-based Polysaccharide Biomaterials in Cartilage Tissue Engineering: A Review."Biomaterials 21.24 (2000): 2589-598. Web. 13 Aug. 2014

ACKNOWLEDGEMENTS

The Authors would like to thank the City University of New York, New York City College of Technology's Dean's Office, and CUNY Research Scholars Program and acknowledge all the previous alumni students in the Scaffolds For Engineered Tissues Laboratory.

Entertainment Connection

Author: Conny Gordon Mentor: Tamrah Cunningham CUNY New York City College of Technology

Abstract

We have developed Entertainment Connection as a website to gather and consolidate information related to the entertainment industry. Entertainment Connection consists of the development of a contributory web application to display and gather information on the Entertainment Industry, as well as to vet users for students. The goal of the website is to create the foundation for a web-based directory of existing jobs within the field. We have designed Entertainment Connection because existing options lack necessary infrastructure. The directory is meant to advise students and career seekers on jobs that are available, and the steps required to achieve those jobs. This is important because there are countless opportunities awaiting those who are in search for their next journey. A directory of what exists, what's to come, and how to accomplish what's needed will help to digitally keep a record of all of those who take the time to create. Also as part of its purpose, the website seeks to engage the general public, including interested professionals and scholars, by incorporating a roster. The "Stay Connected" page will consist of verified workers in case users who come across our website need to be further assisted with questions pertaining to a certain job. As a secondary purpose, the web application was developed to be replicable by others who might choose to take and adapt to Entertainment Connection for their own career-related purposes.

Method

In order to fulfill our vision of Entertainment Connection being a web-based directory, as well as an engaging site for the general public, we held a beta test for students of the ENT tech major at the Voorhees building. In this beta test, we allowed students to get first hand experience with the website thus far to get a better grasp of the information currently available is useful. Alongside using the website, we also curated a small list of questions to help further get insight that will help us improve on the website.

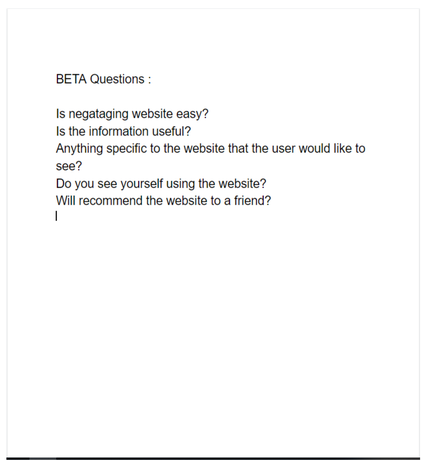

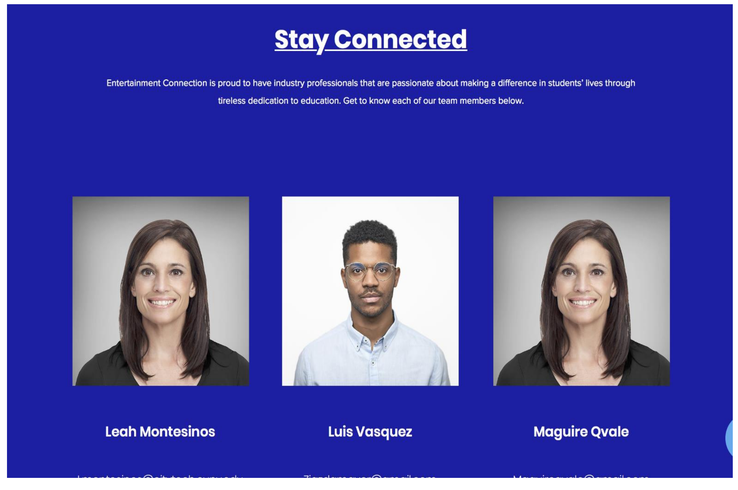

Introduction

As students get closer to the finish line they tend to worry less about courses and more about their careers. Some at this point start to wonder if they are taking the right course of action to land the dream job. Being students in the entertainment department exploring and developing skills in all aspects of the field students quickly realize that there is a lot of information the schools website and department is missing. One of the most important keys to success is essentially knowing where to begin. Of course, the school is a great start… for students, but what about for employees? Developing an online advisement to fill the gap that would bridge together the transformation of student to worker seemed to be the perfect fit. As researchers we reached out to students and faculty members by creating surveys and collecting data. We branched out two different surveys, one focusing on the wants of the current students in our department and the other focusing on the experience and knowledge gained from our professors while they were undergoing the same change of student to professional. The results lead us to develop a resourceful tool where all students questions can be answered. Entertainment Connection gives students the opportunity to explore jobs in the industry, their educational factors, and even has a roaster to connect new and old industry members.

Results

Beta Question:	Summary:
Is navigating the website easy?	The site is manageable but can be greatly improved if things like a "scroll to top" button, table of contents like things are implemented.
Is the information useful?	The information given was found useful but there could be some parts that could offer more insight. For example, be able to click on a job in the directory and taken to another site where they could apply.
Anything specific you would like to see on the website?	Making the job titles clickable as mentioned above, a search bar to allow for specific/faster find, job descriptions instead of just job requirement and more clickable buttons to make navigating easier
Do you see yourself using the website?	The majority have said yes, but have raised question on if it they would do it consistently.
Will recommend the website to a friend?	The majority said they would recommend the website, especially after the improvements

Conclusion / Discussion

Getting feedback from students was very helpful to Entertainment Connection in order to make the website more alluring and useful to the public. The information from the students was very vital since they are the kind of demographic that our website is aiming towards. With their help we can help provide more useful features, better information layout, site navigation and more. Now that we have knowledge of where Entertainment Connection is lacking, we can start making the changes that will make the website better.

-City tech website and Course Catalog - CIS. "Welcome to the Department of Entertainment Technology." *Our Children's Center (OCC) - City Tech*, www.citytech.cuny.edu/entertainment/.
-Professors
- Survey Website - "The Versatile Data Collection Tool for Professionals | Typeform." *Free Beautiful Online Survey & Form Builder | Typeform*, www.typeform.com/product/?tf_campaign=brand_1473009320&tf_source=google&tf_medium=paid&tf_content=58633583713_282120556037&tf_term=typeform&tf_dv=c&gclid=Cj0KCQiAuf7fBRD7ARIsACqb8w7F1BRbYFYpi9Y-QMSmgwTQ4Jbiz1V0hisNA_0KXgeyOjV_-3tBXeoaAiY5EALw_wcB.

-Undergraduate Research
-Computer System Technology Department
-CUNY Research
-Entertainment Department
-ENT Professor Matt Warden
-New York City College of Technology
-Professor Tamrah D. Cunningham

Creation In Art, Architecture, And Geometry Wrapped In Origami

Oliver Hadi

Professor Anne Leonhardt &
Professor Satyanand Singh

Abstract

Origami has been around for centuries known as the art of paper folding. In the 20th century, this ancient art form found its way to applications in the fields of engineering, medicine, and other sciences. We will take a closer look at how origami can be integrated and used as a problem-solving tool in the field of architecture. Our main focus will explore the potentials of origami through tessellations of parallelograms. The target of application will be an interchangeable ceiling that folds like a “Herringbone Tesselation” and alters both the aesthetics and acoustics of the space that it is applied to. The goal of this dynamic application would be to accommodate different needs at different times within the same space. For example: an educational space that at times promotes noise reduction for reading and acoustical enhancement for theater practice. We will make explorations through digital and physical modeling as well as following mathematical principles to identify the limitations and explain the movements of the proposed design.

Precedent

RVTR architects conducted a research on the topic in 2011. “Resonant Chamber”, as the project was called, was developed through an iterative process both as a digital model as well as a full-scale physical prototype. The prototype consisted of electronics, reflector, electro-acoustic and absorptive composite panels. The origami-based design allowed the movement of the panels using hydraulic hinges on the back face edges.

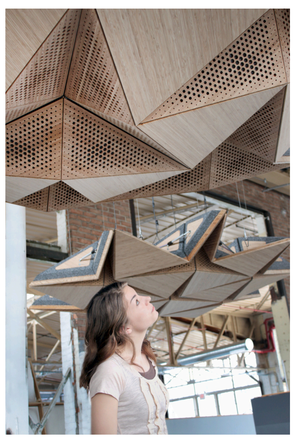

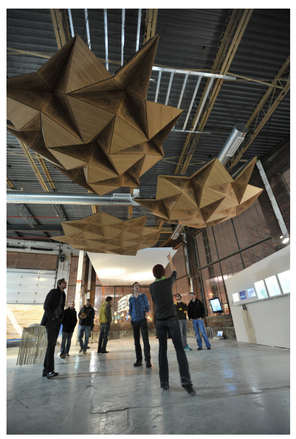

Methods

Rhino 6.0 was used as the primary digital model space and the tessellation was achieved through the Grasshopper plugin and Kangaroo add on. With this software, we can create, adjust and observe the visual outcome of the tessellation in digital space. The Grasshopper uses a parametric language that requires inputs and domains to generate outputs. In the case of the tessellation, by altering the inputs in real-time, the outputs create a visual animation that imitates the movement of the geometry as if it was one sheet of paper folding and flattening at its creases.

Grasshopper algorithm chain layout

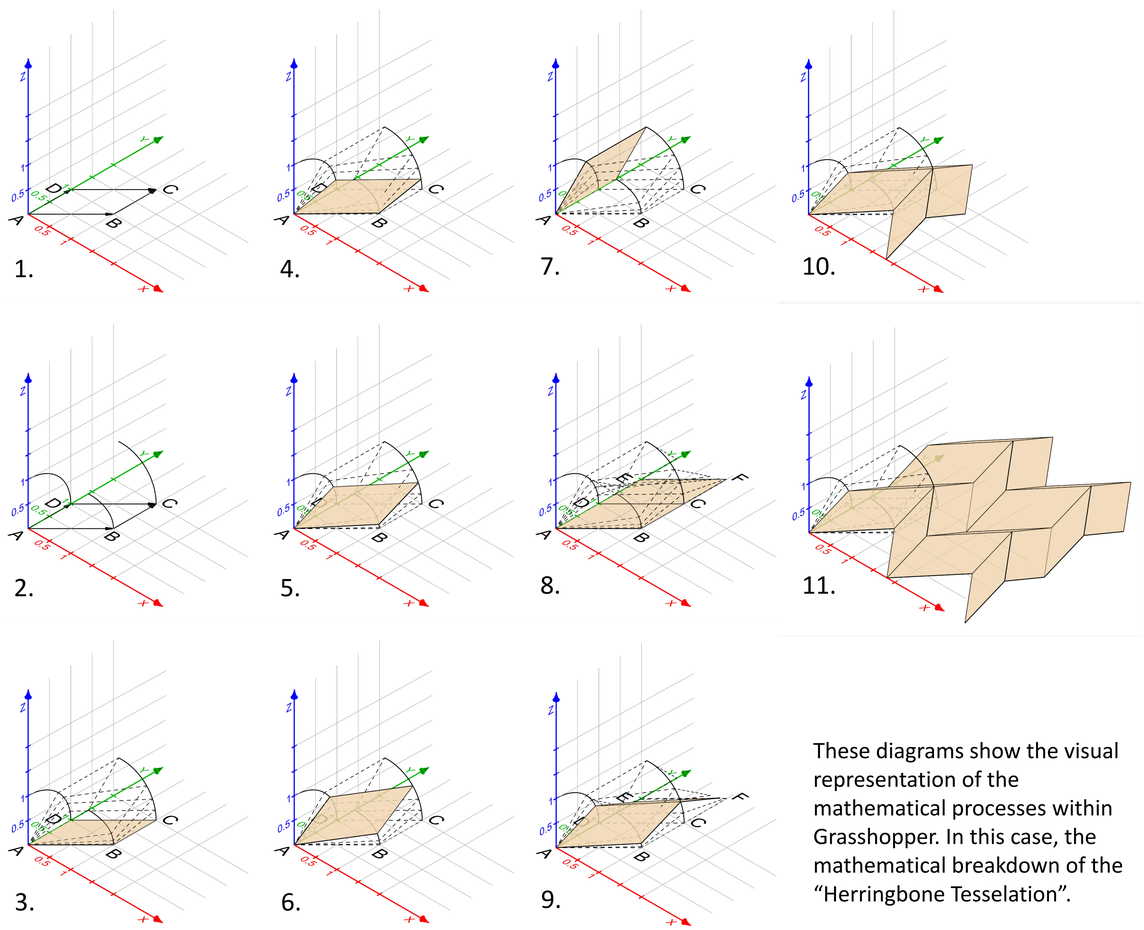

These diagrams show the visual representation of the mathematical processes within Grasshopper. In this case, the mathematical breakdown of the “Herringbone Tesselation”.

Mathematical Break-down

1. -Point “A” is defined as “0” in x, y and z directions.
   -Vectors are used to locate 3 other points to capture a parallelogram on the x-y plane.
2. Two trajectory curves are defined as the path for points “B” and “D” to follow during the folding process. The curve path for point “C” is just a reference, since the parallelogram remains the same, it does not need to be constrained further.

3-7. The surface of the parallelogram is created based on the 4 points. It then shows its corners moving along their trajectories as the parameters of the geometry remain constant.

8. Points “A” and “B” are mirrored on plane “CD” and create points “E” and F”
9. The 2 surfaces are sharing a line “CD” and it acts as the folding edge between them.
10. The two folding surfaces are mirrored on plane “BF” and complete 1 module of the tessellation.
11. The module can be arrayed in a continuous, rectangular manner.

Application Of Design

The investigated ceiling geometry would have the ability to move by employing hydraulic hinges attached at the folding edges of each individual panel. Because of its repetitive fashion, the origami geometry can change by the number, the size, and the shape of the modules to accommodate any ceiling. Besides the aesthetic qualities, the changing angles and directions of the panels can enhance the acoustical performance, therefore can be fitting for theatre and music performance spaces.

Rendering backgrounds done by Studio Gang.

Summary

With today’s technologies, traditional origami paper folds can easily be transformed into real-life applications. To fully understand the function of an architectural feature as the origami ceiling, there are many aspects to consider from acoustics, lightning, structural properties, material, etc. However, using parametric design allows us to analyze and iterate any given project to ensure high efficiency. That alone may result in savings in the construction phase of a project.

References

- Precedent article + images from https://www.archdaily.com/227233/resonant-chamber-rvtr
- Theatre space renderings from https://studiogang.com/project/writers-theatre
- Grasshopper geometry was recreated from https://www.youtube.com/watch?v=MTQtPs2xcRk

Doctor-patient Communication and Patient Continuity of Care: A Mixed-methods Study of Primary Care Services in NYC

Kavita Hariprashad and Professor Noemi Rodriguez (Mentor)
Department of Health Sciences, CUNY New York City College of Technology
Honors Scholars & Emerging Scholars Program

Abstract

Continuity of care is a vital component of patient health status. Doctor-patient communication is basic to the continuity of care. Data is sparse regarding up-to-date surveys done in New York. This study looked at the outcome of patient continuity of care through the survey of patients treated in primary care settings by primary care physicians in New York City. A mixed-methods survey was carried out using validated Likert scales to assess the correlation between doctor-patient communications and dimensions of continuity of care. Surveys were distributed via Google Forms to 20 adult participants whom resided in New York City. Participants were predominantly Non-Hispanic with the majority being 25-44 years of age. Correlational analysis showed a significant negative correlation between the Doctor-Patient Communication variable and Dimensions of Continuity of Care. Importance of the link between family medicine and patient care in the delivery of primary care services is stressed as a means for productivity within the healthcare system spectrum.

Introduction

Continuity of care is defined as carrying out an uninterrupted plan of care with a single physician instead of multiple physicians (Haggerty et.al., 2012).

Primary care services is the stepping stone towards continued care within the healthcare delivery system. A disconnect in communication between primary care physicians and patients can lead to disruptions in ongoing care health needs. According to a Patient Continuity of Care questionnaire given in 2008 to orthopedic patients in family care units, over 50% of patients reported they did not feel their caregiver gave them enough information to continue their healthcare regimen (Biem, et.al, 2008). Effective communication among primary care physicians and patients have been shown to help with symptom alleviation, positive clinical outcomes, better patient behaviors, and medication compliance (Bosson, et. Al, 2018). This is highly critical in the primary care setting, where primary care visits have been on a decline among adults. The most recent data indicates a drop of 18% between 2012-2016 (Frost & Hargraves, 2018). As a result, the investigation of doctor-patient communication in continuity of care is vital to ongoing health service delivery in primary care settings.

Methods

Participants

- ✓ Total of **20 participants (19 utilized for quantitative analysis)**
- ✓ **100% New York Residents** of diverse racial backgrounds
- ✓ Ages ranged from **18 to 64 years old** (mean of 37 years)
- ✓ Gender composition is **45% male** and **55% female**
- ✓ Marital Status: **45% single**, **45% married** & **10% In a Domestic Partnership**
- ✓ **70%** reported being **employed**; remaining **30%** were **students, retired or unable to work**
- ✓ **80%** with a high school diploma, some college credits or a Bachelors Degree
- ✓ **20%** held a Masters degree level or higher

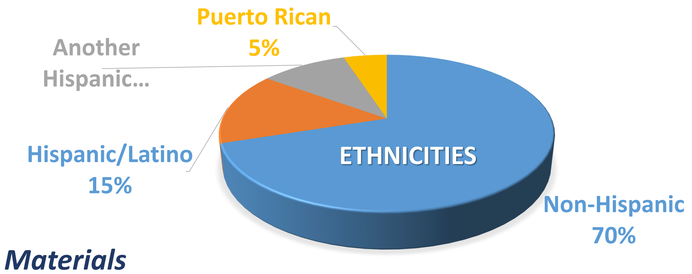

Materials

- For the **Doctor-Patient Communication Test**, an ordinal scale (4-Point Likert scale) of a range of 1 (Yes) to 4 (No) was used to evaluate participants' view of how satisfactory their primary care physicians communicated with them during consultation visits. This survey was used as a behavioral measure to assess whether the primary care physician's communication methods led to discontinuity of care.
- For the **Continuity of Care Test,** an ordinal scale (5-point Likert scale) of a range of 1(Definitely True) to 5 (Definitely False) was used to evaluate part one (the care process) and range of 1 (Agree Strongly) to 5 (Strongly Disagree) was used to evaluate part two (dimensions of continuity). This survey was used as both an affective and cognitive measure to see whether a patients' feelings and knowledge of their care led to care process continuation.

Results

A Pearson Correlation was computed using SPSS software (version 23) to assess the relationship between Doctor-patient Communication (variable 1) and Continuity of Care (variable 2). There was a **negative correlation** between the two variables, with the Continuity of Care variable composed of 2 parts: Care Process [r=-0.245, n=19, p=0.311] and Dimensions of Continuity [r= -0.552, n=19, p=0.014]. As the score for Doctor-patient communication goes up (from yes to no) alternatively the care process goes down as well as the continuity of care. **It should be noted there was a greater, and significant correlation for Dimensions of Continuity in relation to the Care Process.** There was one qualitative response given by a participant who did not have or chose not to have a primary care physician, stating that the reason for not being involved with the primary health system is due to the fear of the accumulation of monetary debt.

Discussion

The main objective of this study was to determine if there was a correlation between Doctor Patient Communication (independent variable) and Continuity of Care (dependent variable). It was hypothesized that less satisfaction with communication between primary care physicians and patients would lend to disruptions with the continuation of care in the delivery of primary care services. The **results did not support the hypothesis. I**t was discovered that a decrease in doctor-patient communication leads to an increase in care process agreement and more perception of continuity of care. This finding was in line with other literature that mentions "patients may report being satisfied with each [physician]visit but still not feeling that they have established a sense of trust"(Thom et. al., 2004). One reason for this could be ethnicity differences among physicians and patients, which has been shown to play a major role in continuity of care with a single primary care physician (Nwabueze & Nwankwo, 2016). This suggests that other factors in the doctor-patient dynamic beyond communication influence continuity of care.

Conclusion

In conclusion, the study carried out with New York City participants gave a more thorough, detailed insight into the two components of the continuity of care aspect of the delivery of primary care health services. The identification of the dimensions of continuity of care being more significant than the care process itself shows that we need to find more ways in which patients can learn to trust their primary care physicians even though satisfactory doctor-patient communication is valuable to care outcomes. The notion of an increased doctor-patient communication leads to a decrease in trust, a major component of the dimensions of continuity, can be explained by differences of trust within ethnicities. This calls for further investigation by ethnicities of physician and their patients using a larger sample to identify trust and doctor-patient communication to better understand why in this study continuity of care scores decreased as communication satisfaction increased.

Acknowledgments

I would like to express special thanks of gratitude to my mentor Professor Noemi Rodriguez for her guidance, time and support in the completion of the research survey process.

References

Beaulieu, C., Breton, M., Freeman, G., Haggerty, J.L. & Roberge, D. (2012). Validation of a Generic Measure of Continuity of Care: When Patients Encounter Several Clinicals. *Annals of Family Medicine Journal*, *10*(5): pp. 443-451. Retrieved https://www.ncbi.nlm.nih.gov/pubmed/22966108

Biem, H., Bourgault-Fagnou, M., Hadjistavropoulos, H., Janzen, J., & Sharpe, D. (2014). Patient Perceptions of Hospital Discharge: Reliability and Validity of a Patient Continuity of Care Questionnaire. *International Journal for Quality in Health Care*, *20*(5): Pps 314-323. Retrieved https://doi.org/10.1093/intqhc/mzn030

Bosson, J., Foote, A., Gauchet, A, Gilbert, C., Kernou, A., Sustersic, M. & et al. (2018). A Scale Assessing Doctor-Patient Communication In A Context Of Acute Conditions Based on Systematic Review. *PLOS One Journal 13*(2): e0192306. Retrieved https://psycnet.apa.org/record/2018-15709-001

Chokshi, D.A., & Ladapo, J. (2014). Continuity of Care for Chronic Conditions, Threats, Opportunities, and Policy. *Health Affairs Journal*: No pps. Retrieved https://www.healthaffairs.org/do/10.1377/hblog20141118.042672/full/

Frost, A. & Hargraves, J.(2018, November 15). *Trends in Primary Care Visits*. Health Care Cost Institute. Retrieved https://www.pcpcc.org/2018/11/15/trends-primary-care-visits

Hall, M.A., Pawlson, L.G. & Thorn, D.H. (2004). Measuring Patients' Trust In Physicians When Assessing Quality of Care. *Health Affairs Journal*, *23*(4) : No pps. https://doi.org/10.1377/hlthaff.23.4.124

Nwabueze, C. & Nwankwo, N.N. (2016). Ethnicity and Doctor-Patient Communication: An Exploratory Study of University of Abuja Teaching Hospotal, Nigeria. *Society of Participatory Medicine Journal*, *8(1)*: E12. Retrieved https://participatorymedicine.org/journal/evidence/research/2016/10/07/ethnicity-and-doctor-patient-communication-an-exploratory-study-of-university-of-abuja-teaching-hospital-nigeria/

Sensor Implementation of an Assistive Technology Mobile Robot

Author: Jannat Hoque -- Mentor: Professor Farrukh Zia

Computer Engineering Technology Department

ABSTRACT

HeathKit Educational Robot (HERO-1) is a robotic educational tool that has been helping colleges and universities across the country teach students about Computer and Robotics Technology since the 1980s. The HERO-1 model at City Tech went into hibernation after 15 years of service. Currently, three students from the CUNY Scholars Research Program, including myself, are reviving City Tech's HERO to provide new features by updating the computer hardware and software technology, such as mobile robot obstacle detection and navigation and speech synthesis and recognition. The two most common modern devices that are used for mobile robot obstacle detection and navigation are ultrasonic sensor using sound waves and infrared sensor using light waves. The main difference between the IR sensors and Ultrasound sensors is that IR sensor detects electromagnetic radiation and the Ultrasound sensors detect mechanical energy. By learning and comparing the advantages and disadvantages with testing and technical specifications of the two devices, we implemented them on a mobile robot to test their effectiveness in real world situations. Both the IR and Ultrasound sensors performed as expected. In the future, a script of servo motor and ultrasonic sensor will be tested and replace the old hardware device in the HERO robot. This will allow HERO to continue teaching students at City Tech. Another interesting benefit of updating HERO's technology is that it will enhance the implementation of Assistive Technology to enable her to help people with disabilities. For example, we are planning to work on connecting HERO to a Bluetooth voice recognition device to replace the remote control panel. This part of experiment was tested for people who need help with vision by producing speech output.

INTRODUCTION

Ultrasonic sensors are made to detect an object's proximity or range using ultrasound reflections to calculate the time it takes to reflect ultrasound waves between the object and the sensor. An ultrasonic sensor measures the distance from the sensor to the object by using sound waves. The ultrasonic sensor measures the distance from the object to the sensor by sending a sound wave at a specific frequency and listening for the sound wave to reflect back, by recording the elapsed time between the sound wave reflecting back and the sound wave that is generated. Ultrasonic distance sensors that uses IR proximity sensor is a photovoltaic sensor that detects Infra-Red light. The Infra-Red light stays outside of the electromagnetic spectrum and is invisible to the human eye. The main difference between the Ultrasound sensors and IR sensors is that IR sensor detects electromagnetic radiation and the Ultrasound detecting mechanical energy . The DHT11 is a digital temperature and humidity sensor. It uses a capacitive humidity sensor and a thermistor to measure the surrounding air, and output a digital signal on the data pin.

ELECTRICAL CIRCUIT

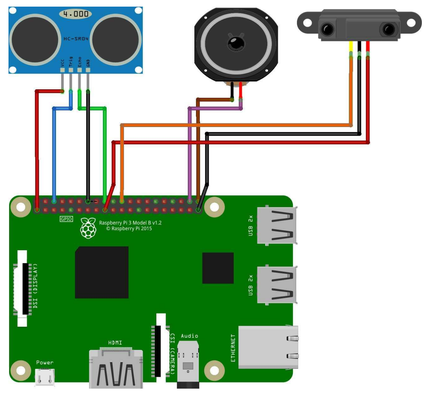

GP2Y0D02YK0F

Distance Measuring Sensor Unit
Digital output (80 cm) type

ACKNOWLEDGEMENTS

Emerging Scholars Program 2019

METHOD

The robot HERO is being upgraded with hardware circuits and features. Since this project was a group project my part was to test all the sensors. Modern hardware devices and sensors will be added and tested to implement assistive technologies that will help people with disabilities. Speech synthesis and recognition and sensors are being tested with Raspberry Pi and by using the installed sensor script and the speech program, combine both to detect and speak about the obstacles.

CONCLUSION

This is a three part project that we are improving an old version of robot to help people who are blind and with many other disabilities. For this research project we tested the HC-SR04 (Distance sensor) and the DHT-11 (Temperature sensor) using Arduino installed programming. The sound sensor was tested using raspberry pi. We tested the modern hardware, using Arduino, C++ Programming, Raspberry Pi, and a modern embedded computer that runs Linux with an SD card and is used for voice synthesis and recognition.

REFERENCES

Felix. "Using a Raspberry Pi distance sensor (Ultrasonic sensor HC-SR04)." *Raspberry Pi Tutorials*, 11 Nov. 2015, tutorials-raspberrypi.com/raspberry-pi-ultrasonic-sensor-hc-sr04/.

HC-SR04 Ultrasonic Range Sensor on the Raspberry Pi. (2017, November 10). Retrieved November 29, 2017, from https://www.modmypi.com/blog/hc-sr04-ultrasonic-range-sensor-on-the-raspberry-piNedelkovski, Dejan . "Ultrasonic Sensor HC-

SR04 and Arduino Tutorial." *HowToMechatronics*, 22 Sept. 2017, howtomhttp://www.sharp-world.com/products/device/lineup/data/pdf/datasheet/gp2y0d02yk_e.pdf

Spectroscopic study of the Interaction of multi-target compounds with DNA

Baljit Kaur and Alberto Martinez
Chemistry Department, New York City College of Technology
285 Jay St, Brooklyn, NY 11201

Abstract

As the basic genetic material of life, and because of its key role in cell replication, DNA plays a fundamental role in cell replication. In addition, the activity and potential toxicity of drugs might be related to the mode and the intensity with which those external compounds interact with the biomolecule. For these reasons, medicinal chemists have been traditionally interested in gaining insights on drug-DNA interaction as a way to understand the mechanism of action, as well as toxicity, of compounds of therapeutic value. Our group is currently working on the design, synthesis and primary testing of multi-target polyphenols as potential anti-Alzheimer's disease agents. As part of our ongoing biological investigation on these compounds, we have determined the binding mode as well as binding affinity of a multi-target polyphenol (AM20) by using fluorescence and UV-visible titrations, and we have compared the results to clioquinol used as control. The results show that both compounds form permanent adducts with DNA with binding affinities in the range of 10^4 – 10^6 M^{-1} and one binding site. In conclusion, we have gained insights into the pharmacological profile of a compound with promising potential in the anti-AD therapeutic scheme.

Introduction

As the basic genetic material of life, and because of its key role in cell replication, DNA is a particularly good target for antiviral, anticancer and antibiotic drugs. In line with this, there is an increasing interest in studying the interaction of potential drug candidates with DNA. Furthermore, the activity and potential side effects of many drugs depends on the mode and the intensity with which they interact with this biomolecule. Therefore, gaining insights on drug-DNA interaction is crucial for the understanding of the mechanism of action, as well as toxicity, of compounds of therapeutic value. Our group is currently working on the design, synthesis and primary testing of ionophoric polyphenols as potential anti-Alzheimer's disease (AD) agents. These compounds have shown promising potential against important aspects related to AD. **Our goal is to use spectroscopy analysis to measure the DNA binding properties of a polyphenols and clioquinol used as reference (Figure 1).**

On the other hand, AM20 ((E)-4-(((2-hydroxynaphthalen-1-yl)methylene)amino)benzene-1,3-diol) is a multi-target polyphenolic compound that shows promising ability to fight important aspects commonly associated to AD, such as amyloid-β aggregation, reactive oxygen species, or toxic concentrations of Cu^{2+} ions.

Clioquinol is a hydroxyquinoline initially developed as antifungal and antiprotozoal agent that has also shown activity against vital and protozoal infections. Importantly, clioquinol completed phase II clinical trials against Alzheimer's disease because of its ability to chelate toxic concentrations of metal ions that are typically associated with the progression of the disease.

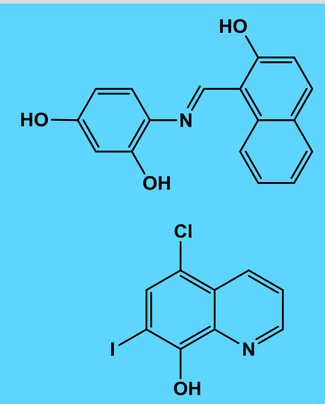

Figure 1: Molecular structure of the tested polyphenol AM20 (top), and clioquinol (bottom).

Methods

UV Visible Titrations:
Samples were prepared in a UV-visible cuvette containing 2 mL of test compound solution by adding 1990 µl of Tris/HCL (5 mM) buffer at a pH of 7.4, 10 µl of clioquinol or AM20 from a 5 mM solution (25 µM working concentration of the corresponding drug), and the additions of 10 µL of CT DNA (340 µM). Prior to each addition of CT DNA, the sample was incubated for one minute before measuring absorption. This was repeated for a total of 15 titrations.

Fluorescence Titrations:
Samples were prepared in a fluorescence cuvette containing 1948 µL of Tris/HCL buffer, at a pH of 7.4, 50 µL of DNA, and 2 µL of Acridine Orange 5 mM (2.5 µM working concentration of AO), then incubated for 5 minutes. Then, 3.4 µL of the drug under study were added from a 5 mM stock solution and allowed to incubate for 1 minute before fluorescence was measured. This was repeated for a total of 15 titrations

Results

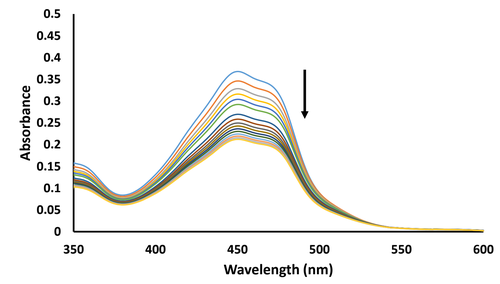

Figure 2: UV-visible titrations of AM20 with CT DNA

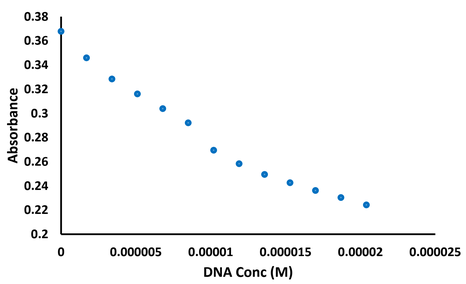

Figure 3: Decay of absorbance at 450 nm upon consecutive additions of DNA

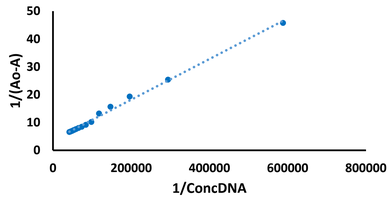

Figure 4: Binding affinity plot for AM20 with CT DNA

$$\frac{1}{A_0 - A} = \frac{1}{A_0} + \frac{1}{K\ x\ A_0\ x\ C_{DNA}}$$

K = Binding affinity
C_{DNA} = concentration of DNA

Chemical Compound	Fluorescence Titrations			UV-Visible Titrations
	n	K (M^{-1})	Ksv (M^{-1})	K (M^{-1})
AM20	1.11 (±0.10)	1.76 E+06 (±1.81E+06)	2.95 E+04 (±1.11E+04)	3.41E+04 (±0.38E+04)
Clioquinol	1.29 (±0.29)	3.43E+06 (±4.71E+06)	6.06E+04 (±2.12E+04)	N/A

Table 1: Stern-Volmer constants (K_{sv}), number of binding sites (n), and binding affinity for each compound (K).

Figure 5: Fluorescence titrations of CT DNA with AM20 and clioquinol

$$\log\frac{F_0 - F}{F} = \log K_b + n\log[M]$$

K_b = Binding affinity
n = number of binding sites

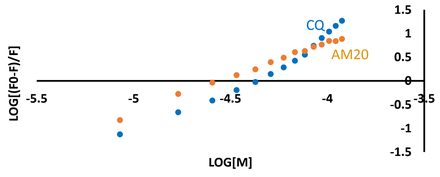

Figure 6: CT DNA binding affinity plot for AM20 and clioquinol

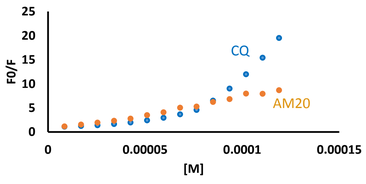

Figure 7: Stern-Volmer plot for AM20 and clioquinol

$$\frac{F_0}{F} = 1 + K_{sv}[M] = 1 + k_q\tau_0[M]$$

τ_0 = lifetime of fluorophore
K_{sv} = Stern-Volmer constant
k_q = Bimolecular quenching constant

Conclusions

- Analysis of the UV-visible spectroscopic data for clioquinol and AM20 showed binding affinities in the range 10^4 to 10^6 M^{-1}.
- UV-visible data could not be collected for clioquinol due to interferences with DNA absorption at 260 nm.
- Fluorescence experiments confirmed the interaction of both AM20 and clioquinol with DNA by forming permanent adducts through one binding site.
- The results presented by both experiments suggest that both AM20 and clioquinol have the potential to interact with DNA.

Acknowledgments

Special thanks to the Emerging Scholars Fall 2019 Program, NYCCT Chemistry Department for supporting and facilitating this project, and Professor Alberto Martinez

References

i. Martínez, A., Alcendor, R., Rahman, T., Podgorny, M., Sanogo, I., & McCurdy, R. (2016). Ionophoric polyphenols selectively bind Cu2+, display potent antioxidant and anti-amyloidogenic properties, and are non-toxic toward Tetrahymena thermophila. *Bioorganic & Medicinal Chemistry*, *24*(16), 3657-3670. doi: 10.1016/j.bmc.2016.06.012
ii. Salahudeen, M., & Nishtala, P. (2017). An overview of pharmacodynamic modelling, ligand-binding approach and its application in clinical practice. *Saudi Pharmaceutical Journal*, *25*(2), 165-175. doi: 10.1016/j.jsps.2016.07.002
iii. Zhang, S., Sun, X., Jing, Z., & Qu, F. (2011). Spectroscopic analysis on the resveratrol–DNA binding interactions at physiological pH. *Spectrochimica Acta Part A: Molecular And Biomolecular Spectroscopy*, *82*(1), 213-216. doi: 10.1016/j.saa.2011.07.037

A Preliminary Health Study Across Student Population; Comparison Between Sexes and Ethnic Groups.

Dianna Khass, Department of Biological Sciences and Professor Niloufar Haque, Department of Biological Sciences

285 Jay Street, Brooklyn NY 11201

Abstract

The human body is comprised of trillions of cells. Each cell group has a unique structure and function that differentiates them from one another. The combination of cells results in the formation of tissues, organs and organ systems. The human body is made up of different organ systems that have the ability to carry out a specific function. It is hypothesized that the present lifestyle among the different genders and ethnicities of the participants will impact their physical functions and present a risk to the individuals health. Our age and lifestyle affects our physiological functions. Our health, nutrition and lifestyle is a major contributor of how our body responds in health and disease conditions. It is necessary to maintain our health such as our weight, body mass index, food consumption, the number of hours slept, our pulse and lung capacity, which can all in all help us promote a healthy mind and body. The objective of the present study was to evaluate if there was any significant difference in our student population. In order to compare we looked at parameters such as our weight, body mass index, food calorie quantitative and qualitative consumption, the number of hours slept, our cardiovascular system pulse and lung capacity, within a time frame of a week. Then we compared the data across sexes and ethnic groups. Our results show that there is a significant difference between male and female sleep patterns. The most significant variation in pulse was within the Asian and Haitian communities. Additional details will be discussed once the project is completed.

Introduction

According to the National Heart, Lung and Blood Institute, calories is associated with the amount of energy individual's produce. As we know, there is energy found in everything that is eaten and in what we drink. In order to maintain a healthy weight, we must maintain the equilibrium of the energy that comes in and comes out of our body. Factors that impact out weight is our metabolism, genes and environment. There are factors that alter our environment that allows us to struggle with maintaining our health and have an impact on our weight. When the energy that is taken in when consuming food is not in equilibrium with the energy we burn from being active we gain weight [1].

To understand the healthy weight of an adult we look at the relationship between the body weight and height. This is known as the body mass index (BMI), it is calculated from the height and weight and the purpose of calculating this score is to identify if the individual is underweight, overweight or obese. Individuals who are considered to be overweight due to the scale of their body mass index indicating they have a great amount of weight on their body for their height. According to National Heart, Lung and Blood Institute, overweight is having a body mass index scale that is greater than 25 and below 30. On the other hand, obese is considered when an individual has a great amount of body fat in comparison to their height. According to National Heart, Lung and Blood Institute, obese s having a body mass index scale that is 30 and greater [2].

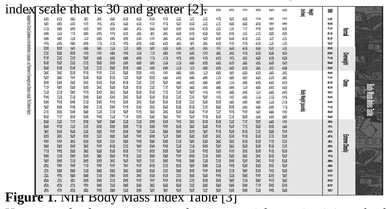

Figure 1. NIH body Mass Index Table [3]

Heart rate also known as your pulse, is essential to maintaining a healthy body. Your pulse is the number of times your heart beats per minute. As you become older your pulse changes and can allude to an underlying heart condition. In order to examine your pulse, you may want to look at your wrists or the side of your neck and put your fingers over your pulse and count the beats per minute. According to the American Heart Association, a normal heart rate varies from one another, yet the normal pulse is between 60 to 100 beats per minute. A beta blocker may be the reason for a lower pulse than 60 beats per minute, beta blocker can be used to control an abnormal rhythm such as arrhythmia [5]. It is common in individuals who are very athletic and exercise a lot. This is due to factor that their heart muscle is in a great condition and will not need to work as hard to maintain a steady beat.

Age	Target HR Zone 50-85%	Average Maximum Heart Rate, 100%
20 years	100-170 beats per minute (bpm)	200 bpm
30 years	95-162 bpm	190 bpm
35 years	93-157 bpm	185 bpm
40 years	90-153 bpm	180 bpm
45 years	88-149 bpm	175 bpm
50 years	85-145 bpm	170 bpm
55 years	83-140 bpm	165 bpm
60 years	80-136 bpm	160 bpm
65 years	78-132 bpm	155 bpm
70 years	75-128 bpm	150 bpm

Figure 2: American Heart Association know your numbers: maximum and target heart rate [5]

According to the American Lung Association, the maximum capacity of air that your lungs can hold is about 6 liters or 600ml [6]. By the time a person reaches between 20 to 25 their lungs have matured. And as we are growing older our lung capacity will slowly de-crease, which makes it difficult to breathe. This is due to the diaphragm becoming more fragile, the lung tissue that aids in keeping airways open are losing elasticity and allowing the airways to minimize. In addition, the rib cage bones will get smaller and there will be a less amount of space for the lungs to expand. Lung capacity can be measured by performing a spirometry test. Spirometry results are used in order to diagnose chronic obstructive disorder (COPD) or asthma to assert if the breathing of an individual has improved after treatment.

Sleep is a necessary component of our lives that helps us maintain energy to stay awake and active throughout the day. An individual may feel wide awake at a time and then drowsy at another, this is due to the circadian rhythm. This is a regulation cycle system that monitors the time an individual feels sleepy and when they are awake. According to the National Sleep Foundation, the circadian rhythm is alike within every individual [7]. The recommended amount or sleep young adults, that are 18 to 25 years old, and adults, that are 26 to 64 years old, are suggested to sleep a range of seven to nine hours [8]. According to the Centers for Disease Control and Prevention, sleeping with less than 7 hours of sleep per night is associated with increased risk for obesity, diabetes, high blood pressure, coronary heart disease, stroke, frequent mental distress, and all-cause mortality [10]. However, there is significant differences between sexes, finding women to be more of the early birds and men tend to be more awake at night.

Circadian rhythms are monitored by the hypothalamus. There are other factors that also come into play, for instance light can signify a new day signaling to the brain it is time to wake up. When it is nighttime, the body will release melatonin which is a hormone that helps the body fall asleep. When the individual is falling asleep and waking up at the same time the circadian rhythm is maintained, and helps reduce insomnia.

According to the National Sleep Foundation, men have a circadian cycle that is six minutes longer than women and that is why they tend to run truer to a full 24-hour cycle or longer. This explains why they tend to feel less tired in the evening [7]. However, for women they tend to run less than a full 24-hour cycle, and that is why they tend to be awake earlier than men. However, according to the National Sleep Foundation, women have an increasing susceptibility to early- waking sleep disturbances like insomnia [7].

Age	Recommended	May be appropriate	Not recommended
Newborns	14 to 17 hours	11 to 13 hours 18 to 19 hours	Less than 11 hours More than 19 hours
4-11 months	12 to 15 hours	10 to 11 hours 16 to 18 hours	Less than 10 hours More than 18 hours
Toddlers 1-2 years	11 to 14 hours	9 to 10 hours 15 to 16 hours	Less than 9 hours More than 16 hours
Preschoolers 3-5 years	10 to 13 hours	8 to 9 hours 14 hours	Less than 8 hours More than 14 hours
School-aged Children 6-13 years	9 to 11 hours	7 to 8 hours 12 hours	Less than 7 hours More than 12 hours
Teenagers 14-17 years	8 to 10 hours	7 hours 11 hours	Less than 7 hours More than 11 hours
Young Adults 18-25 years	7 to 9 hours	6 hours 10 to 11 hours	Less than 6 hours More than 11 hours
Adults 26-64 years	7 to 9 hours	6 hours 10 hours	Less than 6 hours More than 10 hours
Older Adults ≥ 65 years	7 to 8 hours	5 to 6 hours 9 hours	Less than 5 hours More than 9 hours

Figure 3: National Sleep Foundation's Sleep Duration Recommendations [9]

Materials and Methods

Students monitored their health within a range of a week, tracking daily their weight, height, body mass index, blood pressure, pulse, lung capacity, food calorie consumption and the number of hours slept. The information was all recorded within a written report containing a description of the quantity and quality of the parameters, using apps like "MyFitnessPal", "Fitbit", "Apple Watch" and "Mysleepcycle". These parameters were extracted from the report and were studied across the population of students comparing ethnicities and sexes. Using excel to store the analytic data into tables and to create graphs to examine the results within different ethnicities and across genders to identify the average, conduct a t-test to assess the p value, computing the standard deviation, and using ANOVA to help examine the statistical variation within and across the population. Then, using the Centers of Disease Control and Prevention to compare the results to identify if there are any proven significance that were found from the analysis of the data.

Results

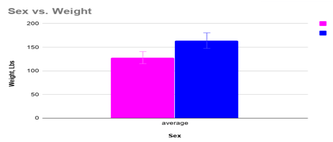

Total number of participants n=40

Female n=31

Male n= 9

Figure 4: Sex vs. Weight Graph: This graph shows there are 40 individuals participating within this study, taking into consideration their different genders and the number of participants within each gender there are. Found within this graph there is an average weight for females of 128lbs meanwhile for male the average weight is 164lbs. Within all the participants, regardless of their gender there is an average weight of 126lbs. There is a noticeable standard deviation for females of 22 meanwhile the standard deviation for male is 24, an overall standard deviation 0f 27.38. There is a standard error of 3, and when conducting a t-test the score computed is t-test 0.000212413, which allows us to determine that the p value is less than 0.05, portraying a significant result.

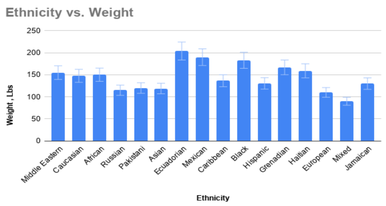

Total number of Participants n=31

Total number of Ethnicities n=16

Figure 5: Ethnicity vs. Weight Graph: This graph shows there are 40 individuals participating within this study, taking into consideration their different ethnicities and the number of participants within each ethnicity there are. Found within this graph there is an average weight for Middle Eastern is 155lbs, Caucasian 147lbs, African American 150lbs, Russian 115lbs, Pakistani 120lbs, Asian 118lbs, Ecuadorian 204lbs, Mexican 190lbs, Caribbean 136lbs, Black 183lbs, Hispanic 13lbs, Grenadian 167lbs, Haitian 159lbs, European 110lbs, Mixed 90lbs, and Jamaican 130lbs. Within all the participants, regardless of their ethnicity there is an average weight of 126lbs. The standard deviation computed is 27.38. Conducting an ANOVA test, our results show we are able to accept the null hypothesis because F, which is equivalent to 0.1749 is < F crit which is 2.3419. This indicates within the different ethnic groups there are different means. The P value computed is 0.1367.

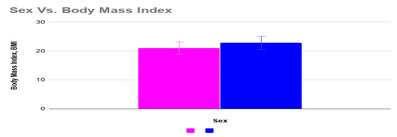

Total number of participants n=22

Female n=18

Male n= 4

Figure 6: Sex vs. Body Mass Index (BMI): This graph shows there are 22 individuals who participated within this segment of the study, taking into consideration their different genders and the number or participant within each gender there is. Found within the visual representation, there are only 4 male participants and 18 female participants. The average female BMI score is 21 and for male it is 22, it shows there is not a significant difference between the gender BMI score. The standard deviation computed is 2.02, and the standard error is 3. Conducting a t-test gave a value of 0.1175, displaying that the p value is greater than 0.05.

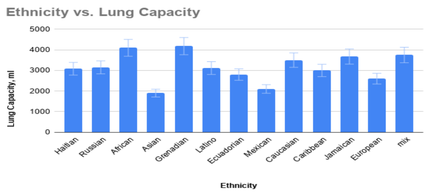

Total number of Participants n=23

Total number of Ethnicities n=10

Figure 7: Ethnicity vs. Body Mass Index (BMI) graph: This graph shows there are 23 individuals participating within this segment of the study, taking into consideration their different ethnicities and the number of participants within each ethnicity there are. Found within this graph there is an average BMI for African American is 26.16, Russian 21.7, Pakistani 23.8, Asian 21.24, Latino 21.73, Grenadian 22.6, European 20.15, Jamaican 18.7, Caucasian 22.70 and Mixed 24.2. Within all the participants, regardless of their ethnicity there is an average BMI of 22. The standard deviation is 3.1. Conducting an ANOVA test, our results show we are able to accept the null hypothesis because F, which is equivalent to 0.2717 is < F crit which is 5.9987. This indicates within the different ethnic groups there are different means. The P value computed is 0.9515.

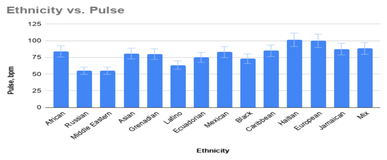

Total number of Participants n=32

Total number of Ethnicities n=14

Figure 8: Ethnicity vs. Pulse graph: This graph shows 32 individuals participating within this segment of the study, taking into consideration their different ethnicities and the number of participants within each ethnicity there are. Found within this graph there is an average pulse for African American is 84 bpm, Russian 55 bpm, Middle Eastern 55 bpm, Asian 80.90 bpm, Grenadian 80 bpm, Latino 63.5 bpm, Ecuadorian 75 bpm, Mexican 83 bpm, Black 73 bpm, Caribbean 85 bpm, Haitian 101 bpm, European 100 bpm, Jamaican 87 bpm and Mixed 88 bpm. Within all the participants, regardless of their ethnicity there is an average pulse of 81 bpm. The standard deviation computed is 17.36. Conducting an ANOVA test, our results show we are able to accept the null hypothesis because F, which is equivalent to 0.0176 is < F crit which is 5.8733. This indicates within the different ethnic groups there are different means. The P-value computed is 0.9999.

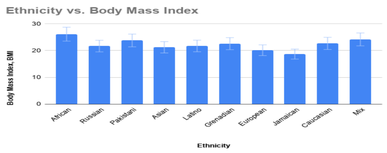

Total number of Participants n=30

Total number of Ethnicities n=13

Figure 9: Ethnicity vs. Lung Capacity graph: This graph shows there are 30 individuals participating within this segment of the study, taking into consideration their different ethnicities and the number of participants within each ethnicity there are. Found within this graph there is an average lung capacity for Haitian 3083ml, Russian 3150ml, African American 2789ml, Asian 2641ml, Grenadian 4183 ml, Latino 3214 ml, Ecuadorian 2800 ml, Mexican 2100 ml, Caucasian 3000 ml, Jamaican 3675ml, European 2600 ml, and mx 3001 ml. Within all the participants, regardless of their ethnicity there is an average lung capacity of 2977ml. The standard deviation is 828.108. Conducting an ANOVA test, our results show we are able to accept the null hypothesis because F, which is equivalent to 0.3602 is < F crit which is 5.9117. This indicates within the different ethnic groups there are different means. The P-value computed is 0.9237.

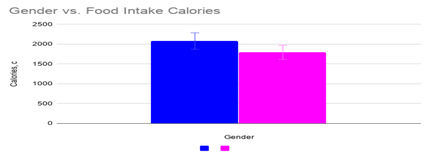

Total # of Participants n=40

Male n= 7

Female n=33

Figure 10: Gender vs. Food Intake Calories. This graph shows there are 40 individuals who participated within this segment of the study, taking into consideration their different genders and the number or participant within each gender there is. Found within the representation, there are only 7 male participants and 33 female participants. The average calorie intake for males is 2078 calories, meanwhile for females the average calorie intake is 1792 calories. There is a significantly higher number for males versus there components female. The standard deviation is 602.12, conducting a t-test gave a value of 0.258, displaying

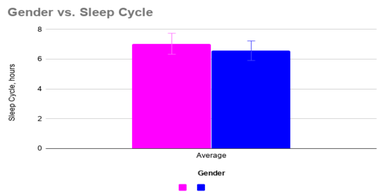

Total # of Participants n=39

Female n=32

Male n= 7

Figure 11: Gender vs. Sleep Cycle: This graph shows there are 39 individuals who participated within this segment of the study, taking into consideration their different genders and the number or participant within each gender there is. Found within the graph, there are only 7 male participants and 32 female participants. The average amount of sleep for females is found to be 7 hours meanwhile, the average amount of sleep hours for males is 6.57 hours. The standard deviation is 1.46, and conducting a t-test gave a value of 0.453, displaying that the p value is greater than 0.05.

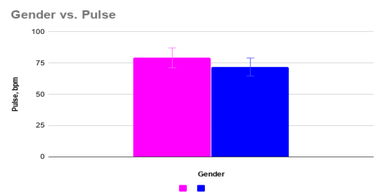

Total # of Participants n=47

Female n=42

Male n= 5

Figure 12: Gender vs. Pulse: This graph shows there are 47 individuals who participated within this segment of the study, taking into consideration their different genders and the number or participant within each gender there is. Found within the representation, there are only 5 male participants and 42 female participants. The average pulse rate for females is found to be 79 bpm meanwhile, the average pulse rate for males is 71 bpm. The standard deviation is 14.8, conducting a t-test gave a score of 0.278, portraying that the p-value is greater than 0.05.

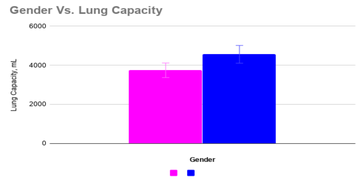

Total # of Participants n=39

Female n=36

Male n= 3

Figure 13: Gender vs. Lung Capacity: This graph shows there are 39 individuals who participated within this segment of the study, taking into consideration their different genders and the number or participant within each gender there is. Found within the graph, there are only 3 male participants and 39 female participants. The average lung capacity for females is found to be 3743.76 mL meanwhile, the average lung capacity for males is 4561 mL. The standard deviation is 4561.50, and conducting a t-test gave a score of 0.7699, portraying that the p-value is greater than 0.05

Discussion

Looking at **figure 6**, displaying the Body Mass Index versus sex, the average female BMI score is 21 and for male it is 22, it shows there is not a significant difference between the gender BMI score. According to the National Heart, Lung and Blood institute, both genders will not fall within the overweight scale, and will fall in the normal range [2]. Studies have shown there is an equal percentage of male and females maintaining a normal BMI range [12].

Meanwhile, in **figure 7**, displaying the ethnicity of the individuals versus the Body Mass Index. There are 23 participants within this segment of the study. There are 10 different ethnicities, and there is an average BMI for African American is 26.16, Russian 21.7, Pakistani 23.8, Asian 21.24, Latino 21.73, Grenadian 22.6, European 20.15, Jamaican 18.7, Caucasian 22.70 and Mixed 24.2. African American have the greatest BMI scale, and according to the National heart, Lung and Blood Institute, the ethnic group would be found as overweight [2]. The highest BMI among the ethnicities is African American. According to the U.S. Department of Health and Human Services Office of Minority Health, African American women have the highest rate of being overweight or obese in comparison to other ethnic groups [13]. Studies in 2015 have shown, that African Americans women were 60% more likely to be obese than non-Hispanic white women [13]. The ethnicities of the Asians and Russians have very similar BMI scores. According to a study done by *The NY Times*, the ethnic group of Asians might have lower obesity rate than other ethnic groups yet they have twice the susceptibility of having Type 2 diabetes, which promotes heart attacks and strokes [14]. The individuals who fall within the Pakistani and Mix ethnic groups are found to be very similar.

In **figure 8**, Ethnicity vs. Pulse graph, shows there are 32 individuals participating within this segment of the study, taking into consideration their different ethnicities and the number of participants within each ethnicity there are. There are 14 different ethnicities to take into consideration. Found within the graph there is an average pulse for African American of 84 bpm, Russian 55 bpm, Middle Eastern 55 bpm, Asian 80.90 bpm, Grenadian 80 bpm, Latino 63.5 bpm, Ecuadorian 75 bpm, Mexican 83 bpm, Black 73 bpm, Caribbean 85 bpm, Haitian 101 bpm, European 100 bpm, Jamaican 87 bpm and Mixed 88 bpm. Within all the participants, regardless of their ethnicity there is an average pulse of 81 bpm, which concludes they are in range of the normal heart rate [5]. The pulse rate of the individuals of the ethnicities of Middle Eastern and Russian are the same, and below normal that might be due to a beta blocker [5]. The pulse rate of Haitians and European for much alike, having the highest pulse rate among the different ethnicities and might be careful because they have the ability to be over the normal pulse range.

Viewing **figure 11**, Gender vs. Sleep Cycle, shows the average amount of sleep for females is found to be 7 hours meanwhile, the average amount of sleep hours for males is 6.57 hours. Our results agree with the National Sleep Foundation, examining that women tend to sleep more than men. This explains why women tend to be awake in the morning versus men, because they are receiving their recommended hours of sleep. The recommended hours of sleep and individual should receive is 7 hours, according to the National Sleep Foundation [7]. Studies have shown that individuals who experience less than 7 hours of sleep are associated with low adherence to a healthy diet and regular meal patterns [11].

In **figure 12**, Gender vs. Pulse, shows there are 47 individuals who participated within this segment of the study, taking into consideration their different genders. The average pulse rate for females is found to be 79 bpm meanwhile, the average pulse rate for males is 71 bpm, remaining within the normal pulse rate [5]. Our evidence agrees with studies, that high frequency heart rate and the overall complexity of heart dynamics are statistically higher in women than men [15].

Acknowledgements: I would like to thank the Emerging Scholars Program for giving me this opportunity. I would like to genuinely thank Professor Hamid Norouzi and Abdou Bah.

Reference:

[4] "All About Heart Rate (Pulse)." *www.heart.org*, www.heart.org/en/health-topics/high-blood-pressure/the-facts-about-high-blood-pressure/all-about-heart-rate-pulse.

[3] "Body Mass Index Table 1." *National Heart Lung and Blood Institute*, U.S. Department of Health and Human Services, www.nhlbi.nih.gov/health/educational/lose_wt/BMI/bmi_tbl.htm.

[2] "Calculate Body Mass Index, Healthy Weight Basics." *National Heart Lung and Blood Institute*, U.S. Department of Health and Human Services, www.nhlbi.nih.gov/health/educational/wecan/healthy-weight-basics/body-mass-index.htm.

[1] "Healthy Weight Basics." *National Heart Lung and Blood Institute*, U.S. Department of Health and Human Services, www.nhlbi.nih.gov/health/educational/wecan/healthy-weight-basics/index.htm.

[8] "How Much Sleep Do We Really Need?" *National Sleep Foundation*, www.sleepfoundation.org/articles/how-much-sleep-do-we-really-need.

[7] "How Sleep Cycles Vary Between Men and Women." *National Sleep Foundation*, www.sleepfoundation.org/articles/how-sleep-different-men-and-women.

[12] Kuan, P X, et al. "Gender Differences in Body Mass Index, Body Weight Perception and Weight Loss Strategies among Undergraduates in Universiti Malaysia Sarawak." *Malaysian Journal of Nutrition*, U.S. National Library of Medicine, Apr. 2011, www.ncbi.nlm.nih.gov/pubmed/22135866.

[6] "Lung Capacity and Aging." *American Lung Association*, www.lung.org/lung-health-and-diseases/how-lungs-work/lung-capacity-and-aging.html.

[9] "National Sleep Foundation Recommends New Sleep Times." *National Sleep Foundation*, www.sleepfoundation.org/press-release/national-sleep-foundation-recommends-new-sleep-times.

[14] O'connor, Anahad. "Why Do South Asians Have Such High Rates of Heart Disease?" *The New York Times*, The New York Times, 12 Feb. 2019, www.nytimes.com/2019/02/12/well/live/why-do-south-asians-have-such-high-rates-of-heart-disease.html.

[13] "Office of Minority Health." *Obesity - The Office of Minority Health*, www.minorityhealth.hhs.gov/omh/browse.aspx?lvl=4&lvlid=25.

[10] "Prevalence of Healthy Sleep Duration among Adults - United States, 2014." *Centers for Disease Control and Prevention*, Centers for Disease Control and Prevention, 25 Aug. 2017, www.cdc.gov/mmwr/volumes/65/wr/mm6506a1.htm.

[15] Ryan, S M, et al. "Gender- and Age-Related Differences in Heart Rate Dynamics: Are Women More Complex than Men?" *Journal of the American College of Cardiology*, U.S. National Library of Medicine, Dec. 1994, www.ncbi.nlm.nih.gov/pubmed/7963118.

[11] Theorell-Haglöw, Jenny, et al. "Sleep Duration Is Associated with Healthy Diet Scores and Meal Patterns: Results from the Population-Based EpiHealth Study." *Journal of Clinical Sleep Medicine : JCSM : Official Publication of the American Academy of Sleep Medicine*, U.S. National Library of Medicine, 26 Nov. 2019, www.ncbi.nlm.nih.gov/pubmed/31770092.

[5] "Understanding Blood Pressure Readings." *Www.heart.org*, www.heart.org/en/health-topics/high-blood-pressure/understanding-blood-pressure-readings.

Static analysis of circular plates under Mechanical Loads

Author :Harpreet Lalia
Mentor : Prof.Farhad Alinaghizadeh

Civil Engineering and Construction Management Technology

Abstract

In this research statics analysis of circular plates is performed using SolidWorks.

Circular plates with different material properties, thickness to radius ratios, and boundary conditions under mechanical loads are modeled and analyzed in SolidWorks.

The results are obtained for deflections of circular plates under uniform and point loads.

A three-dimensional (3D) model of circular plates is first created in SolidWorks. Then the material properties, mechanical loads and boundary conditions are defined for the plate.

It is found deflection of plates is depended on magnitude of mechanical loads, geometrical parameters, boundary conditions and material properties. Responses of SolidWorks for deflections of plates versus loads are obtained and shown in figures. The effects of boundary conditions, geometrical parameters, material properties and mechanical loads on deflection of plates is investigated. Furthermore, equilibrium equation of circular plates under load is obtained by writing equilibrium condition for an element of circular plate under mechanical loads

Introduction

Circular plates have different applications in engineering field. In this research we studied static analysis of circular plates under transverse mechanical loads. The analysis is performed in Solidworks. A three-dimensional (3D) model of circular plates is created in Solidworks. The material properties, boundary condition, and load are then defined. Deflection of the plates with clamped boundary condition is obtained. Furthermore, equilibrium equation of circular plates under transverse loading is obtained.

SolidWork is widely used in different engineering fields, e.g., Civil, Structural, and Mechanical engineering. SolidWorks has different features such as creating a plate with a distributed load or point load.

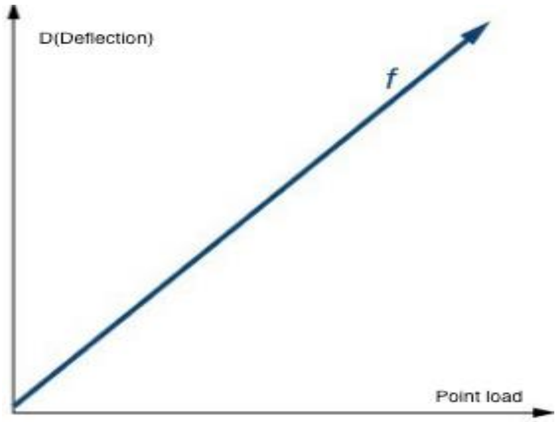

The objective of this research is to study analysis of circular plates under transverse loading using SolidWorks.
To model the problem, circular plates are first created in SolidWorks and then material properties and boundary conditions are defined.

We experimented with SolidWorks and saw so many outstanding forces features that can be applied to the subject area of static analysis of structural members .

Equation of circular plates

the equilibrium equation of circular plates is written as follows:

$$\frac{1}{r}\frac{d}{dr}\left\{r\frac{d}{dr}\left[\frac{1}{r}\frac{d}{dr}\left(r\frac{dw}{dr}\right)\right]\right\} = \frac{q}{D}$$

This is equation is obtained by considering equilibrium condition for an element of the circular plate. More detail about this equation can be found in Ref. [2].

Experimental Study

Deflections of circular plates with clamped boundary conditions are obtained using SolidWorks.
The results are obtained for plates made of alloy steel.
Deflection of plates under transverse loading is shown in the below figure.

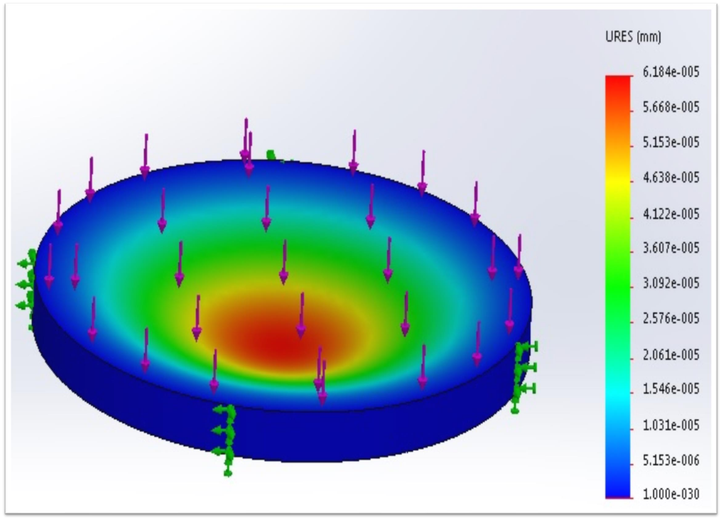

References

"Deflection Check / Serviceability Check in SDC Verifier." *SDC Verifier*, 23 Apr. 2019, https://sdcverifier.com/articles/deflection-check-serviceability-check/.

[2] *Definition of DEFLECTION*. https://www.merriam-webster.com/dictionary/deflection. Accessed 27 Nov. 2019.

[2] Timoshenko SP, Woinowsky-Krieger S. Theory of plates and shells. McGraw-hill; 1959.


NEW YORK CITY
COLLEGE OF TECHNOLOGY
CUNY

Kevin Rojas, Ericka Saldana, and Mandy Li

Mentor: Dr. Angran Xiao

New York City College of Technology

Abstract

Most people who are not in a field or career path that requires the use of a laser engraver, as we were, would never encounter such a device in their lives. Our team of nine students decided to embark on this journey of understanding how to create our own laser engraver in order to sell this product for an affordable cost compared to conventional lasers. Our focus is on an educational and small business setting. However, we also wanted to do something else besides a basic laser engraver. Our project's purpose was to create a feasible and cheap DIY laser engraver that encompasses a rotational feature that almost all DIY laser engravers do not have, while also making it lightweight and portable.

Introduction

Our project will have two main functions which are, having the laser follow only x axis motion and have the lower part where the chuck will be holding the steel bar will be rotation one direction. The issue we face is the possibility that our method will not work. We have all the idea down and the procedure of what we will manufacture. However, the coding will be a little difficult to create or to improve its original code. We might have a minor situation with time management and the effort we sure put. To prevent this issue is by having good communication. Communication is key when it comes to teamwork and getting things done the right way. Once, time management is fixed, we can move on to improving this project a lot faster. We will have enough time to catch our mistake verse rushing and having half completed work.

Methodology

The main things we needed to figure out was the design of the chassis or frame that would house the engraver, to find a software that would control the engraver or make our own, and to buy hardware that would be compatible with the software and fit into our design. We also had to keep in mind things like engraving speed, battery capacity, laser strength, laser safety standards, the material of the frame, ease of use, and other issues, while making this product. The team went through numerous product design methodologies of deciding what would work and what would not. We also asked our mentor, other professors that had coding knowledge, and a few CNC technicians in our mechanical engineering department.

Through our online research, we found a free source software called, K40 Whisperer, that had our desired rotational component that we had sought after. We finalized a CAD design on Solidworks that would allow for enough space to exist for the rotational engraving effect, while also keeping it big enough to engrave objects of lengths of about less than 2ft, but small enough that it would be travel-friendly. We used aluminum metal bar extrusions to make the frame. We also designed mounts and holders and 3D printed them so that everything could be snuggly put into place.

Schematic

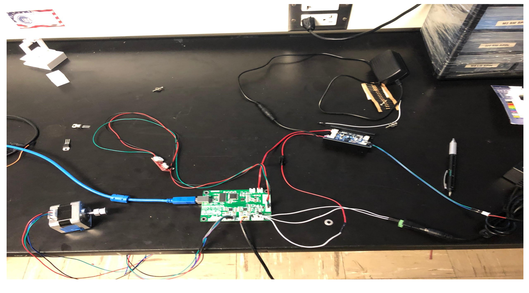

CAD Assembly and Equipment

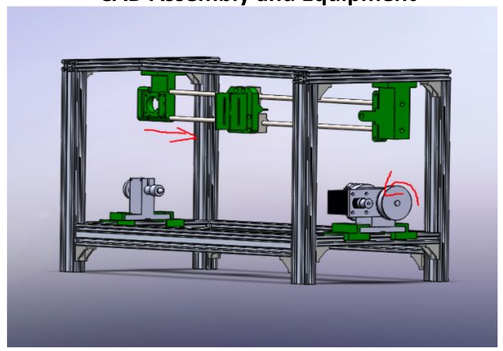

The laser will be running along rods that are attached two mounts underneath the top of the frame. The laser will be moving back and forth on the x-axis. The chuck is attached at the bottom of the frame in between two pivots which rotates along the same axis.

Parts	Names	Descriptions
	#1 Aluminum extrusions	T-Slotted Aluminum Extrusion a technique used to transform aluminum alloy into objects with a definitive cross-sectional profile for a wide range of uses
	#2 Belt	A loop of flexible material used to link two or more rotating partsmechanically, most often parallel.
	#3 Charger	A device for charging a battery or battery-powered equipment.
	#4 Wiring	Long thin pieces of metal used to transport an electric current
	#5 3D Printer	A machine allowing the creation of a physical object from a three-dimen-sional digital model by creating llayers of material in succession
	#6 Stepper Motors	DC motors which move in discrete steps. They have several coils that are ut together in groups called "phases"
	#7 Purple Blue Laser Module	Device that emits light through a process of optical amplification based on the stimulated emission of electromagnetic radiation
	#8 UNO Project Super Starter Kit	Kit based on arduino used for programming
	#9 Three-Jaw Rotary Chuck	Device that holds a workpiece in place and has a number of adjustable jaw gears to move together in order to centralize a piece.
	#10 8mm Bore Pulley Synchronous Wheel with Bearing	Grooved wheel used to change the direction of an ojbect of force.
	#11 M2 Nano	The M2 is the standard mainboard in many laser engravers and provides basic motion and firing control

End Result

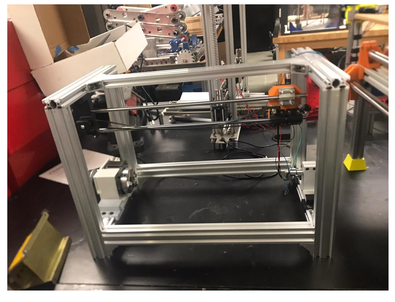

Safety Analysis and FMA Chart

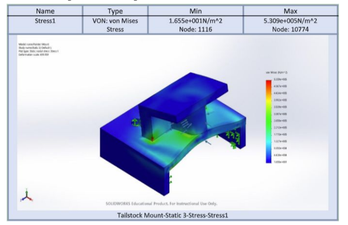

The corrective actions used by our design team included adding extra thickness (material) to mount and holder connectors. After coming up with a prototype that works, we then reprinted the parts using 25% infill instead 10% infill to increase rigidity. We added two tension parts for the laser and rod system to reduce tension caused during laser operation. It also is designed to tighten the laser and rod system without having to completely disassembling the whole drive belt.

	Severity		Occurrence		Detection			
Fail Mode	**Effects**	**Rating**	**Causes**	**Rating**	**Tests**	**Rating**	**RPN**	**Recommended Action**
Laser Overheating	Doesn't engrave	6	Prolonged Use	5	Testing on Material	6	180	Make sure there is cooling unit for the laser
3D Prints-Motor holder breaking due to vibration	Power Supply falls off	8	Impurities in print	5	Static Simulation	9	360	Increase Safety Factor
3D Prints-Motor holder breaking due to vibration	Laser to go off axis	7	External Loads/Forces	6	Static Simulation	9	378	Increasing overall sturdiness of design
Programming Errors	Mistakes occur in the engraving process	5	Wrong Codes	4	Testing Codes	6	120	Check programming codes multiple times
Timing Belt breaking	the laser won't move	7	Tension of belt being too tight or too loose	6	Tension Testing	5	210	Finding out max tension of timing belt

The structural for this project is to create a stabilize frame for the laser to engrave. This analysis is to identify the different ways in our design could possibly fail in operation. The laser engraver is design with some guidance are similar to a 3D printer. The components of the 3D printed parts could break due to vibrations of the engraver. Issues for an open engraver therefore safety glasses is needed to prevent eyes damage. Other issue is if imputing and incorrect code will cause the engraver to do a different operation. These problems help us identify the safety for this engraver.

Software

The software is used to create jpgs and svg files to convert into g-codes for the laser engraver. The g-codes are used to move the laser engraver. For this case the x- axises will be running normally and and y-axises will be rotating on the chuck. This software is special to this laser engraver because it creates a special g-code for the engraver to rotate. Most software can't rotate.

Conclusion:

We had a semester to complete this project and we finished before our deadline. Assembly time for our product came out to under an hour and anyone would easily be able to start engraving a cylindrical bar or hydro flask bottle after assembling our product in less than minutes using the provided software on their computer. We want to continue our research and work into making it autonomous from using the computer and having an interface on the engraver for more ease of use. This project showcased how to work in a large group of people while also furthering our understanding of how to finalize a product.

Acknowledgements and References

We would first and foremost like to thank Dr. Angran Xiao, our professor, mentor, friend, and guide for this project. He steered us into the right direction and made sure we met the most professional standards our project could be upheld to.

"ANSI Z136 Standards." ***The Laser Institute*****, 3 Oct. 2018,** **www.lia.org/resources/laser-safety-information/laser-safety-standards/ansi-z136-standards.**

"CFR - Code of Federal Regulations Title 21." ***Accessdata.fda.gov*****, www.accessdata.fda.gov/scripts/cdrh/cfdocs/cfcfr/CFRSearch.cfm?FR=1040.10.**

Hardware Implementation of Assistive Technology Robot

Author: Joycephine Li - Mentor: Professor Farrukh Zia

Computer Engineering Technology Department

ABSTRACT

SuperHERO is an on-going research project in Computer Engineering Technology department which involves upgrading Heathkit Education Robot (HERO) hardware circuits and features by using modern hardware devices and sensors. The current phase of the project will focus on upgrading the motor drive system hardware as well as implementation and testing of features such as mobile robot obstacle detection and other assistive technologies to help people with disabilities. This involves the reattachment of the robot arm after repairing and updating with 3D printing and using modern hardware and software technology. We observed that the robotic arm has rotary and translation movements after testing with a sample code. Also, the arm gripper has a rotary movement with an open and close function. This part of the experiment will help people with limited arm movements, so the robot arm can help to reach and grab objects.

INTRODUCTION

In the previous phase, the two modern microcontroller devices, Arduino and Raspberry Pi, are incorporated on the HERO-1 model with the correct wiring connections to be made from the schematic diagrams in Google Drive. The base of robot is ready to be tested with its overall movements. While in preparation for its performance, the arm is ready to be implemented after the stepper motors are tested individually for their condition. This part of the experiment helps people with limited arm movements, so the robot arm can help to reach and grab objects.

HARDWARE

The robot arm consists of 3 stepper motors to control its translation and rotation movements. The arm extend motor creates a translation motion of the robotic arm. The arm rotation motor is part of the arm drive circuit board that is used to rotate the robotic arm. The wrist rotation motor and gripper rotation is used to rotate the wrist and gripper at 180 degrees, respectively. Lastly, gripper is used to grab objects with its open and close function. The block diagram of the arm is shown on the right.

ACKNOWLEDGEMENTS

Emerging Scholars Program 2019 Fall

Honors Scholars Program 2019 Fall

BLOCK DIAGRAMS

Modern SuperHERO Robot

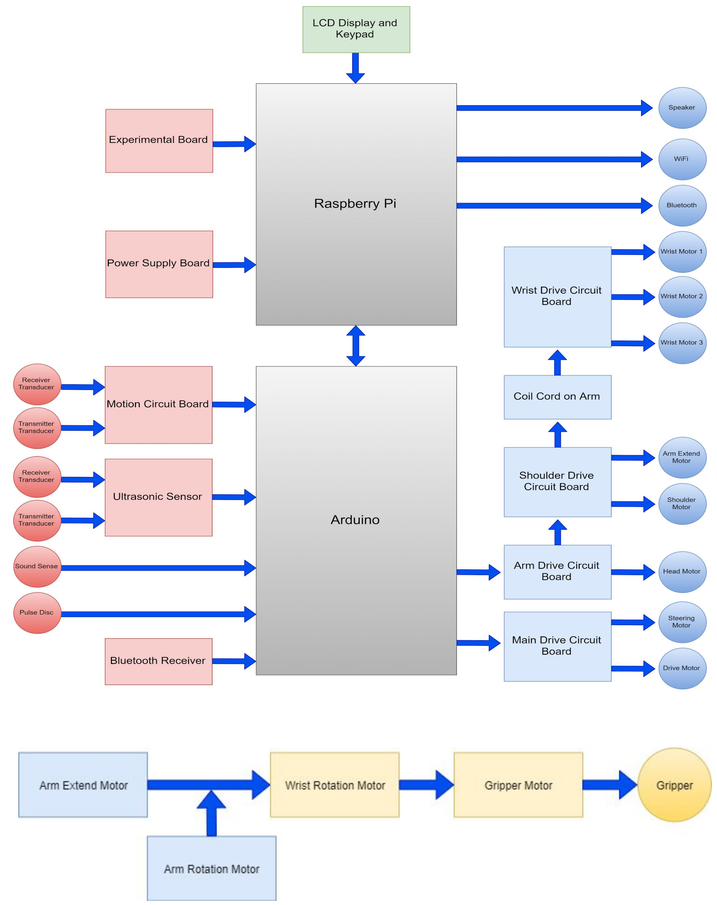

ELECTRICAL CIRCUIT

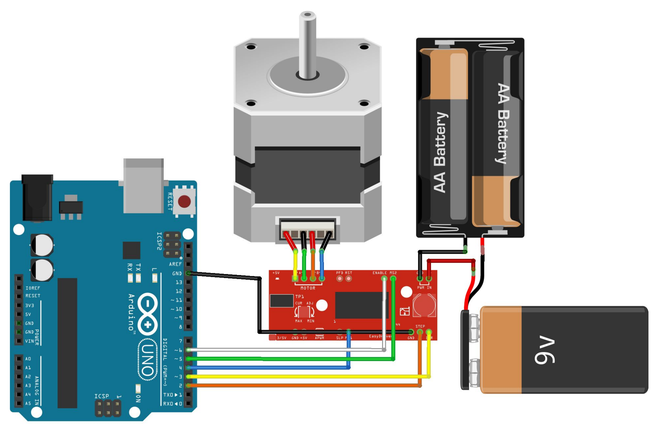

PROGRAM CODE

Small section of the Easy Driver Arduino Code

```
//Declare pin functions on Redboard
#define stp 2
#define dir 3
#define MS1 4
#define MS2 5
#define EN  6

//Declare variables for functions
char user_input;
int x;
int y;
int state;

void setup() {
  pinMode(stp, OUTPUT);
  pinMode(dir, OUTPUT);
  pinMode(MS1, OUTPUT);
  pinMode(MS2, OUTPUT);
  pinMode(EN, OUTPUT);
  resetEDPins(); //Set step, direction, microstep and enable pins to
  Serial.begin(9600); //Open Serial connection for debugging
  Serial.println("Begin motor control");
  Serial.println();
  //Print function list for user selection
  Serial.println("Enter number for control option:");
  Serial.println("1. Turn at default microstep mode.");
  Serial.println("2. Reverse direction at default microstep mode.");
  Serial.println("3. Turn at 1/8th microstep mode.");
  Serial.println("4. Step forward and reverse directions.");
  Serial.println();
}
```

CONCLUSION

An Arduino sample code that is used to test the Easy Driver bipolar motor circuit and gear stepper motor of the arm works successfully. Transistors are connected to the arm drive circuit board to test the arm.

FUTURE WORK

After testing the arm's overall performance, it will be attached to the base of the robot. Some arm components will be 3D printed to replace the plastic parts of the old robotic arm. Lastly, the robot will be tested with its overall performance.

REFERENCES

"Easy Driver Hook-up Guide." *Sparkfun*, https://learn.sparkfun.com/tutorials/easy-driver-hook-up-guide/all.

"Japan Servo KP4M15G w/ gearhead 1:20." *InterinarElectronics*, 2013 Sept 23, http://www.interinar.com/public_docs/KP4M15G.pdf.

"1.8° 42MM High Torque Hybrid Stepping Motor." *Adafruit*, https://cdn-shop.adafruit.com/product-files/324/C140-A+datasheet.jpg.

Software Implementation of Assistive Technology Mobile Robot

Authors: Jannatul Mahdi, Jannat Hoque, Joycephine Li Mentor: Professor Farrukh Zia

New York City College of Technology - CUNY

ABSTRACT

Heathkit Educational Robot (HERO-1) went into hibernation after helping students in colleges and universities across the country for over 15 years to learn Computer and Robotics Technology. Currently, the members of City Tech Women Engineers Club are reviving HERO to give it new features by using modern computer hardware and software technology. This will enable the implementation of Assistive Technology in the robot to help people with disabilities.

INTRODUCTION

The two most common modern devices that are used for mobile robot obstacle detection and navigation are ultrasonic sensor using sound waves and infrared sensor using light waves. By learning and comparing the advantages and disadvantages with testing and technical specifications of the two devices, we implement them on a mobile robot to test their effectiveness in real world situations. The hardware that is used for this project are the HERO-1 robot (model and circuits), DC motor, servo motor, stepper motor, ultrasonic sensor, Arduino, and Raspberry Pi. For the software, Arduino programming is used to upgrade the light wave sensors using C/C++ and Raspberry Pi programming is used to upgrade sound wave sensor using Python. Upgrading the sensors of the robot can help the robot to sense if there is something in front of it and react to it, and upgrading the sound sensor can help the robot to react to any sound. The four original 6 Volts batteries were replaced with two 12 Volts rechargeable batteries, one powering the circuits and one powering the motors. The original power supply and main drive circuits are being reused. Festival Lite program is used to implement speech synthesis by using the ultrasonic sensor.

BLOCK DIAGRAM

This is a SuperHERO robot block diagram that is based on the old block diagram on HERO-1 model with its modern features.

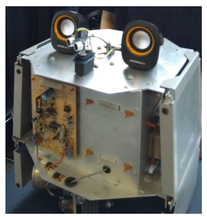

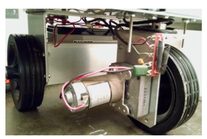

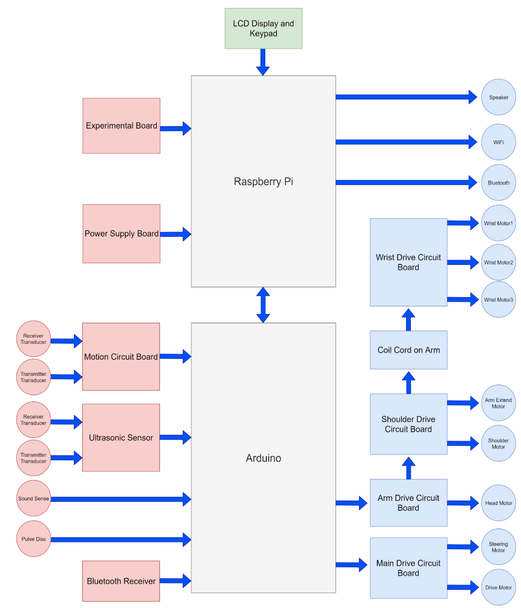

REFERENCES

- Felix. “Using a Raspberry Pi distance sensor (Ultrasonic sensor HC-SR04).” *Raspberry Pi Tutorials*, 11 Nov. 2015, tutorials-raspberrypi.com/raspberry-pi-ultrasonic-sensor-hc-sr04/.
- “Heathkit HERO RevB.” *Google Drive*, drive.google.com/drive/u/0/folders/1ULcLsusVFjnbY-m60zj6nBsRdIHkFt
- HC-SR04 Ultrasonic Range Sensor on the Raspberry Pi. (2017, November 10). Retrieved November 29, 2017, from https://www.modmypi.com/blog/hc-sr04-ultrasonic-range-sensor-on-the-raspberry-pi
- “Speech Synthesis on the Raspberry Pi” https://learn.adafruit.com/speech-synthesis-on-the-raspberry-pi/introduction
- HC-SR04 Ultrasonic Range Sensor on the Raspberry Pi. (2017, November 10). Retrieved November 29, 2017, from https://www.modmypi.com/blog/hc-sr04-ultrasonic-range-sensor-on-the-raspberry-pi

HARDWARE

The main difference between the ultrasonic sensors and IR sensors is that IR sensor detects electromagnetic radiation and the ultrasonic sensor detects mechanical energy. A Python script that was installed for Raspberry Pi to test the ultrasonic sensor and servo motor, an electric motor that consists of rotary actuator, was tested separately with no mistakes. These two scripts are then combined with an LED script to increase the measuring range and indication of obstacle detection from the ultrasonic sensor. Also, an old model of DC motor that is attached on the old model of HERO robot works using 12 Volts battery. An old charging circuit was reused and reexamined successfully to charge the batteries that is attached to the robot without removing the batteries.

CONCLUSION

In the future, we are planning to work on connecting the robot to a Bluetooth device to replace the remote control panel of the old HERO robot. Also, we plan to implement voice recognition to control the robot with voice commands. Lastly, an arm gripper will be incorporated after the base assembly of the robot is complete.

Determinism of Stochastic Processes through the Relationship between the Heat Equation and Random Walks

Gurmehar Makker, Faculty Mentor: Dr. Lin Zhou
Mathematics Department, New York City College of Technology, CUNY

Abstract

We study the deterministic characteristics of stochastic processes through investigation of random walks and the heat equation. The relationship is confirmed by discretizing the heat equation in time and space and determining the probability distribution function for random walks in dimension $d = 1, 2$. The existence of the relationship is presented both through theoretical analysis and numerical computation.

Introduction

A random walk is a stochastic process that consists of a sequence of random steps taken with a fixed or random time step on a well-defined space. For dimensions $d = 1, 2$ the spaces used are lines and planes.

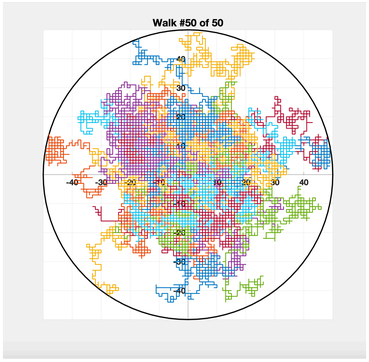

Fig. 1. 50 random walks in 2D space with 500 steps each

The heat equation is a special case of the diffusion equation. It is a partial differential equation that describes the flow or distribution of heat with respect to time in a solid surface or medium. The general form of the heat equation is given by:

$$u_t = k\nabla^2 u$$

Analysis

1. For 1-Dimensional Random Walks, using discretized notion of time and space, the probability of a particle to be at a position x after n steps is given by a binomial distribution:

$$P(x,n) = \binom{n}{k} p^k (1-p)^{n-k}, k = \frac{x+n}{2}$$

where, p is the probability that, for fixed time intervals, the walker will move to the right or to the left by Δx.

For a large number of steps, as $n \to \infty$, approximations for the factorials can be done using the Stirling's formula:

$$P(x,n) = \frac{2}{\sqrt{2\pi\sigma_x^2}} e^{\frac{-\Delta x^2}{2\sigma_x^2}}, \sigma_x^2 = 4np(1-p)$$

here, $P(x, n)$ resembles a Gaussian distribution. Using continuous limits and approximations, the probability density function, with starting $P(x, 0) = \boldsymbol{\delta}(x)$, where $\boldsymbol{\delta}$ is the Dirac Delta function, is given by:

$$P(x,t) = \frac{1}{\sqrt{4\pi kt}} e^{\frac{-(x-mt)^2}{4kt}}, k = 2p(1-p)\frac{\Delta x^2}{\Delta t}, m = p(1-p)\frac{\Delta x}{\Delta t}$$

The 1-Dimensional heat equation, with the flux being a negative proportion of the gradient of heat and no internal heat generation, is given by:

$$u_t(x,t) = k u_{xx}(x,t)$$

Fundamental solution of this heat equation with initial condition $u(x, 0) = \boldsymbol{\delta}(x)$ is given by:

$$\Phi(x,t) = \frac{1}{\sqrt{4\pi kt}} e^{\frac{-x^2}{4kt}}$$

2. Let N_x be the number of walkers at position x at a given time $t + \Delta t$, then:

$$N_x(t+\Delta t) = N_x(t) - R\Delta t N_x(t) - R\Delta t N_x(t) + R\Delta t N_{x-1}(t) + R\Delta t N_{x+1}(t)$$

Observing that the last four terms on the right-hand side of the equation are a centered difference formula for the second-order derivative of N_x with respect to space, then the equation above is equivalent to:

$$\frac{\partial N}{\partial t} = R\Delta x^2 \frac{\partial N^2}{\partial x^2}$$

Describing the system using $c(x, t) :=$ density of particles, the diffusion equation is achieved:

$$\frac{\partial c}{\partial t} = D\frac{\partial c^2}{\partial x^2}, D = R\Delta x^2$$

where, D is the diffusion constant.

Computational Results

The 2-Dimensional heat equation is solved numerically with finite difference method with the central source at 1000 degrees as initial condition and the bottom boundary at 100 degrees and other boundaries at 0 degrees.

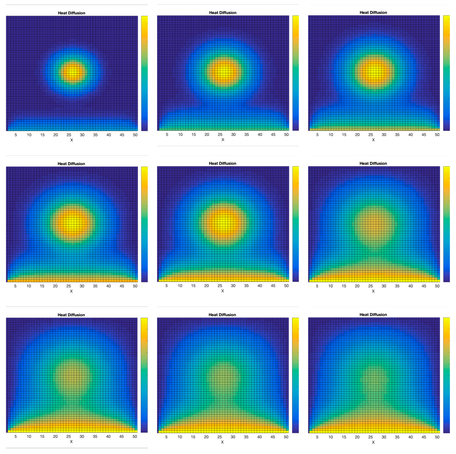

Fig. 2. Two-Dimensional Heat Dissipation, Central Source

In Fig. 2, the heat source at the center at the initial time diffuses in all direction to the boundary. The temperature evolves in time and as it reaches the steady state, it becomes equal to the prescribed boundary condition. The heat dissipation in Fig. 2 resembles the random walk in Fig. 1.

Conclusion

In this poster, two different types of analysis have been used to show that the fundamental solution of the heat equation resembles the probability distribution function of random walks and the net change in the number density of random walkers at a given time yields the diffusion equation, specifically the heat equation. Therefore, the determinism of some macroscopic partial differential equations is related to some far-fetched stochastic processes at the microscopic level.

Future Work

This analysis can be further used to understand and investigate various mathematical concepts from Super-Brownian motion as a limit of critical branching random walks to Fractal Dimension using perspectives from Cantor measure and Hausdorff measure and dimension. Random walks could be further explored to understand even more complex stochastic processes such as Lévy flights.

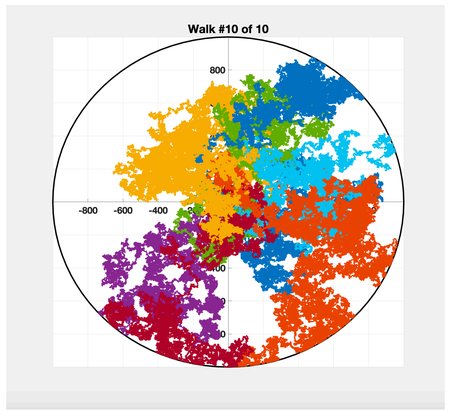

Fig. 3. Million-Step Random Walks with Fractal Patterns

References

1. Nakashima, and Makoto. "Super-Brownian Motion in Random Environment as a Limit Point of Critical Branching Random Walks in Random Environment." *ArXiv.org*, 24 Apr. 2013, https://arxiv.org/abs/1207.1755.
2. "Introduction to Diffusion and Random Walks", https://www.uio.no/studier/emner/matnat/fys/FYS2160/h17/simuleringsopgaver/virrevandrer_diffusjon.pdf
3. "Random Walks", https://www.princeton.edu/~akosmrlj/MAE545_S2018/lecture17_slides.pdf

Acknowledgments

This research is supported by the Emerging Scholars Program at the New York City College of Technology, CUNY.

Roboqueen 3D

Authors: Jensy Maldonado and Anny Baez - Mentor: Professor Farrukh Zia

Computer Engineering Technology Department

Roboqueen is a persistent research project in the Computer Engineering Technology Department. It is being designed as a full body interactive robotic mannequin in response to the needs of the fashion technology industry. The Roboqueen's hardware circuits and components will be improved and updated with the help of 3D printed electronic, embedded circuits and sensors. These custom 3D printed devices and circuits will be used to add functionality and features to the Roboqueen project. Thus, a challenge is proposed to use MATLAB, to study forward and inverse kinematic equations and their solutions in 3D, to control the body movements. Furthermore with the upgraded hardware the movements of the robot are more fluent compared to the previous version.

INTRODUCTION

There are two aspects of the project; hardware and software. The 3D body profile is designed using cardboard segments and 3D CAD tools to image a human body. The voice synthesis and recognition that's synced with the bar graph lips and RGB LED based eyes helped attained this purpose. Besides, we are using Blynk to control the head and arm movement in a synchronized way based on kinematic calculations.

HARDWARE & PARTS LIST

The hardware for this project includes extruded aluminum frame and 3D laser cut cardboard body, two microcontrollers (Arduino and Raspberry Pi), 8 servo motors, USB microphone, probe sensor, audio amplifier and speakers. Two RGB LEDs for the eyes, LED for the lips and AC / DC power supplies are also used.

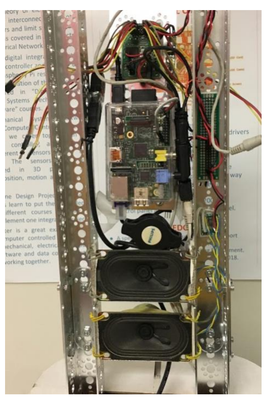

BLOCK DIAGRAM

The diagram below displays a detailed chart of the electrical circuit built on Roboqueen.

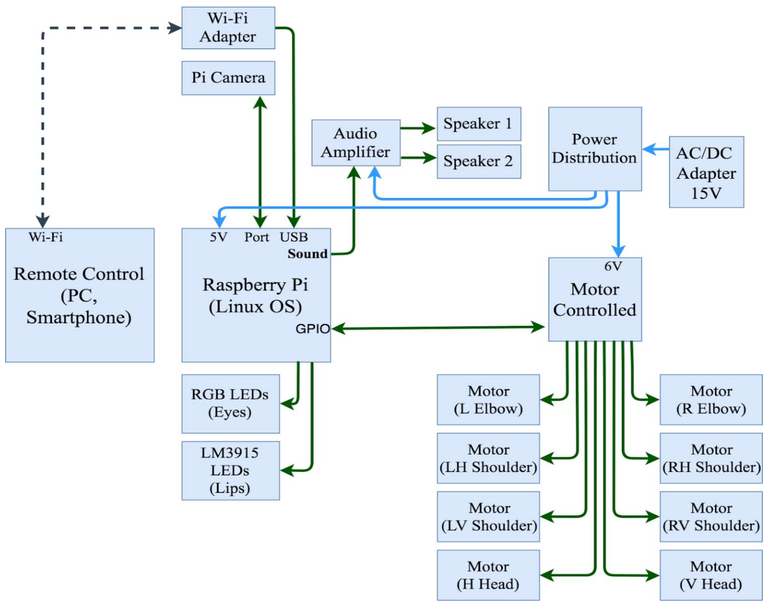

ELECTRICAL CIRCUIT

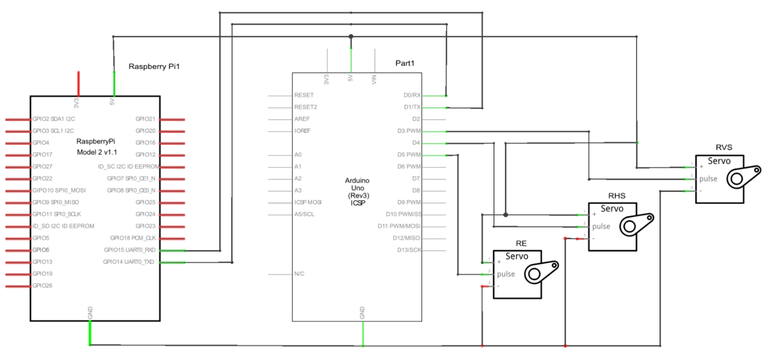

ACKNOWLEDGEMENTS

Emerging Scholars Program 2019

CUNY Research Scholars Program 2019

PROGRAM CODE

The code shown to the right shows a simulation run in MATLAB. This simulation helps us discover the angles needed to move the arms in 3D dimensions (X, Y, and Z Axis).

```
scara = cgr_create(theta, d, a, alpha, offset, type, base, ub, lb);
scara = cgr_self_update(scara, [0; 0; 0]);
g = ncgr_plot(g, scara);

pause(1);
scara = cgr_self_update(scara, [0; 0; 0]);
g = ncgr_plot(g, scara);

pause(1);
scara = cgr_self_update(scara, [0; 0; 0]);
g = ncgr_plot(g, scara);

%% inverese kinematics
[q, k, err]= cgr_ikine1(scara, [0.5; 0.5; -0.5], 0.01, 100);
scara = cgr_self_update(scara, q);
g = ncgr_plot(g, scara);
pause(0.1);
```

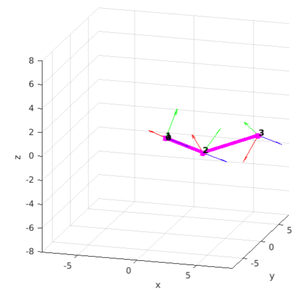

CONCLUSION & FUTURE WORK

The advances that have been implemented and improved in terms of movement the mounting frame of the servomotor, open up the possibilities of future improvements that can be implemented not only for Roboqueen but also for other projects involving the servomotors. In addition, improvements will be made in speech synchronization with communication with arm and head movements.

REFERENCES

Instructables. "Robotic Claw Business Card." *Instructables Workshops*, Instructables, 1 Nov. 2017, www.instructables.com/id/Robotic-claw-business-card/.

Students' Perceptions of the Impact of Peer-led Workshops on their Team-working and Problem Solving Skills

David Mastalerz, Faculty Mentor: Melanie Villatoro

Construction Management & Civil Engineering Department, New York City College of Technology, CUNY

Abstract

The Department of Construction Management and Civil Engineering Technology (CMCE) has incorporated Peer Led team Learning (PLTL) in the CMCE 115 Statics course since 2015. The implementation of PLTL has contributed to increased pass rates and decreased withdrawal dates in this critical course. Statics is the first course in the four course design sequence required for all Associate and Bachelor Degree students. The study will explore students' perceptions of the benefits of PLTL workshops on their team working and problem-solving skills. The workshops are facilitated by Peer Leaders and are designed to promote team-working and problem-solving skills. This study seeks to measure students perceptions of their improvement of these skills. The participants in the study are the students attending the weekly one-hour peer-led workshop over the course of one semester. Data will be collected through surveys, and organized, analyzed, and presented in a poster.

Introduction

Peer-led team learning (PLTL) is an innovative model in science education. Student-leaders (peers) guide the activities of small groups of students in weekly Workshop meetings. The students work through challenging problems that are designed to be solved cooperatively. The peer leaders are trained to ensure that the students are actively and productively engaged with the material and with each other. This methodology offers a number of educational opportunities: the supportive format encourages questions and discussions that lead to conceptual understanding; students learn to work in teams and to communicate more effectively; peer leaders learn teaching and group management skills. The purpose of this study is to examine the students' perceptions of the effects of the peer-led workshop on their problem solving and team-working skills.

Literature Review

The PLTL model encourages students to actively engage in their own learning. Differing from traditional cooperative learning strategies, however, this model provides guidance to the students in a setting outside of lecture and without teacher intervention [Deming, 2001]. Since its conception, PLTL has been introduced into other undergraduate science courses, including organic chemistry, biology, and anatomy and physiology [Julia Snyder-Jason Wiles 2015]. In the PLTL model, students work in small groups of six to eight students led by an undergraduate peer who has previously taken and been successful in the course. Peer leaders work collaboratively with the course instructor to facilitate small group problem-solving after being trained in learning theory, pedagogical methods, and the conceptual content of the course [Roth V 1998]. Leaders are not experts in the content, nor are they expected to provide answers to the students in their workshop groups. Rather, they guide and mentor students to develop their own understanding of concepts. Of the many studies that have examined the effectiveness of the PLTL model, only one tested the model as a predictor of critical thinking gains. Quitadamo, Brahler, and Crouch [2009] examined the impact of PLTL on critical thinking gains in six undergraduate science and math courses at a research university in the Pacific Northwest. Results showed that the PLTL model had a positive impact on critical thinking gains in science, regardless of gender, ethnicity, or other variables. In addition, grade performance and retention improved, particularly for females.

Acknowledgment

Professor Nadia Kennedy and Armando Cosme

PLTL Program and CMCE Department

The project is supported by the Emerging Scholars Program at the New York City College of Technology, CUNY.

Research Questions

The study focuses on the following research questions:

1) Does the impact of peer-led workshops improve students' perception on their team-working skills?

2) Does the impact of peer-led workshops improve students' perceptions on their problem solving skills?

Data Collection

Data was collected using the online service, Surveymonkey. Two surveys were created, and each focused on one of the two research question. Each survey consisted of 6 questions. Both surveys were distributed to the students, who took part in the peer-led workshops of the Statics shortly after the students' first midterm exam. Below are the questions in each of the two surveys:

Q#1-6 for Research Question 1

1. The peer-led workshops have helped me to feel more confident solving problems with another peer.
2. The peer-led workshops have helped me to become better at communicating during teamwork.
3. The peer-led workshops have helped me to become a better listener during teamwork.
4. The peer-led workshops have helped me to become more comfortable working with others.
5. I have started to work more often on homework or test prep with a partner outside after class.
6. The peer-led workshops have helped me to come to like studying with a partner outside of class.

Q#1-6 for Research Question 2

1. The peer-led workshops have taught me to think about the process first before solving a problem.
2. The peer-led workshops have helped me to be more persistent in problem solving.
3. I am less willing to give up if I encounter problems I think are difficult.
4. I am more confident with the topics covered.
5. I try my own method in solving problems more frequently.
6. My problem solving skills have improved.

Data Analysis

Based on the surveys, we found that the students who are attending the PLTL workshops regularly perceive that they:

- Improved their communication skills.
- Improved their ability to work effectively with other students.
- Improved their listening skills.
- Improved their determination in solving problems.
- Improved confidence in solving problems
- Improved their thinking process in problem solving

The raw data from the surveys is given below.

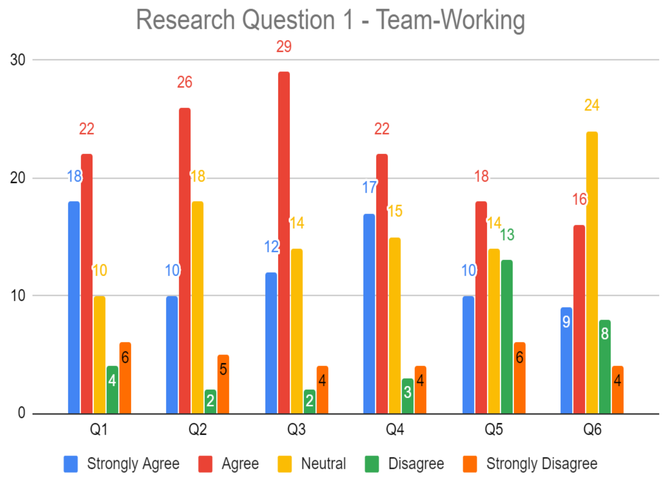

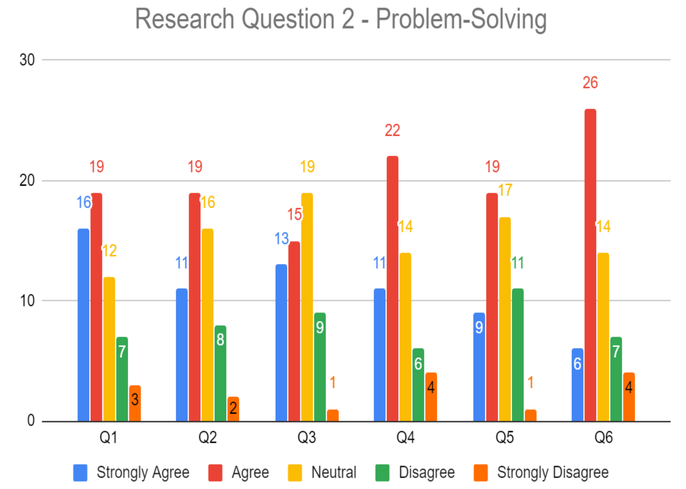

Results

Overall, 82% of the students perceived that there was improvement in their communication and interpersonal skills; this was greater than the previous 75% we received earlier this year. Most of the students agreed that working together was much better for them than working alone. About 81% of the students believe that they became better at explaining ideas, at listening more carefully, and became more comfortable working in a group. This was about the same as the previous 80%. Only 71% of the students felt that their thinking about the process of problem solving has improved. This improved from the previous 60%. Primarily the perception was that 78% of the students improved their problem solving skills. This was the biggest increase in our results from the previous 65%. In addition, most students felt that the workshop helped them to understand each other's ideas through interactions. In turn, this motivated students to work on the problems and find ways to solving them. Overall there was a clear consensus that the workshops had a positive impact on students' team-working and problem solving skills had improved as well.

Conclusions

The overwhelming perceptions of the students was that the peer-led workshops have helped them to improve both their team-work and problem solving skills. The biggest challenge was getting the students to begin conversing with one another because this workshop has not been integrated into more classes. This time around we were able to have more students complete our surveys. As such our results would have more credibility because of the larger sample size.

References

Quitadamo IJ, Brahler CJ, Crouch GJ (2009) *Peer-Led Team Learning: A Prospective Method for Increasing Critical Thinking in Undergraduate Science Courses.* Retrieved November 14th, 2019 from : https://ecommons.udayton.edu/cgi/viewcontent.cgi?referer=https://scholar.google.com/&httpsredir=1&article=1042&context=dpt_fac_pub

Cracolice MS, Deming JC (2001) *Peer-Led Team Learning.* Retrieved November 14th, 2019 from : https://search.proquest.com/openview/20361828617f570ced688fc7199c6d7c/1?pq-origsite=gscholar&cbl=40590

Julia Snyder-Jason Wiles (2015) *Peer Led Team Learning in Introductory Biology: Effects on Peer Leader Critical Thinking Skills*. Retrieved November 14th, 2019 from : https://journals.plos.org/plosone/article?id=10.1371%2Fjournal.pone.0115084

Gosser D, Roth V (1998) *The Workshop Chemistry Project: Peer-Led Team Learning. Journal of Chemical Education.* Retrieved November 14th, 2019 from: https://pubs.acs.org/doi/abs/10.1021/ed075p185

Study of Communication Delay in Servo Actuator Networks

Student: Gene Nadela Faculty Mentor: Dr. Xiaohai Li
Department of Computer Engineering Technology | City Tech Robotics Research Lab | www.citytechrobotics.org

Abstract

Robotics has seen greater widespread use and implementation in recent decades. Automating complex tasks in industry will require a proportionally complex robotics system. It becomes necessary to examine the effect of a large network of servos (an important component in robotic systems) on the communication delay between command and action. Communication delay will have a fundamental impact on system's stability and performance. An experimental study of the delays through the servo network will help us analyze and ensure stability of the system. To accomplish this, we developed an experimental apparatus which will determine the time delay between the system controller and the servo action. We then compare the effect of a single servo to three servos, then six, then nine servos. Across hundreds of trials, we determined that there is little difference in the time delay when increasing the number of servo motors in a network.

Introduction

The motivation of this study is a result of the development of a bipedal humanoid robot, which uses up to twenty AX12 servos simultaneously in order to perform functions such as legged locomotion. AX12 servos are high performance servos capable of precise position control, and are also capable of continuous rotation, making them useful in developing particularly complicated robots. Demonstration of this system may be viewed at the following URLs:

https://youtu.be/M-Mx4f-Z-WA
https://youtu.be/ItA4fxoOeQk

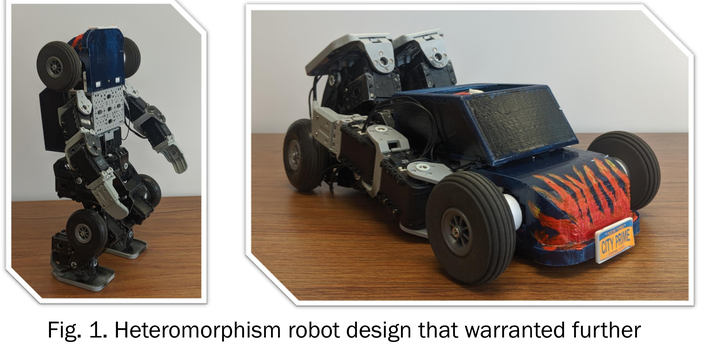

Fig. 1. Heteromorphism robot design that warranted further study of servo networks.

Methodology

To determine the delay between the microcontroller command signal and the servo response, an oscilloscope probe is placed at the signal wire between the microcontroller and the servo, while another probe is similarly placed at the voltage wire, between the supply and the servo. As the command is executed, the microcontroller sends out a command packet to the servo, and the servo will draw current from the power supply in order to move. This procedure is done on a single servo setup, a three servo setup, a six servo setup and a nine servo setup.

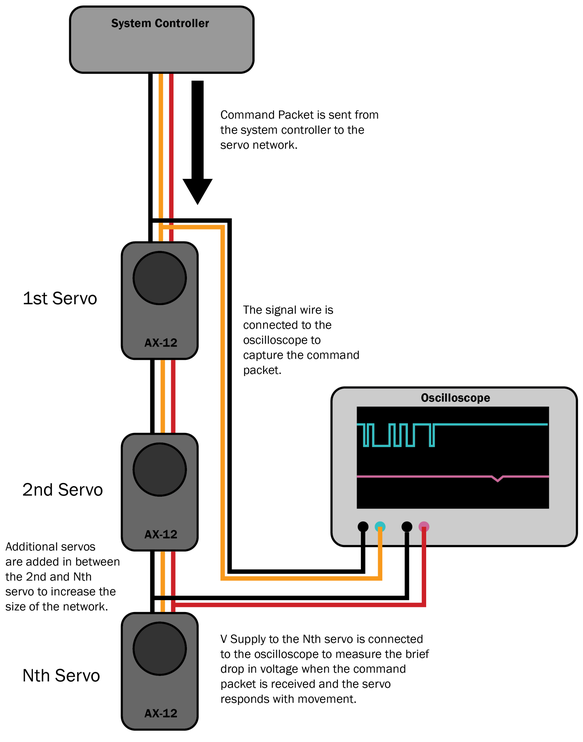

Fig. 2. Diagram of the experimental apparatus that is used for all servo network setups.

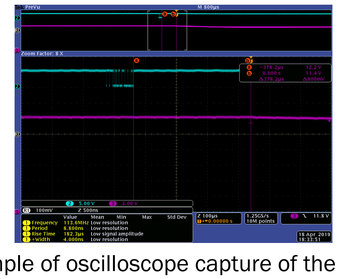

Fig. 3. Example of oscilloscope capture of the servo response.

Results

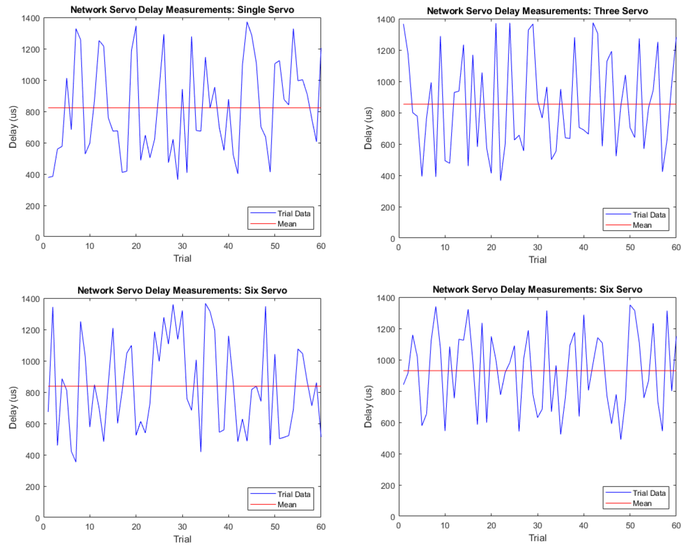

Sixty trials were performed for each setup, making for a total of 240 trials:

- Single servo setup had a mean delay of 822.95 us.
- Three servo setup had a mean delay of 854.25 us.
- Six servo setup had a mean delay of 837.63 us.
- Nine servo setup had a mean delay of 876.71 us.

Conclusion

Based on the results, we can conclude that the communication delay between the control signal and the servo response is largely not affected by increases in the number of servos in the network.

References

[1]. Smith, J. and Jivraj, J. *Analysis of Robotis Dynamixel AX-12+ Actuator Latencies.* Symposium on Brain, Body and Machine. Montreal, Canada. Nov. 2010.
[2]. Mensink, A. *Characterization and modeling of a Dynamixel Servo.* University of Twente. (2008).
[3] *Dynamixel AX-12 User's Manual*. Robotis. Seoul, South Korea. (2006).

Morgan Injection Molding Machine

Abel Tapia, Dany Nolasco, Prof. Angran Xiao

New York City College of Technology

Abstract

In this project, the professor and students in Department of Mechanical Engineering Technology will set up a Morgan Press injection molding machine and experiment injection molding using 3D printed molds. The main task in this semester is to design an injection mold using the measurements of the table pan. Most of the work so far are focused on creating a computerized model of the mold, which lays the foundation for the following activities including 3D printing and CNC machining of the mold.

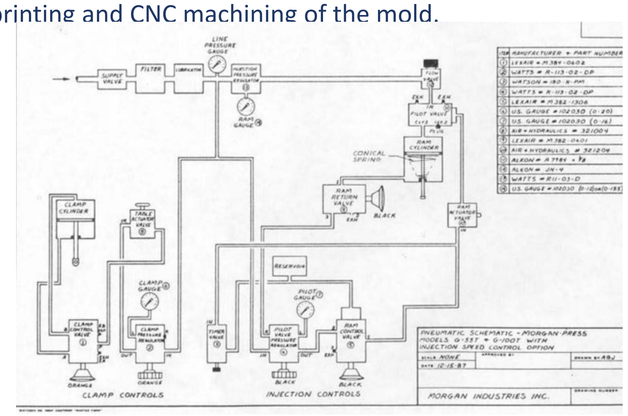

Background

The plastic industry is one of the fastest growing major industries in the world. The *Morgan-Press Injection Modeling Machine* is a good example of a machine used today to produce plastic production. The *Morgan-Press Injection Modeling Machine* developed to make injection molding of plastic parts practical and cheap in the quantities for fast prototyping and low-volume production. It provide services from tool design, to manufacturing feasibility, to production runs of simple and complex parts and multi-component assemblies, low-risk, low-cost alternative option to get prototypes and samples developed by plastic injection molders. The *Injection Modeling Machine can be found in* model shops, medical device manufacturers, research & development labs/projects, many educational institutions research.

Method

1. Remove the Injection Molding Machine from its wooden container.
2. Set the machine on the workbench where it will be operated before installing the Temperature Control System. The control system is fragile so it is best not to physically move the machine with control cabinets attached. Mount machine to a bench or table for this part of the project faculty and our mentor in the Mechanical Engineering Technology work together.
3. Install Temperature Control Systems there will be two heat controls with a temperature range 32-800F that provides the machine melting capability. They are located in a separate electrical cabinet mounted on the left side of the Mount Plate. The chart on the front of the table platen is a general guide to temperature setting required for various material. When ready to operate plug the machine into a 120 volt, 20-amp electrical outlet using the three-conductor cord supplied. If an extension cord is used, it should be as short as possible and constructed with 14 gauge wire.
4. The machine is equipped with Injection Speed Control installed the hose, muffler, and pressure control.
5. Connect main air supply to ¼ FPT air inlet fitting in rear base of machine
6. The machine is now ready for operation

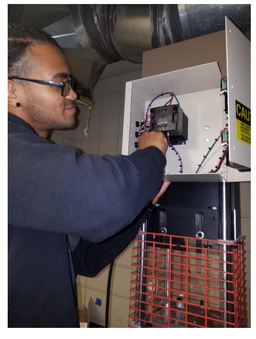

Molding Specification Table

DEFECT	POSSIBLE CAUSES	CORRECTIVE ACTION
Mold not full(short shot)	Material too cold Mold too cold Insufficient cavity venting of mold Injection pressure too low Time cycle too short Gates and/ or runners too small	*Raises Barrel and nozzle zone temperatures *Apply heat to mold Rework mold to allow more venting *Raises injection pressure Increase the size of runners and gates
Flashing at mold parting lines	Injection pressure too high for clamp force selected	*Lower in injection pressure or raise clamp force, or both
Part discolored	Heat to high Cycle time too long	*Lower selected temperatures Shorten cycle time
Excessive "sink" in part	Part design Injection pressure too low Gate too small Cycle time too short Material too hot Mold too hot	Avoid thick sections *Raise injection pressure Adjust mold to allow more gating Increase injection cycle time *Lower nozzle and barrel temperatures *Cool mold
Surface of part streaked, blistered, and/or bubbles in part	Moisture in material granules Material temperature too high	*Dry material thoroughly before molding * Lower nozzle and barrel temperatures

Conclusion

Although the machine is still in the process of being assembled due to lack of parts, we were able to make a 3-D design model of one part of the mold pieces. Once all parts are ordered the machine will be fully operational coming of the next ESP semester. Along with that there will be a 3-D printed version of the completed mold design.

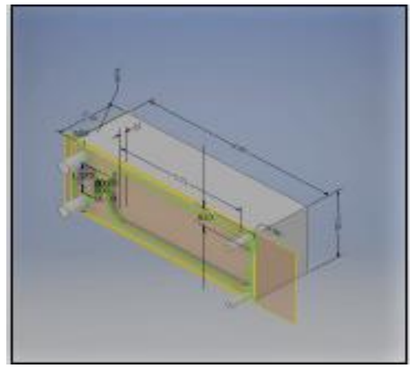

Acknowledgements

This project is supported by the Emerging Scholars Program at New York City College of Technology with Proof A Xiao

1. www.morganindustriesinc.com
2. Morgan-Press Injection Molding Machine Operating Instructions
3. Cutting costs in short-run plastics injection molding
4. https://www.homedepot.com/p/1-2-in-x-260-in-PTFE-Tape-0178502/202280370
5. https://www.mcmaster.com/general-purpose-hose
6. https://www.mcmaster.com/pilot-valves

Characterization of one of tetrahymena Thermophila calpains using bioinformatics tools.

Titilope Odumuwagun, Ralph Alcendor, PhD, New York City College of Technology

Introduction

Tetrahymena thermophile are free-swimming freshwater protists that are surprisingly useful for multiple interesting questions in biology. They're a predatory species that will eat anything that fits in their mouth. These cells are free-living unicellular organism that belongs to the ciliated Protozoa, a major, ecologically successful monophyletic group of unicellular eukaryotes. Their closest known relatives, Dinoflagellates and Apicomplexans, which include Plasmodium and other obligate parasites, are also unicellular (Orias, 2011). **Calpains** are a group of calcium-sensitive cysteine proteases that are ubiquitously expressed in mammals ans many other organism. This family contains 14 members with μ-calpain (calpain 1) and m-calpain (calpain 2) being the most well-characterized (Siklos, 2015).

Calpains are regulated by Ca2+ concentration, phosphorylation, calpastatin and probably by altering their subcellular localization (limiting access to substrate). These endopeptidases have numerous functions including, but not limited to, remodeling of cytoskeletal attachments to the plasma membrane during cell fusion and cell motility, proteolytic modification of molecules in signal transduction pathways, degradation of enzymes controlling progression through the cell cycle, regulation of gene expression, substrate degradation in some apoptotic pathways, and an involvement in long-term potentiation (Tocris Bioscience, 2019)

Perturbations in calpain activity have been associated in pathophysiological processes contributing to type II diabetes (calpain 10), Alzheimer's disease (calpain 1), gastric cancer (calpain 9) and muscular dystrophy (calpain 3).

Bioinformatics tools that have aided in highlighting differences and similarities between genomic computational analysis which include phylogenetic trees and cladograms were used throughout the project. These tools includes BLAST (basic local alignment searching tool), Multiple sequence alignment tools (MAFFT (multiple alignment using fast Fourier transform), T.Coffee , MUSCLE(multiple sequence alignment of protein and nucleotide sequences)) . Other bioinformatics tools that ere used in these project are MEGA (molecular genetics analysis) and VMD(Visual Molecular display)

Objective/Hypothesiss

The purpose of this project was to characterize one of *Tetrahymena thermophila* calpain. We hypothesize *T. thermophila* calpains are similar to human calpains, therefore, information from human calpains can be used to identify the function, localization and other characterization of *T.thermophile calpains.*

Methods and Materials

Teterahymena Genome Database Wiki : To obtain information on the genome, genes, and proteins of Tetrahymena. For theses project used the database to extract information on TTHERM_00529560 gene.

NCBI BLAST (The Basic Local Alignment Search Tool)

To find regions of local similarity between sequences. The program compares nucleotide or protein sequences to sequence databases and calculates the statistical significance of matches

MULTIPLE SEQUENCING ALIGNMENT TOOLS: To align the full calpain gene of interest as well as its domain with the full sequences of all human calpains as well as its domain level .

- MAFFT (multiple alignment using fast Fourier transform)

To create multiple sequence alignments of amino acid or nucleotide sequences.

- MUSCLE(multiple sequence alignment of protein and nucleotide sequence)

To perform multiple sequence alignment. MUSCLE is claimed to achieve both better average accuracy and better speed than ClustalW2 or T-Coffee,

- T.coffee: To align sequences or to combine the output of your favorite alignment methods into one unique alignment.

MEGA (molecular genetics analysis). To conduct automatic and manual sequence alignment, inferring phylogenetic trees, mining web-based databases, estimating rates of molecular evolution, and testing evolutionary hypotheses.

VMD (Visual Molecular Dynamic) To display, animate, analyze and draw the structure of the gene of interest, human calpain 15 and human calpain 7.

Results

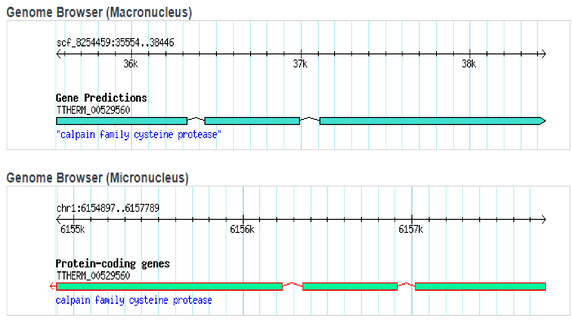

Figure 1: Macro and micro nuclei gene structure of TTHERM_00529560. Both have 2 introns and 3 exons.

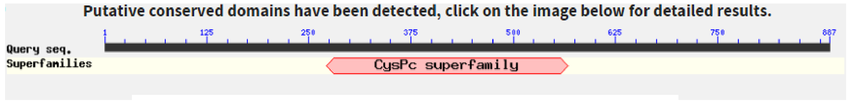

Figure 2: Conserve domain of TTHERM_00529560. Like other calpains, it has the CysPc conserve domain.

Description	Max Score	Total Score	Query cover	E-value	Per. Iden	Accession
homolog (Drosophila)	58.9	58.9	28%	1.00E-07	23.31%	AAH21854.1
calpain-15 isoform X2	59.3	59.3	28%	1.00E-07	23.31%	XP_011520928.1
calpain-15 isoform X4	58.9	58.9	28%	1.00E-07	23.31%	XP_011520930.1
calpain-15 isoform X1	58.9	58.9	28%	1.00E-07	23.31%	XP_011520922.1
calpain-15 isoform X3	58.9	58.9	28%	1.00E-07	23.31%	XP_011520929.1
calpain-11 isoform X5	58.2	58.2	35%	2.00E-07	21.62%	XP_006715050.1

Table 1: Result from BLAST. TTHERM_00529560 is more closely related to human calpain 15. The max score help to determine which one is most closest to the Te*terahymena* calpains.

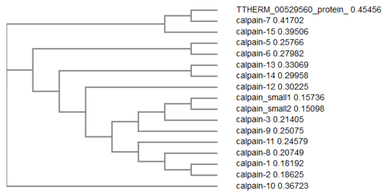

Figure 3 :: Cladogram structure after comparison with human calpains using MUSCLE. Human Calpain 15 is most closely related to TTHERM_00529560

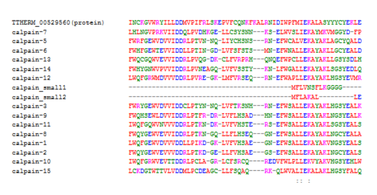

Figure 4:There are 2 conserved amino acid observed and one column with an identical sequence in the alignment

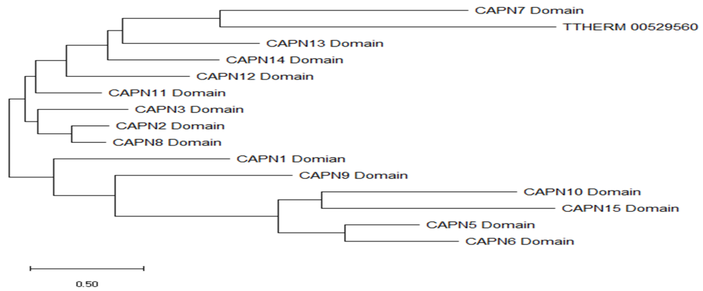

Figure 5: The phylogenic structure of mega maximum shows Calpain 15 domain is most closely related to TTHERM _00529560

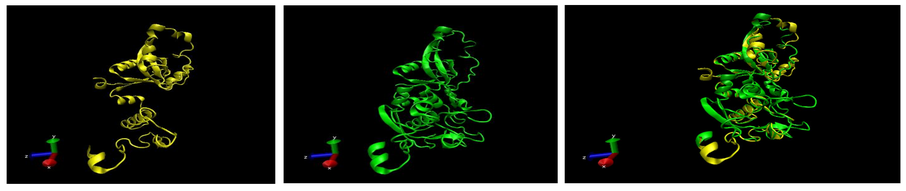

A B C

Figure 28: Structure of human Calpain 7 and TTHERM _00529560 shows a similar structure implying how nearly closely related they are. The structure has a QH number 0.6671 , a RMSD of 1.5685 and a percent identity of 11.55

Summary of Results

- Both macro and micro nuclei of **TTHERM_00529560** consist of three exons and two introns.
- TTHERM_00529560, like other calpains, contains a CysPc domain
- BLAST query showed TTHERM_00529560 is more closely related to human calpain 15, with a max score 59.3 and percent identity of 23.31%.
- T-Coffee and MAFFT showed TTHERM_00529560 is more closely related to calpain 7.
- Phylogenic tree analysis using MEGA and Phylogeny.fr showed TTHERM_00529560 is more closely related to calpain 7.
- VMD analysis comparing the domains of TTHERM_00529560 with domains of calpain 7 and 15, as more closely related to calpain 7.

Conclusion

These results suggest TTHERM_00529560 may be more closely related to human calpain 7. The similarity between these two genes may help with providing location and function of TTHERM_00529560

Future Studies

More analysis is required to confirm the similarity of these genes. Other bioinformatics analysis could involve examining the localization of TTHERM_00529560 and comparing it with calpain 7.

References

E. Melloni, S. Pontremoli, The calpains, Trends in Neurosciences, Volume 12, Issue 11, 1989, Pages 438-444,

The EMBL-EBI search and sequence analysis tools APIs in 2019.

(PMID:30976793) Madeira F, Park YM, Lee J, Buso N, Gur T, et al. Nucleic Acids Res. [2019]

Calpains. (n.d.) *Collins Dictionary of Medicine*. (2004, 2005).

Calpain research for drug discovery: challenges and potential, Yasuko Ono et al , *Nature Reviews Drug Discovery* **volume 15**, pages 854–876 (2016)

Tocris Bioscience. (2019). *Pharmacology*. [online] Available at: https://www.tocris.com/pharmacology/calpains [Accessed 3 Dec. 2019].

Siklos, M., BenAissa, M., & Thatcher, G. R. (2015). Cysteine proteases as therapeutic targets: does selectivity matter? A systematic review of calpain and cathepsin inhibitors. *Acta pharmaceutica Sinica. B*, *5*(6), 506–519. doi:10.1016/j.apsb.2015.08.001

Orias, E., Cervantes, M. D., & Hamilton, E. P. (2011). Tetrahymena thermophila, a unicellular eukaryote with separate germline and somatic genomes. *Research in microbiology*, *162*(6), 578–586. doi:10.1016/j.resmic.2011.05.001

Acknowledgements

Special thanks to CUNY, Biological sciences dept., BIB program, Emerging scholar and our mentor Professor Ralph Alcendor.

Characterization TTHERM_00190820, a *Tetrahymena Thermophila* Calpain Family Member

Ebunoluwa Okunade, Ralph Alcendor, New York City College of Technology

Introduction

Calpains are proteins that are members of the calcium-dependent protease family, found in different organisms[1]. Calpains are involved in various cellular processes such as apoptosis, cellular proliferation, and cell motility. Although calpains are dependent on calcium in order to be activated, but they could also go through ERK-mediated phosphorylation in order to be activated[2]. Over the course of a few years, Calpains have been studied in different organisms to find out the functionality of these proteins. Humans have 15 different Calpains. Many of these have been characterized however, more information is still needed on their full function.

Tetrahymena thermophila is a ciliate that exhibits nuclear dimorphism; which is when an organism has two different kinds of nuclei in a cell. It has a macronucleus which is the nucleus that controls the non-reproductive cell functions, while micronucleus is the nucleus which controls the cell's reproductive functions. Therefore, since it carries out different functions and biological properties similar to humans and other mammals, this makes it a model experimental organism for biologists. *Tetrahymena thermophila* is a ciliate that alternates between sexual and asexual stages in its life cycle[6]. When in a nutrient rich media during vegetative growth, the cells usually reproduce asexually through binary fission. However, in starvation conditions(dehydration…) cells will reproduce through sexual conjugation. If there is a mating strain *T.thermophila* can mate with any of the other mating types(6) without preferring anyone [6].

In this research, a *Tetrahymena thermophila* calpain gene was selected and queried using Basic Local Alignment Search Tool (BLAST) . The goal was to see which human calpain the *Tetrahymena thermophila* calpain is more similar to. Identifying the similarities in structure can help identify the function of a gene. In addition, different bioinformatic tools like Multiple Alignment using Fast Fourier Transform (MAFFT), Tree based Consistency Objective Function For alignment Evaluation (T-Coffee), and Multiple Sequence Comparison by Log- Expectation (MUSCLE), were also used to derive the phylogenetic tree, cladogram, and alignments of the *T.thermophila* protein sequence with the human genome calpain sequence and the human calpain domain with TTHERM_00190820 domain sequence. In addition, Molecular evolutionary genetics analysis (MEGA) and Phylogeny.fr were used for constructing phylogenetic tree, and Visual Molecular Dynamics (VMD) was used to visualize the molecular structure of the calpains with TTHERM_00190820. This research investigated that *Tetrahymena thermophila* calpain gene will be similar to that of one of the human calpain.

Objective/Hypothesis

Using bioinformatics tools to derive information about TTHERM_00190820. Our hypothesis is that TTHERM_00190820 will have similar structure and function to one of human Calpains.

Methods and Materials

Tetrahymena Genome database wiki

The protein sequence of TTHERM_00190820 was taken from this database.

Basic Alignment Search Tool (BLAST)

Protein sequence of TTHERM_00190820 was compared with the database to confirm that the sequence was that of *Tetrahymena thermophile.* The sequence was then compared to *Homo sapiens* protein sequences.

Multiple Sequence Alignment tool and phylogenetic tree

MAFFT, T-COFFEE, and MUSCLE were used to align the full human calpain sequence with TTHERM_00190820 protein sequence. The human calpain domain sequence was also aligned with TTHERM_00190820 domain sequence T-Coffee and MUSCLE constructed a cladogram. In addition, phylogeny.fr, MAFFT and MEGA were used to construct the phylogenetic tree using protein and domain sequences of the calpains and TTHERM_00190820 gene.

Visual Molecular Dynamics (VMD)

Visualization of the molecular structure of the calpains, and TTHERM_00190820 gene

Results

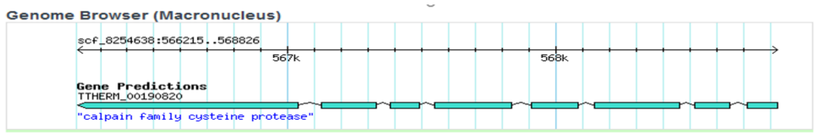

Figure 1: Macro nuclei gene structure of TTHERM_00190820. It has 7 introns and 8 exons

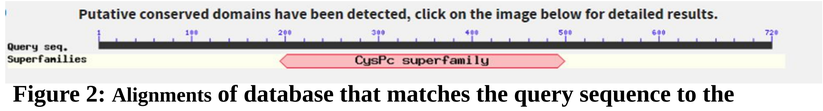

Figure 2: Alignments of database that matches the query sequence to the reference sequence.

Description	Max Score	Total Score	Query Cover	E value	Per. Ident	Accession
homolog (Drosophila)	94.4	94.4	45%	6.00E-19	24.03%	AAH21854.1
calpain-15	91.7	91.7	45%	7.00E-18	23.97%	NP_005623.1
calpain-15 isoform X4	91.7	91.7	45%	8.00E-18	23.97%	XP_011520930.1
calpain-15 isoform X1	91.3	91.3	45%	1.00E-17	23.97%	XP_011520922.1
calpain-15 isoform X2	91.3	91.3	45%	1.00E-17	23.97%	XP_011520928.1
calpain-15 isoform X3	91.3	91.3	45%	1.00E-17	23.97%	XP_011520929.1
calpain 11, isoform CRA_d	63.5	63.5	40%	2.00E-09	24.20%	EAX04253.1
calpain-11 isoform X5	63.5	63.5	40%	3.00E-09	24.20%	XP_006715050.1
calpain-11 isoform X1	63.5	63.5	40%	3.00E-09	24.20%	XP_006715047.1
calpain-11 isoform X4	63.5	63.5	40%	3.00E-09	24.20%	XP_011512577.1

Table 1:Results from BLAST that shows gene similarity between calpain found in humans and TTHERM_00190820

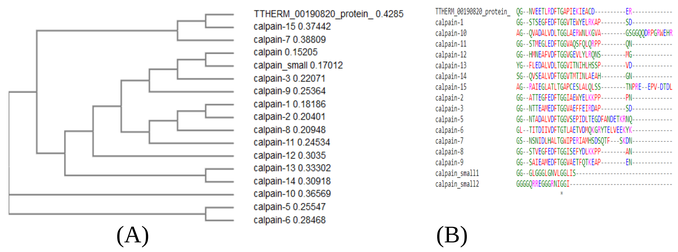

Figure 3: (A) Cladogram result from T-Coffee which shows that human calpain 15 is the closest to TTHERM_00190820. (B) Multiple sequence alignment from T-COFFEE. There is 1 column with identical sequence from the alignment result

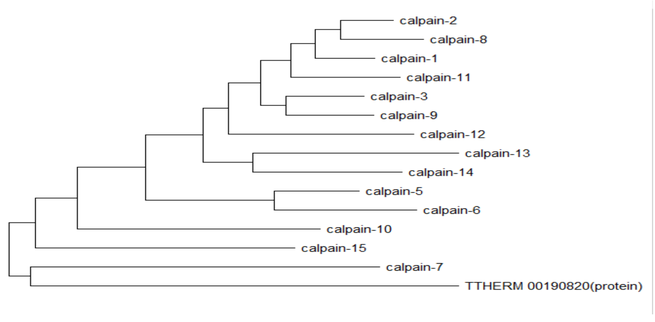

Figure 4: MEGA result shows that Calpain 7 is the closest to TTHERM_0019082

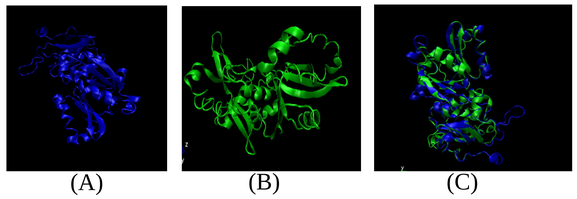

Figure 5: (A)The structure of calpain 7. (B) The structure of the gene of interest . (C) The molecular structure of the gene of interest and calpain 7 using the domain sequences. gene of Interest=green, calpain 7= Blue.

Summary of Results

- TTHERM_00190820 macro and micro nuclei both contains 7 introns and 8 exons.
- As a calpain family member it contains a CysPc domain which is about 300 amino acid long.
- BLAST showed TTHERM_00190820 is more closely related to human calpain 15
- T-Coffee and MAFFT multiple sequence alignment and cladogram suggested TTHERM_00190820 is also more closely related to human calpain 15, while MEGA showed it is more closely related to calpain 7.
- Further analysis using MEGA and Phylogeny.fr suggested TTHERM_00190820 is more closely related to calpain 7.
- VMD protein structure analysis indicated TTHERM_00190820 is more closely related to human calpain 7.

Conclusion

These results demonstrate that TTHERM_00190820 may be more closely related to human calpain 7, although more analysis is required. Confirming these results would suggest that TTHERM_00190820 may share similarities in location and function with human calpain 7.

Future Studies

Future experiments can include more computational analysis to characterize other *Tetrahymena thermophila* calpains. In addition, other types of bioinformatics tools could be used to further analyze the functionality and location of *Tetrahymena*.

References

1. Ohno, S., Emori, Y., Imajoh, S., Kawasaki, H., Kisaragi, M., & Suzuki, K. (n.d.). Evolutionary origin of a calcium-dependent protease by fusion of genes for a thiol protease and a calcium-binding protein? Retrieved from https://www.nature.com/articles/312566a0.

2. The ERK Signal Transduction Pathway. (n.d.). Retrieved from https://www.rndsystems.com/resources/articles/erk-signal-transduction-pathway.

3. Orias, E., et al. "*Tetrahymena thermophila*, a unicellular eukaryote with separate germline and somatic genomes". *Research in Microbiology.* 2011. Volume 162. p. 578-586

4. Calpain. (n.d.). Retrieved from https://www.sciencedirect.com/topics/neuroscience/calpain.

5. BLAST: Basic Local Alignment Search Tool. (n.d.). Retrieved from https://blast.ncbi.nlm.nih.gov/Blast.cgi.

6. TGD: Gene Details. (n.d.). Retrieved from http://ciliate.org/index.php/feature/details/TTHERM_00190820.

7. Cervantes, M. D., Hamilton, E. P., Xiong, J., Lawson, M. J., Yuan, D., Hadjithomas, M., … Orias, E. (n.d.). Selecting One of Several Mating Types through Gene Segment Joining and Deletion in Tetrahymena thermophila. Retrieved from https://journals.plos.org/plosbiology/article?id=10.1371/journal.pbio.1001518.

Acknowledgements

Special thanks to RF CUNY, CSTEP SURP, and my mentor Professor Ralph Alcendor.

Discovering Blockchain Technology

Tajamul Rabbani, Marcos S. Pinto

New York City College Of Technology

Abstract

A blockchain is a decentralized peer-to-peer network consisting of blocks also known as records. Each record is unique and contains a unique history that is added to the chain in chronological order after it is verified by several computers, known as nodes. Every block that is added contains a hash of the previous block linking them to each other, forming a chain hence the term blockchain. The data added to the blockchain is not immutable.

By allowing digital information to be distributed, but not copied, blockchain technology created the backbone of a new type of internet. It is this difference that makes blockchain technology so useful — representing an innovation in registering and distributing information, that eliminates the need for a trusted party to facilitate those relationships.

Technologies Utilized

Blockchains need to be extremely fast to be able to process several transactions in limited time and update them as fast across several nodes. To accomplish this, I used the following technologies:

- **.NET Core**
- **C#**
- **Blazor**
- **Bulma CSS**
- **HTML**

Blazor is a web framework which runs on ASP.NET Core server.

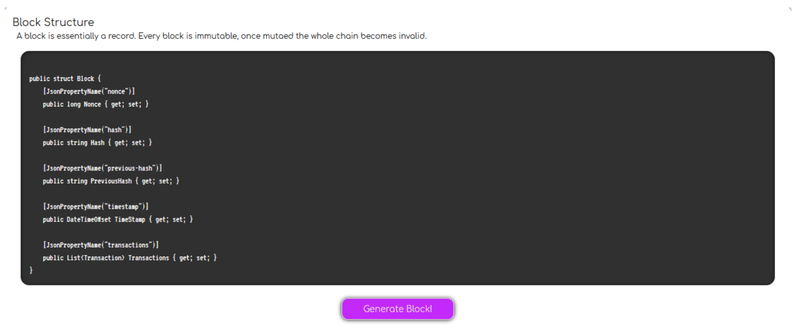

Background

Stuart Haber & **W. Scott Stornetta** were the first one to work on blockchain. In 2008, a person or group known as **Satoshi Nakamoto** were able to gestate blockchain by implementing it as the fundamental element in bitcoin cryptocurrency, to show and have a public ledger for all transactions.

To boil down, blockchain is a decentralized public ledger which removes the need for having any 3rd party authentication. It records all the transactions across many computers, if any block is altered the chain is invalidated.

Below an overview of bitcoin transactions can be seen from 2009-present.

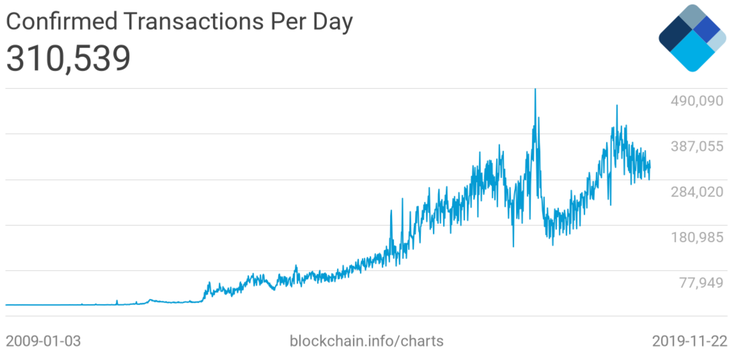

All transactions taking place on Keybase Space Drop account:

115637166901751809	[Keybase Space Drop] GDV4…JT53 transferred 688.4065454 XLM to GBTD…A4PK.	22 Nov 2019 22:56:23 UTC
115637166901747713	[Keybase Space Drop] GDV4…JT53 transferred 688.4065454 XLM to GCMS…ZR46.	22 Nov 2019 22:56:23 UTC
115637166901743617	[Keybase Space Drop] GDV4…JT53 transferred 688.4065454 XLM to GDCC…2SKL	22 Nov 2019 22:56:23 UTC
115637166901739521	[Keybase Space Drop] GDV4…JT53 transferred 688.4065454 XLM to GB34…FIRB.	22 Nov 2019 22:56:23 UTC
115637166901735425	[Keybase Space Drop] GDV4…JT53 transferred 688.4065454 XLM to GDSM…HH37.	22 Nov 2019 22:56:23 UTC
115637166901731329	[Keybase Space Drop] GDV4…JT53 transferred 688.4065454 XLM to GCOJ…EHNC.	22 Nov 2019 22:56:23 UTC
115637166901727233	[Keybase Space Drop] GDV4…JT53 transferred 688.4065454 XLM to GCGG…E46Y.	22 Nov 2019 22:56:23 UTC
115637166901723137	[Keybase Space Drop] GDV4…JT53 transferred 688.4065454 XLM to GCIR…EV22.	22 Nov 2019 22:56:23 UTC
115637166901719041	[Keybase Space Drop] GDV4…JT53 transferred 688.4065454 XLM to GDBM…S3WS.	22 Nov 2019 22:56:23 UTC

Usages

Besides cryptocurrency, blockchain is used in several industries ranging from automotive to health care. Here are a couple of industries that utilize blockchain technology:

- **Government**
- **Waste Management**
- **Health care**
- **Payment processing**
- **Supply chains**
- **Music**
- **Shipping**
- **Digital IDs**

Example

For my research project, I created a .NET Core Blazor server. The following objects were created to represent a blockchain:

- **Block**
- **Transaction**
- **Blockchain**

Since, the project is a web application temporary blockchains can be created by accessing the web interface.

Sample output below:

Acknowledgements

I'd like to thank Professor Marcos S. Pinto for having me on this research, it was an absolute honor and a wonderful experience to work with him.

I used the following GitHub repositories for my research. The actual application code can be found on my GitHub: **https://github.com/yucked/breadloaf**

- INNOQ, INNOQ Blockchain CSharp, 2019, GitHub Repository, **https://github.com/innoq/innoq-blockchain-csharp**
- Programming Blockchain, Programming Blockchain, 2019, GitHub Repository, **https://github.com/ProgrammingBlockchain/ProgrammingBlockchain**
- Hyperledger, Education, 2019, GitHub Repository, **https://github.com/hyperledger/education**

Light-Matter Interactions in Emerging Two-Dimensional Materials

Shaina Raklyar, German V Kolmakov, PhD

Polaritons in Transition Metal Dichalcogenides

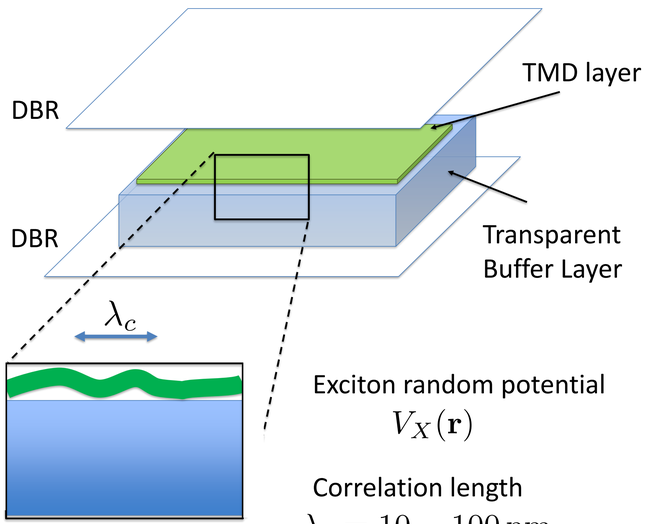

Exciton random potential

$V_X(\mathbf{r})$

Correlation length

$\lambda_c = 10 - 100\,\mathrm{nm}$

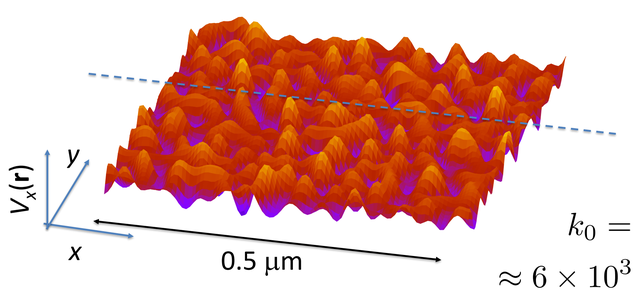

$k_0 = 2\pi/L$

$\approx 6 \times 10^3\,\mathrm{cm}^{-1}$

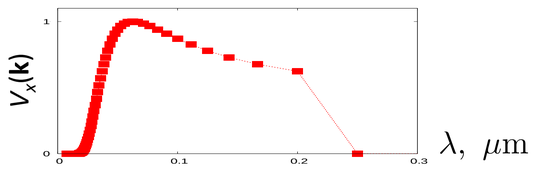

Energy Spectra

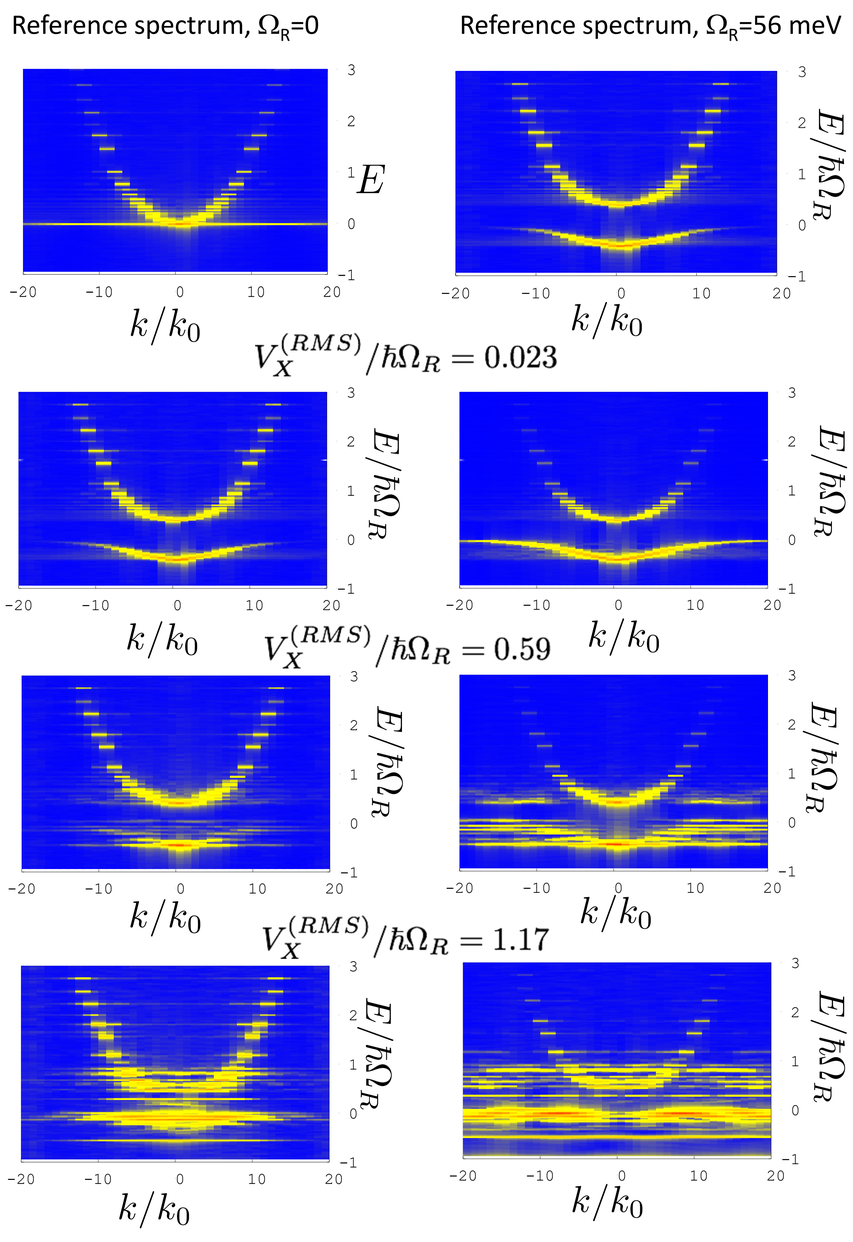

Long-Range Correlations in Topologically Disconnected TMD Flakes

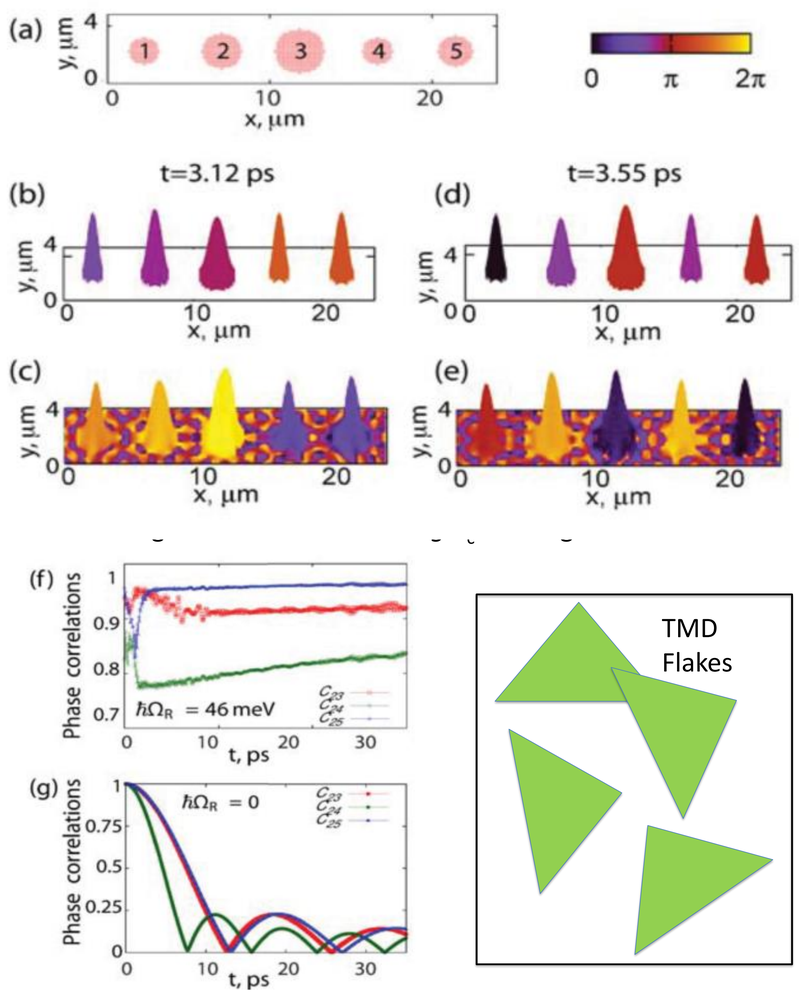

Numerical Simulations

- Mean-field two-component dissipative Gross-Pitaevskii equation

$$i\hbar\frac{d}{dt}\begin{pmatrix}\psi_C(\boldsymbol{r},t)\\ \psi_X(\boldsymbol{r},t)\end{pmatrix} = \left[\boldsymbol{H}^0 + \begin{pmatrix}-i\frac{\gamma_C}{2} & 0\\ 0 & V_X(\boldsymbol{r}) - i\frac{\gamma_X}{2} + g|\psi_X(\boldsymbol{r},t)|^2\end{pmatrix}\right]\times\begin{pmatrix}\psi_C(\boldsymbol{r},t)\\ \psi_X(\boldsymbol{r},t)\end{pmatrix}$$

$$\boldsymbol{H}^0 = \hbar\begin{pmatrix}\omega_C(-i\nabla) & \frac{1}{2}\Omega_R\\ \frac{1}{2}\Omega_R & \omega_X(-i\nabla)+\mu_X\end{pmatrix}$$ -- Linear Hamiltonian of cavity photons and TMD excitons

Conclusions

- Exciton polariton features persist in the energy spectrum even at strong disorder ~ Ω_R
- Strong exciton correlation established In topologically disconnected flakes due to exchange of virtual photons in the cavity

Acknowledgment

- Army Research Office grant # W911NF1810433 (SR, YP, GVK)

Synthesis of TiO_2 –$H_3PW_{12}O_{40}$ Composite Material, Characterization and Photocatalytic Studies

Farah Rammal and Dr. Ivana Jovanovic Ph.D.
Department of Chemistry, New York City College of Technology, CUNY

ABSTRACT

Due to an increase in industrialization and pollution, it is necessary to look into the remediation of polluted sites to eliminate contaminants. This study will focus on how TiO_2 based materials can be used as photocatalysts by improving its photocatalytic efficiency using polyoxometalates (POMs) such as Phosphotungstic Acid ($H_3PW_{12}O_{40}$ or PTA). TiO_2-PTA bounded molecules will be used to confirm the degradation of the Methylene Blue dye, a pollutant found in water and the reduction of silver metal cations ($AgNO_3$). This technique will allow researchers in determining how advanced photocatalytic materials can provide a significant solution for environmental cleanup as they allow for the complete oxidation of the pollutants and reduction of metals.

INTRODUCTION

Titanium Dioxide (TiO_2) is a naturally occurring metal oxide. Due to its high abundance, low-cost, and nontoxicity it is widely used as a photocatalyst. Photocatalysts have been extensively studied and are used as self-cleaning, self-sterilizing films, and cannot work without the use of light.[1] TiO_2 has a large energy gap of 3.2eV, therefore requiring exposure to ultra violet light in order to make TiO_2 particles photoactive. PTA is known for its fast reversible multi-electron redox reactions under mild conditions, electrochromism, and high thermal stability. [2] The binding of PTA on the surface of TiO_2 can help in charge separation in the UV illuminated TiO_2.

METHODS

PTA Functionalization of TiO_2

0.30 g of PTA was dissolved in 10 mL of distilled water in a glass vial. It was placed on a stir plate until the compound completely dissolved. 10mg of TiO_2 was added to the mixture and left to stir overnight.

The solution was centrifuged to separate the particles of TiO_2 coated with PTA. It was decanted to remove the supernatant, while leaving the particles behind. The particles were washed 3 times with water to remove unbound PTA and centrifuged to isolate particles again. Each wash was checked with UV-Vis spectrometer to observe if PTA was in the supernatant. (Fig.5)

Fig 1. TiO_2 – PTA in water

Photo degradation of Methylene Blue with TiO_2-PTA

A stock solution of Methylene Blue (MB) high concentration and low concentration were prepared. Two samples of 10mg of TiO_2 and 10mg of TiO_2-PTA were dispersed in 48ml of H_2O and 2 mL of the stock solution was added . The samples were placed in the dark for 30 minutes to allow the dye to attach to the surface. The samples were placed under UV light for 2h in order to activate photocatalysis. The absorbance peak was checked every 45 minutes to observe if the peak maximum of MB at 660 nm was decreased.

Fig 2. High concentration of MB with TiO_2 (left) and TiO_2 +PTA (right) under UV light; MB has not degraded completely with TiO_2-PTA.

Fig 3. Low concentration of MB with TiO_2 (left) and TiO_2 +PTA (right) under UV light; the MB has significantly degraded over time.

TiO_2 +PTA as a Photocatalyst for Precipitation of Metal Cations

A 10mM solution of $AgNO_3$ was prepared. 3.1 ml of $AgNO_3$ was added to 2.5 ml of TiO_2-PTA in water with 0.6 ml of 2-propanol. This was placed under UV light on a stir plate. In 30 minutes a gray-black precipitate was observed, showing a reduction of Ag^+ to Ag.

Fig 4. The white solution (left) is prior to using UV light, the gray-black solution (right) is the result of the reduction of Ag under UV light

RESULTS

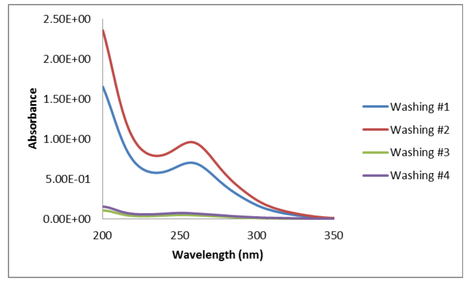

Fig 5. UV-Vis Absorbance of the supernatant after each washing of TiO_2- PTA. The characteristic peaks of PTA in water at 260 nm decreased.

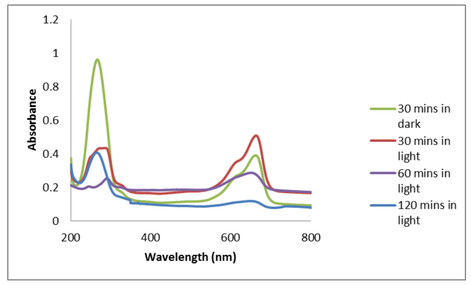

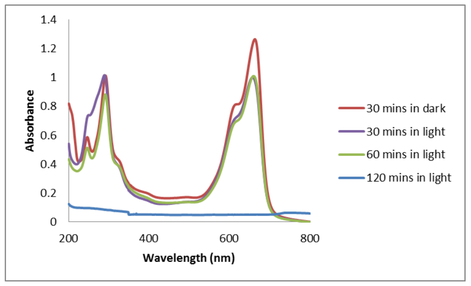

Fig 6. Photodegradation of high concentration of Methylene Blue.
The degradation of methylene blue dye using TiO_2-PTA (left) and TiO_2 only (right). TiO_2 was able to degrade the high concentration MB dye much better than PTA.

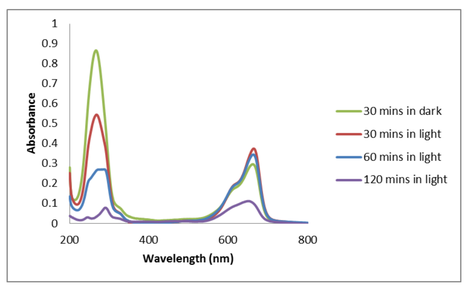

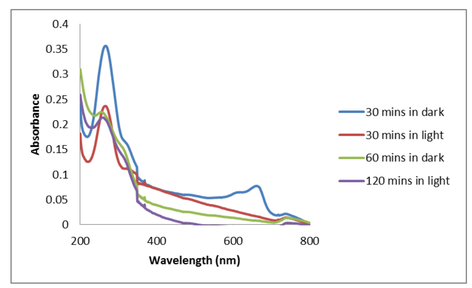

Fig 7. Photodegradation of low concentration Methylene Blue.
The degradation of methylene blue dye using TiO_2-PTA (left) and TiO_2 only (right). Both compounds were able to degrade a low concentration of MB dye.

CONCLUSION

TiO_2-PTA was observed to be a viable photocatalyst for the degradation of methylene blue and works well as a reducing agent for metal cations. This technique will allow researchers in determining how advanced photocatalytic materials can provide a significant solution for environmental cleanup. As they allow for the complete oxidation of the pollutants and reduction of metals. It would be interesting to further conduct more research on the different types of dyes and metals that act as pollutants to help to properly destroy them.

ACKNOWLEGEMENTS

I would like to thank Dr. Ivana Radivojevic Jovanovic for allowing me to do research with her and for being a great mentor.

REFERENCES

[1] Pearson, A., Bhargava, S. K., & Bansal, V. (2011).. Langmuir, 27(15), 9245–9252.
[2] Pelaez, M., Nolan, N. T., Pillai, S. C., Seery, M. K., Falaras, P., Kontos, A. G., Dionysiou, D. D. (2012). *Applied Catalysis B: Environmental*, *125*, 331–349.

Implication of local weather on heat transfer rates by infiltration

Anthony Rivera and Kyungmin Park

Department of Environmental Control Technology and Facilities Management, New York City College of Technology

Mentor: Prof. Daeho Kang

ABSTRACT

The first law of thermodynamics, also known as "Law of Conservation of Energy", states that energy can neither be created nor destroyed; energy can only be transferred or changed from one form to another. The natural transfer of heat flows from a warmer environment to a colder environment. Infiltration through a building entrance door has major impacts on the indoor thermal environment, indoor air quality and energy performance. In our research, we measured differential pressure and air velocity across entrance doors. We also monitored the indoor and outdoor environments in the Environmental Building by collecting data using specialized instruments and sensors. After analyzing the measured data, we were able to calculate the heat transfer of the infiltration through the entrance doors. Finally, we were able to compare the heat transfer rates calculated from local weather and standard weather.

INTRODUCTION

The Architectural Design for a building has an effect on the day to day operations and functionality. This is especially true when it comes down to deciding what materials to choose for the building envelope, determining where to place the entrance doors & what types of entrance doors to use. These factors have a direct impact to the indoor thermal environment, indoor air quality & the building energy performance. For this project we conducted research on infiltration through the entrance doors in the Environmental Building. On a cold winter day, we measured local weather conditions, along with other environmental parameters in the Environmental building. With the measured data we were able to accurately calculate the airflow rates & quantify energy losses through the entrance doors. This poster presents the methods we developed & the significance of the weather sources in the calculation of heat transfer rates by natural air flow through building entrance.

RESULTS

Table 2 Heat loss calculated by two weather data sources in Environmental Building

Variable	Measured Weather		Standard Weather	
	Door 1	Door 2	Door 1	Door 2
Velocity (fpm)	109	139	350	351
Flow Rate (CFM)	2179	2756	6999	7017
Temp Difference (F)	9.8	9.6	11.3	11.6
Heat Loss (MBTU)	24	29	86	86

DISCUSSION

This is part of a long-term project to investigate the impact of infiltration through building entrance doors. This poster focuses on the influence of weather resources on the prediction of the infiltration through entrance doors. We have developed a method to accurately quantify infiltration rates and successfully estimate the heat losses due to the infiltration as shown in Table 2.

Table 2 shows that using the local measured weather is critical in the accurate prediction of heat losses through building entrance door. Standard weather data is widely used to predict physical phenomena taking place in buildings and their surroundings. The heat transfer rates of infiltration are solely dependent on the weather data since the energy equation is the function of an air flow rate and a temperature difference. The results indicate that if the standard weather data is continuously used to quantify heat loss through buildings entrance door will lead to the system being oversizing and the heat loss being overestimated. As infiltration may improve indoor air quality, this aspect should also be studied.

METHODS

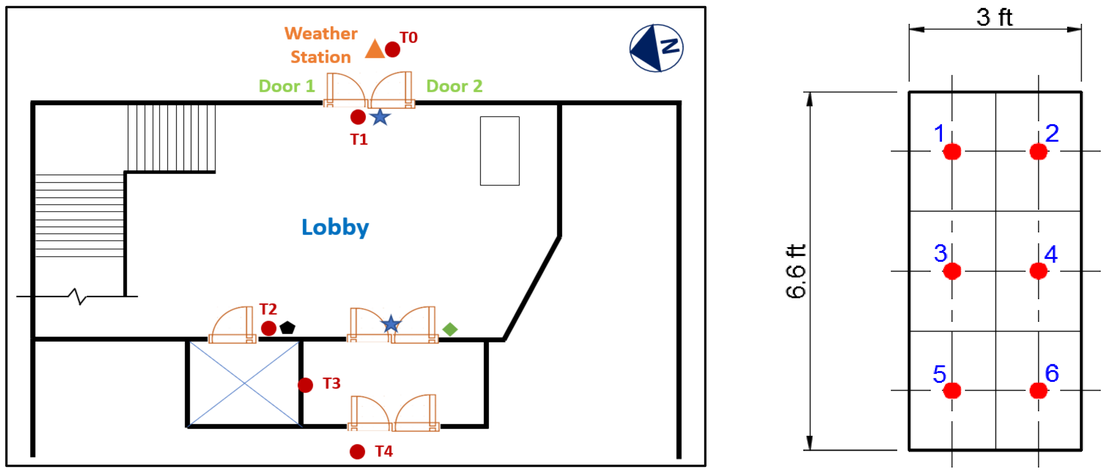

Figure 1 The measuring points on a building plan and the section of entrance doors

This differential pressure across the entrance doors in *in. wg.* can be expressed as

$$P_{diff} = P_h - P_l$$

where P_h is high-pressure side in *in. wg.* and P_l is low-pressure side in *in. wg.* The air flow rate in *CFM* across the entrance doors is expressed as

$$Q = AV$$

where *A* is the area of doors and *V* is the velocity of incoming air in *fps*. The energy equation is used to calculate the heat transfer rate of the natural airflow as

$$\dot{q} = 1.1Q\Delta t$$

where Δt is temperature difference in *°F* between outdoor air and indoor air.

Table 1 Measuring parameters and specification of the measuring instruments

Parameters	Instrument	Measuring Interval	Range	Accuracy	Resolution
OA Temp/RH	HOBO MX2301	1 min	-40-70°C	±0.2°C	0.04°C
Indoor Temp	HOBO U10	1 min	-20-70°C	±0.53°C	0.14°C
Door Opening	HOBO UX90-6M	1 sec	12m / 102°	-	-
Velocity	TSI Velometer	-	0-20 m/s	±5%	0.01 m/s
Wind Speed	HOBO U30	1 min	0-76m/s	±4%	0.5m/s
Wind Direction	HOBO U30	1 min	0-355°	±5°	1.4°

REFERENCES

H Cho, K Gowri, and B Liu. "Energy saving impact of ASHRAE 90.1 vestibule requirements: modeling of air infiltration through door openings." Technical Report PNNL-20026, 2010.

B.A. Cullum, O Lee, S Sukkasi, and D Wesolowski. "Modifying habits towards sustainability: a study of revolving door usage on the MIT campus., 2006.

Lin Du. "Air Infiltration through Revolving Doors." Master's Thesis. 2009.

Yuill GK. 1996. Impact of high use of automatic door on infiltration. ASHARE Research Project 763-TRP. PA: University Park.

Low–cost Near Infrared Diffuse Optical Imaging System

Dr. Chen Xu[1], Mohammed Shakil[2]

[1,2]Depertment of Computer Engineering Technology, New York City College of Technology

Abstract

Diffuse Optical Tomography (DOT) and Optical Spectroscopy using near-infrared (NIR) diffused light has demonstrated great potential for the initial diagnosis of tumors and in the assessment of tumor vasculature response to neoadjuvant chemotherapy. The aims of this project are 1) to test the different types of LEDs in near-infrared range, and design the driving circuit, and test the modulation of LEDs at different frequencies; 2) to test the APDs as detector, and build the receiver system and compare efficiency with pre-built systems. In this project we are focusing on creating a low-cost infrared transmission system for tumor and cancer diagnosis.

Introduction

- The NIR technique utilizes intrinsic hemoglobin contrast, which is directly related to tumor angiogenesis development, a key process required for tumor growth and metastasis.
- The NIR diffuse tomography holds great promise in distinguishing early-stage invasive breast cancers from benign lesions.
- This technique also provides insight into tumor metabolism and tumor hypoxia, important indicators of tumor response to various forms of therapy.

Methods

- The high cost of the DOT system is mainly because of three components, the cost of laser diodes, the cost of optical switches, and the cost of detectors, Photon Multiplier Tubes (PMT).
- With recent advances in photonics, the performance of light-emitting diodes (LEDs) is becoming increasingly comparable in terms of output power and spectral width.
- One of the most appealing strengths of LEDs is the cost, which is several dollars at a similar output power level as that of laser diodes. Besides, LEDs have demonstrated to be safer and more reliable in medical use due to their high resistance to physical lacerations, heat, and electrical damage. Because of the low cost of LEDs, multiple sources can be installed simultaneously.
- The expensive and fragile optical switch can be eliminated. On the detector side, silicon-based avalanche photodiodes (APDs) have the advantage of low cost, similar or even better sensitivity and resolution in the red and near-infrared spectral regions.

System Requirements

- Biological tissue usually undergoes relatively low absorption at the near infrared (NIR) at optical window range from 700nm to 900nm. Hence NIR light can penetrate deep into biological samples and has been used widely to monitor important hemodynamic parameters in tissue non-invasively.
- A low budget NIR system is needed to perform phantom experiments.
- The system needs to have at least two wavelengths and expandable to more wavelengths.
- The system needs to have p-p 20mV sensitivity at 7cm source-detector distance.
- The noise level at 7cm source-detector distance is smaller than p-p 10mV.
- Use optical solution for concentrating LED beam and increase power output per square inch.

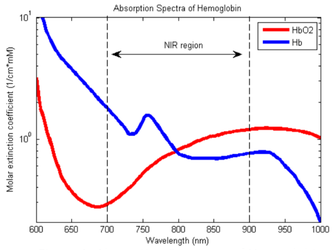

Figure 1: Absorption Spectrum of Hemoglobin

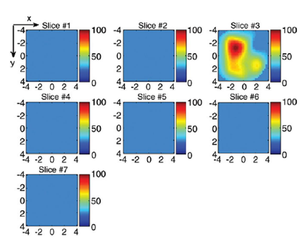

Figure 2: Total HB Map

Digital Control System

- We are using Arduino Nano as a microcontroller for our project.
- LED780E 780nm wavelength led is used for transmission. We are also testing with wavelengths of 670nm, 808nm and 830nm.
- The X9C104 digital potentiometer is used in this project for voltage division.
- The MCP4725 single channel DAC is used for generating AC signals and frequency modulation.
- The SSD1306 display is used for easy mode selection and displaying information to the user.

Data Acquisition

- The control systems includes a mini display as a user interface. User can choose DC only, AC only or DC coupling mode before every operation.
- A potentiometer is present to control the frequency of the signal generator.
- Arduino serial monitor or any serial data monitor system can acquire data from the Arduino.
- For the detector side, we can use official detecting software made by Thorlabs.
- Once the data is collected, we can plot the data and use software like MATLAB, MS excel for further analysis.
- Due to noise in the system, some data may come inaccurate. Further software analysis can fix the problem.
- We can store data locally or send to other places for analysis.
- We can make an Arduino based data acquisition system that runs offline with little to no maintenance.

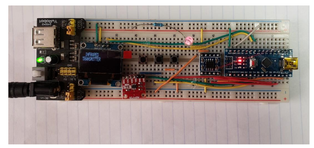

Figure 3: Test Circuit

Results

- We can observe the output of our system via using detector. The LED transmits light at and angle of 30°. Most of the light energy don't reach the detector. The light can transmit maximum 180mW but out highest measurement was 25mW.
- We have only tested the system with DC voltage, once the AC circuit is build, we will try different frequencies.
- Power consumption is very low compared to existing solutions.
- Proper shielding is necessary for better output.
- Further testing is necessary before applying this device to humans.
- Overall, a cheaper and low maintenance alternative that needs further development before applying to humans.

Future Goals

- Use electronic components to reduce noise in the circuit which will give us more accurate data to work with.
- An optical system is necessary for this project. Once the light beam is concentrated via optics the system becomes more efficient with little to none system loss.
- Use fiber optical cable to travel light beam to human skin or affected area for diagnosis.
- Test LEDs with different wavelengths and compare their results.
- Build case that can protect all the components.
- Continue research and increase efficiency of the device.

Reference

1. C. Xu, H. Vavadi, A. Merkulov, H. Li, M. Erfanzadeh, A. Mostafa, Y. Gong, H. Salehi, S. Tannenbaum, and Q. Zhu, "Ultrasound-Guided Diffuse Optical Tomography for Predicting and Monitoring Neoadjuvant Chemotherapy of Breast Cancers: Recent Progress", *Ultrasonic Imaging*, 1-13(2015)
2. Q. Zhu, E. Cronin, A. Currier, M. Huang, NG. Chen, C. Xu, "Benign versus Malignant Breast Masses: Optical Differentiation using US to Guide Optical Imaging Reconstruction," *Radiology*, 237(1), 57-66 (2005).

A Data Visualization System for Wireless Sensor Network Using Thingsboard

Student: Julia Shin

Mentor: Professor Xinzhou Wei

Abstract

The Internet of Things (IoT) conceptualizes the idea of a multitude of devices being able to collect and share data by being interconnected through the Internet. Data visualization presents an organized way to display all this data in a manner that can be easily understood. This can ultimately assist us in making fast, informed decisions with more certainty and accuracy than ever before.

Introduction

Thingsboard, an open source platform for IoT, will generate a real time graphical representation of the data on its dashboard. This application allows people to analyze the condition of a smart home or smart building to ensure that the environment is providing optimal comfort while still be energy efficient.

With ThingsBoard, users are able to:

- Collect and visualize data from devices and assets on IoT based applications.
- Analyze incoming telemetry and trigger alarms with complex event processing.
- Control your devices using remote procedure calls (RPC) on IoT.
- Build work-flows based on device life-cycle event.
- Design dynamic and responsive dashboards to users.
- Push device data to other systems on IoT.

Our system combines sensing network with cloud based visualization tools. Using Arduino Uno as the main controller, the DHT22 sensor collects temperature and humidity data which is connected to the WiFi network by means of the ESP8226 module. The data gathered from the sensor are stored onto Thingsboard through the MQTT protocol (See Figure 1 below) and visualized on the dashboard.

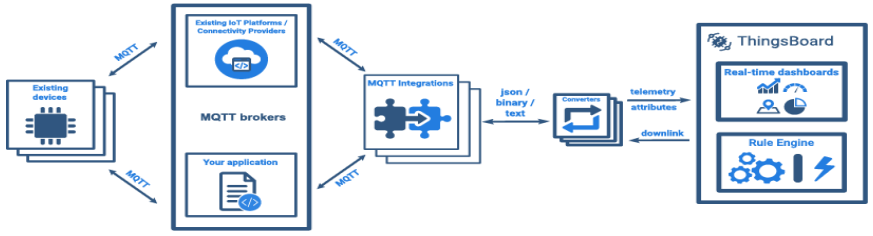

Fig. 1 MQTT Protocol in ThingsBoard

```
  if ( !client.connected() ) {
    reconnect();
  }

  if ( millis() - lastSend > 1000 ) { // Update and send only after 1 seconds
    getAndSendTemperatureAndHumidityData();
    lastSend = millis();
  }

  client.loop();
}

void getAndSendTemperatureAndHumidityData()
{
  Serial.println("Collecting temperature data.");

  // Reading temperature or humidity takes about 250 milliseconds!
  float h = dht.readHumidity();
  // Read temperature as Celsius (the default)
  float t = dht.readTemperature();

  // Check if any reads failed and exit early (to try again).
  if (isnan(h) || isnan(t)) {
    Serial.println("Failed to read from DHT sensor!");
    return;
  }

  Serial.print("Humidity: ");
  Serial.print(h);
  Serial.print(" %\t");
  Serial.print("Temperature: ");
  Serial.print(t);
  Serial.print(" *C ");

  String temperature = String(t);
  String humidity = String(h);


  // Just debug messages
  Serial.print( "Sending temperature and humidity : [" );
  Serial.print( temperature ); Serial.print( "," );
  Serial.print( humidity );
  Serial.print( "]   -> " );

  // Prepare a JSON payload string
  String payload = "{";
  payload += "\"temperature\":"; payload += temperature; payload += ",";
  payload += "\"humidity\":"; payload += humidity;
  payload += "}";

  // Send payload
  char attributes[100];
```

Fig. 3 Part of Arduino code of system

System Methodology

The wiring schematic (Figure 2) for this system consists of the Arduino Uno, the DHT22 sensor, the ESP8266, and a single resistor of value between (4.7k and 10kΩ). The heart of the system definitely lies within the code (Figure 3). The combination of the different For and While functions within the code govern the way the data collected from the sensor is analyzed and presented. Not only that, but the code also dictates the way it is connected to the Wifi which would be specified by the user

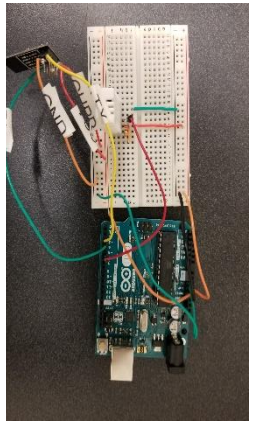

Fig. 2 System Schematic

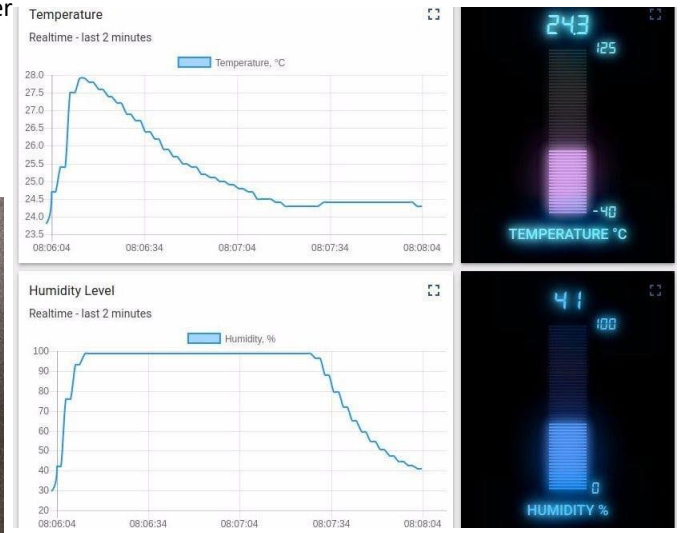

Fig. 4 Dashbaord in ThingsBoard

Conclusion

Thingsboard is a powerful IoT platform with many different applications. It is able to visualize a variety of data and update it in real time on its dashboard (See Figure 4). With a simple wiring schematic and an open source Arduino code, user can easily develop an IoT system for collecting temperature and humidity data in a smart building or smart city.

Implementing READ (Reading Effectively across Disciplines) in the classroom

Anisa Shkembi B.S; Michael Gotesman, Ph.D

Department Of Biological Sciences, New York City College of Technology, CUNY

ABSTRACT

Biology 1101 is the first introductory biological course offered at NYC College of Technology. It is a reading intensive science course, which prepares students for careers in the field of medicine and science.

The purpose of this study is to investigate the effects of using "Annotation," a READ strategy to enhance academic performance and achievement for Bio 1101 students. The experimental design of the study involved the use of a pre-assignment and post assignment challenge to evaluate students progress as well as implementing the READ strategy of annotations to enhance student learning. For sample size, twenty students in a particular section of Bio 1101 administered at New York City College of Technology participated in the study. The first trial was a demonstration of how to read effectively using annotations. All students were advised to read a text on the process of mitosis (the particular subject for that lesson) A similar assignment was used in class where students learned about bacteria and antibiotic resistance. The results of the study indicate that annotation is a successful and effective tool that enhances students' performance and therefore, implementation of READ strategies should be encouraged to improve student learning.

INTRODUCTION

BIO 1101 is the first course of freshman introductory biology. Students learn about the chemistry of life. Bio 1101 deals with various topics such as taxonomy, cell structure, nutrition and important macromolecules, reproduction, hereditary, development and evolution. Concepts of molecular biology and the method of DNA fingerprinting are also introduced in the course. Furthermore, students learn how to use and care of the microscope during laboratory hours. (Clark, 2018)

In " Annotation Tool for Enhancing E-Learning Courses" the author refers to annotations as the highlighting tool which supports the so-called active-reading, an efficient way of learning. Annotations help students to engage with the text and emphasize different parts of it. The highlighting tool proposes to turn reading from an individual activity to a shared one, since reading remains as the fundamental method of learning. (Pereira, 2012)

In " A Teaching Tool for Parasitology: Enhancing Learning with Annotation and Image Retrieval" The author shows the effectiveness of using annotation tool, as an alternative learning approach, to compare morphological characteristics among different species. Based on the results of the study, the author states that students found this approach very helpful. (Kozievitch, 2010)

To improve student's understanding of BIO 1101 reading skills, we wanted to test whether incorporation of READ strategy would enhance reading skills and comprehension. The study was designed to evaluate annotation as a learning tool for the entire class of BIO 1101.

METHODS

Section E016 of the Biology students participated in the study. Annotation was used as a learning tool for the entire class.

Students were asked to read a short text regarding bacteria and to answer questions based on the text.

The first trial was a demonstration of how to read effectively using annotation.

Students were asked to read the process of mitosis and to annotate, which means to take notes while reading, underlining, writing key words and definitions, questions and short summaries of the paragraph.

Figure 1. shows annotation during class activity

A. Shows Bio1101 students during class activity .

B . Shows a tutorial video, as an annotation guide for students.

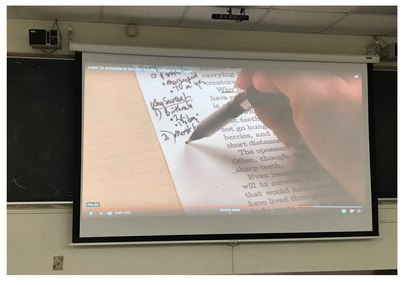

Figure **C-D** shows students learning how to use annotations while reading

PRELIMINARY RESULTS

Participation of the students was 100%. Based on the student's average before practicing annotation and after, there is an increasing score. After practicing annotation as an effective learning tool , students built their knowledge on the process of mitosis and were able to distinguish the differences between the phases of mitosis.

Each Exam is worth 22.5% of the grades

Average of the score is 15.99/22.5 which is 71% for Exam1.

Average of the score is 17.05/22.5 which is 75% for Exam2

PRELIMINARY RESULTS

Fall 2019 Pre-Assessment Bio1101 Section E016

	Q 1C	Q 2C	Q 3C	Q 4A	Q 5A
Avg = 2.6		2.5	2.7	1.9	1.7
Avg		C =	2.6	A =	1.8

Q1C-3C: were questions that tested students Text Comprehension.
Q4A-5A: were questions that tested students ability to analyze the given text

DISCUSSIONS

Overall students did better in the second exam, after practicing the highlighting tool referred to as annotation, a READ method which improved significantly their reading skills and academic performance. Annotation is a tool that helps students to engage in the active-reading, understand, and simplify difficult concepts by underlying key words or symbols, definitions, and writing short summaries. The preliminary results of the study indicate that annotation is a successful and effective teaching tool that enhances students' performance. It is a better way of learning and understanding conceptual knowledge than other conventional teaching methods and therefore, implementation of READ strategies should be encouraged to improve student learning.

REFERENCES

1 . Clark, Mary Ann, et al. *OpenStax Biology*, 28 Mar. 2018, https://openlab.citytech.cuny.edu/openstax-bio/course-outline/.

2. Pereira Nunes B., Kawase R., Dietze S., Bernardino de Campos G.H., Nejdl W. (2012) Annotation Tool for Enhancing E-Learning Courses. In: Popescu E., Li Q., Klamma R., Leung H., Specht M. (eds) Advances in Web-Based Learning - ICWL 2012. ICWL 2012. Lecture Notes in Computer Science, vol 7558. Springer, Berlin, Heidelberg https://doi.org/10.1007/978-3-642-33642-3_6

3. Kozievitch N.P., da Silva Torres R., Andrade F., Murthy U., Fox E., Hallerman E. (2010) A Teaching Tool for Parasitology: Enhancing Learning with Annotation and Image Retrieval. In: Lalmas M., Jose J., Rauber A., Sebastiani F., Frommholz I. (eds) Research and Advanced Technology for Digital Libraries. ECDL 2010. Lecture Notes in Computer Science, vol 6273. Springer, Berlin, Heidelberg https://doi.org/10.1007/978-3-642-15464-5_58

ACKNOWLEDGEMENT

I am thankful to the Emerging Scholars Program and to my mentor, Professor Michael Gotesman for guiding me throughout the study.

The privacy preserving framework with virtual ring and identity-based cryptography for Smart Grid

Leonard Sutanto, Professor Yu-Wen Chen

New York City College of Technology

Abstract

One of the main challenges in the smart grid is how to efficiently manage the high-volume data from smart meters and sensors and preserve the privacy from the consumption data to avoid potential attacks (e.g., identity theft) for the involved prosumers, retail electricity providers and other clusters of distributed energy resources. This poster proposes a two-layer framework with the cloud computing infrastructure. The virtual ring and identity-based cryptography are utilized in each layer to preserve privacy efficiently. The methods of the virtual ring and identity-based cryptography are introduced. The purposes and needs are discussed at the end of this poster.

Introduction

In the age of IoT, Internet of Things, where the idea of billions of smart objects, from devices to sensors that have self-awareness and interaction capabilities with the environment and network of IT systems connecting on a scale never seen before. The legacy electrical grid system is becoming absolute. There is an urgent need to move towards smart grid (SG) system as a solution. SG is electrical power transmission and distribution networks embedded with an information layer and enhanced by automation, interconnectivity, and centralized IT systems to allow two-way communication and power flow.

Weaknesses and Threats

Unfortunately, SG is subject to multiple threats and attacks such as identity theft, denial of service (DoS), false data injection, traffic manipulation attack and replay attacks among others. In addition to that, the consumption data collected by SM may also be used to invade prosumers' privacy. An unauthorized user may use the data to have access to prosumers' information such as household habits behaviors and activities. Such information is subject to serious privacy and security concerns.

To overcome these challenges, we proposes a two-layer framework that utilized the cloud computing infrastructure. The framework combines the virtual ring and the identity-based cryptography. To perform efficiency and provide robust privacy protections, the virtual ring is adopted in the first layer . To process a huge amount of data and handle a high volume of connection, identity-based cryptography is proposed in the second layer.

Proposed Framework

The first layer provision the platform for virtual communities and retail electric providers (REPs). The virtual community is formed by the groups of prosumers who agree on the provided plans by the REP. Prosumers are able to virtually trade the produced renewable energy production within the community with other prosumers or the REP. With the layer-1 cloud infrastructure, the REP manages the owned virtual community and maintain the platform for realizing the trading and billing for the involved prosumers. It is the REP's responsibility to guard the data privacy and security for prosumers in the virtual community and be achievable by utilizing the virtual ring for communication between the virtual community and REP, which is also operated in the second layer.

The second layer is a platform for Distributed System Operator (DSO) to have multi-directional communication between clusters of Distributed Energy Resources (DERs) and multiple REPs. The clusters of DERs are the small-scale electricity-producing resources or controllable loads that are connected to local distribution systems such as solar panels, smart-charging electric vehicles, and demand response applications. DSO coordinates data from various REPs and clusters of DERs and provides the management for the operation and scheduling.

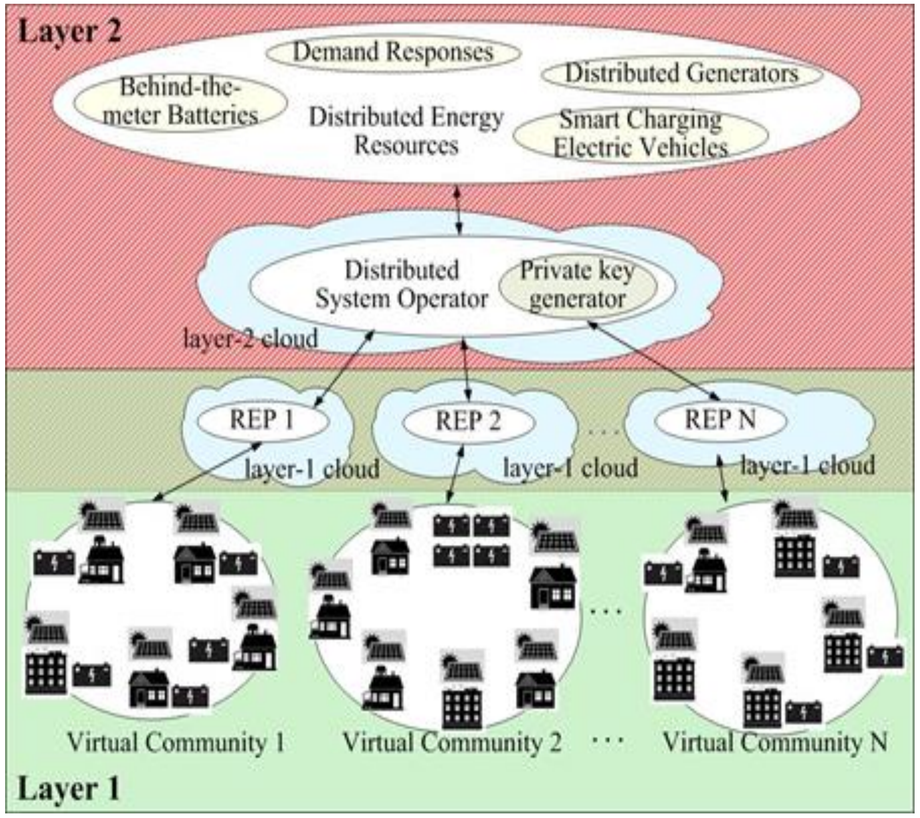

Virtual Ring

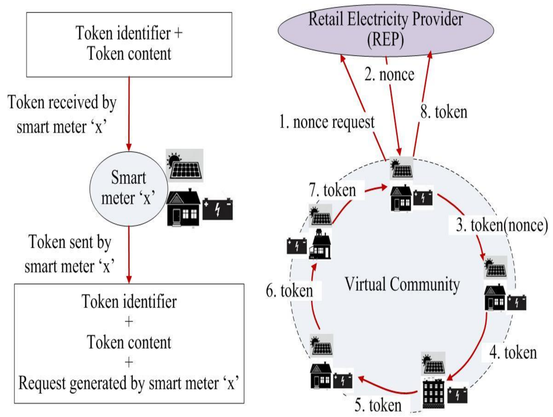

The virtual ring produces a minimum computational cost while providing robust data and privacy protection equivalent to homomorphic encryption. This is possible because of the uniqueness of the ring architecture. The advantage originates from connecting one node to two other nodes, forming a ring with a single continues pathway through each node.

Identity-Based Cryptography

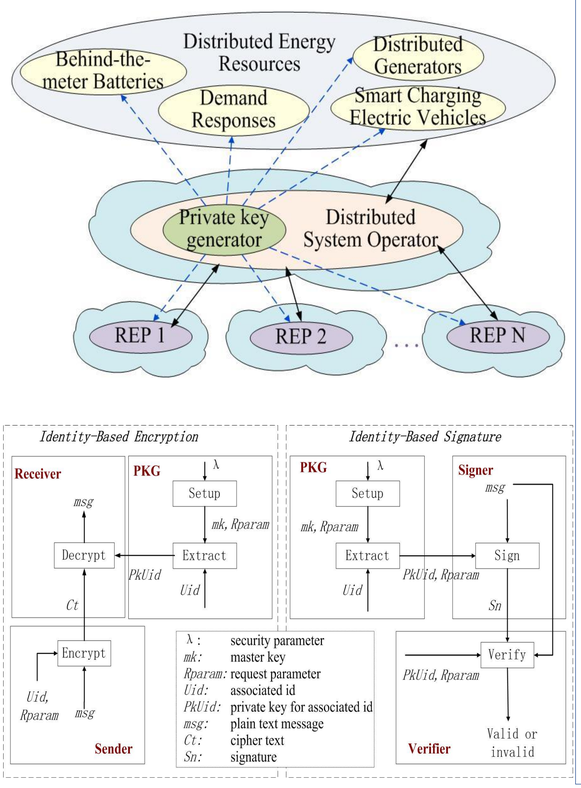

The identity-based cryptography is composed of identity-based encryption (IBE) schemes and identity-based signature (IBS). The private key generator (PKG) is operated and managed by DSO in the second layer. PKG produces the private keys to all involved entities, i.e., clusters of DERs, and REPs. The identity-based cryptography is proposed to handle a heavy load produced by a high volume of connection within the same timeframe. However, The cryptography is subject to processing capabilities because while it can process a heavy load of information, it does so with a high computational cost.

Conclusions

The two-layer framework is proposed with the cloud computing infrastructure and adopt virtual ring and identity-based cryptography for the smart grid. Operating the virtual ring in the first layer provides the efficiency, robust data security and privacy protection between the prosumers and the REP. The identity-based cryptography is utilized in the second layer to process a huge amount of data and handle a high volume of connection. The proposed framework can efficiently provide the privacy preservation solution and achieve the elasticity, scalability, and availability.

Modular Design of an Elevator Control System

Author: Orouba Tagout - Mentor: Professor Farrukh Zia

Computer Engineering Technology Department

ABSTRACT

Modular Design of Elevator Control System is a project that is meant to present a real-life application which is an elevator or lifts. Elevators are used on a daily basis to lift people or merchandise or anything from one floor to another, which inspired me to work in this project. The elevator will be controlled using software and embedded systems with the integration of sensors and logic circuits, stepper motor. The mean controller used in this project is the Arduino Uno ATmega328P that comes with its IDE sketch. For the logic circuit, a multiplexer will be used as the component to control which floor number will be displayed using a seven-segment display.

INTRODUCTION

As we know elevators became essential in our life when navigating buildings with multiple stories. The design built will present an elevator control system for four floors. The microcontroller Arduino uno will control the subsystem, using the code on IDE sketch . Based on the switch pressed and sensor, the elevator cabin can move either in upward or downward direction. H-bridge driver is used to control direction and speed of stepper motor. Inputs of H-bridge are connected to Arduino Uno which controls direction and PWM duty-cycle. Output of an H-bridge is a voltage between 0 V and 12 V, and which depends on input's duty-cycle.

HARDWARE

Arduino Uno is a microcontroller board based on the ATmega328P. It has 14 digital input/output pins, 6 analog inputs.

Multiplexer is a device that selects between several analog or digital input signals and forwards it to a single output line

Stepper Motor is operates with one winding with a center tap per phase. Each section of the winding is switched on for each direction of the magnetic field.

Photointerrupter is a transmission-type photosensor, which hasa light emitting elements and light receiving elements aligned facing each other in a single package, that works by detecting light blockage.

7-segment Display is a form of electronic display device for displaying decimal numerals that is an alternative to the more complex dot matrix displays.

PARTS LIST

Arduino Uno
Multiplexer
7_Segment Display
Stepper motor
Photointerrupter
H Bridge(Motor Driver)
9V battery
Wires and resistors

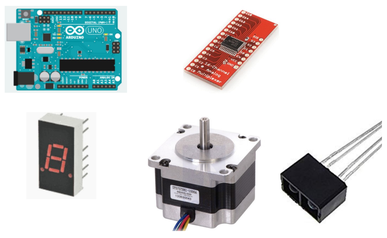

BLOCK DIAGRAM

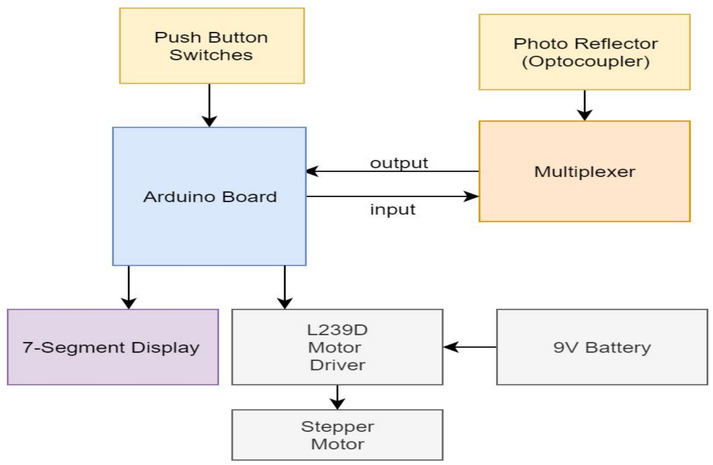

ELECTRICAL CIRCUIT

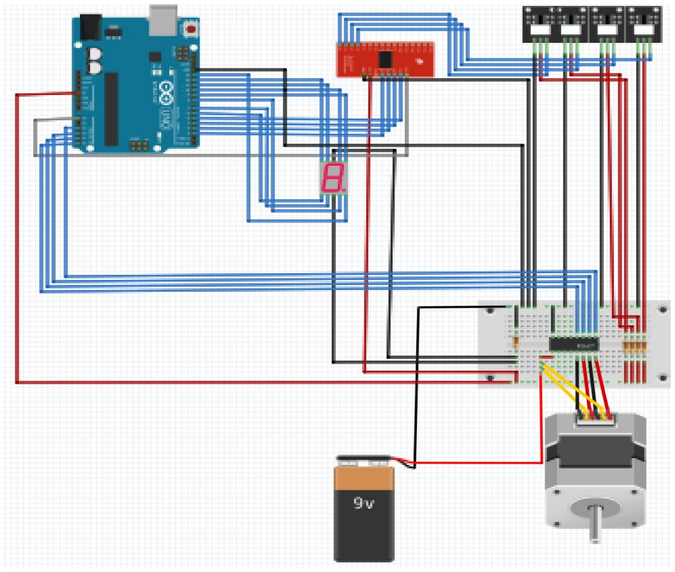

ACKNOWLEDGEMENTS

A special thanks to professor Zia for his help and support.
Emerging Scholars Program 2019
Honors Scholars Program 2019

PROGRAM CODE

CONCLUSION

Elevator control systems were widely used in most buildings. This thesis was based on design and implementation of arduino microcontroller based elevator control system. The main components were used in this thesis are Arduino microcontroller, push button, multiplexer, photointerrupter, 7-segment Display, H-Bridge driver circuit, stepper motor, 12V power supply board, personal computer and USB interfacing device. The Arduino Uno ATmega328P microcontroller was used as the main controller unit to display and control section. This project has been constructed with low cost, very compact, very low power requirement and high efficiency components.

FUTURE WORK

This module can be developed and more features can be added to make it more interactive, for example we can add voice interaction.

REFERENCES

https://www.rohm.com/electronics-basics/photointerrupters/what-is-a-photointerrupter
https://www.electronics-tutorials.ws/combination/comb_2.html
https://www.researchgate.net/publication/318653972_Laboratory_model_of_the_elevator_controlled_by_ARDUINO_platform

Video OER for Physics Education

Author: Parikshit Thapa, Mentor: Darya Krym, Lufeng Leng
New York City College of Technology, Physics Department

Abstract

This is a multi-faceted project in physics education, with several complimentary goals. Firstly, students will produce one or more video demonstrations of laboratory experiment(s). These demonstrations will be shared on Open Lab. The intention is to eventually create an expanding OER for students from City Tech and beyond. The demonstrations will include explanations of equipment and procedure which are already available in written form. Additionally, the demonstrations may include personal observations and hints from the students, which can make the videos more fun and useful for future students. Moreover, students will investigate the mechanism of the experiment in greater depth, including identifying sources of systematic error and producing theoretical estimates of some of these. Students will record an explanation and discussion of the results of these advanced activities, and this will also be a resource for future students.

Introduction

Ballistic pendulum can be defined as a pendulum with a bifilarly suspended bob that retains objects striking it and registers the amplitude of the swing caused by the impact, the velocity of the object (such as a rifle bullet) penetrating the bob being computed by application of the principles of conservation of momentum and energy.
Ballistic pendulum is used to measure the velocity of projectiles through the conservation of linear momentum and mechanical energy. The spring loaded gun shoots a metal ball , the hollow pendulum bob is suspended at its heights which as a result the pendulum and the projectile swing upward and a catch mechanisms stops the pendulum at its height of the position of swing.

Method

The experiment has two parts, the initial velocity of the ball is to be determined from the measurements of the masses of Pendulum M and the ball m and the measurement of the distances between y1 and y2, when the pendulum is in the lowest and the highest position. In the second part, the ball's initial velocity is determined by calculating the horizontal distance between the projectile direction and the time taken by the ball to travel between the photogates which are measured from the middle of the photogates. Measure the mass of the ball, m and the mass of the Pendulum, M. When the pendulum is hanging at its lowest position, we measure the vertical distance, y1 between the position of the center mass and the base of apparatus. We then position the ball at the end of the firing rod and by compressing the spring together we make the gun ready to fire. Fire the ball into the free-hanging stationary pendulum. The pendulum will catch the ball, swing up, and use the catch mechanism to stop the pendulum. Place the catch mechanism in the average position in the knot and measure the vertical distance y2. Place the photogates so that the firing ball intersects the beam of photogate. Place the photogates to intersect the photogate beam with the firing ball and adjust the height and measure the horizontal distance d between the photogates from middle to middle. Measure the flight time that the ball takes, the distance between the photogates taken from middle as photogates are thicker.

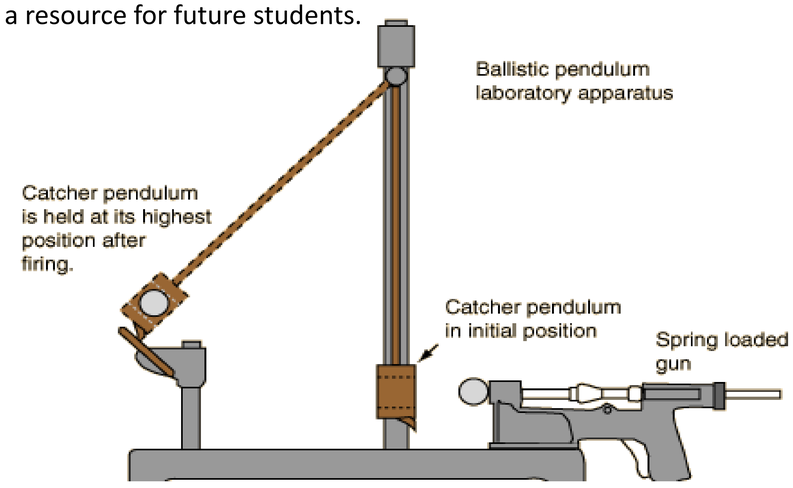

Results

Determination of the initial velocity of a ball with Ballistic pendulum.

Mass of the ball(m) Kg	Mass of the pendulum(M) kg	Distance Y_1 m	Distance Y_2 m	Height $H=Y_2-Y_1$ m	Velocity Of ball Pendulum $V=\sqrt{2gh}$ m/s	Initial Velocity Of ball $V=\{(m+M)/m\} * \sqrt{2gh}$ m/s
0.0651kg	.2078kg	.065m	.148m	.083m	1.27 m/s	6.55 m/s
0.0698kg	.2078kg	.065m	.157m	.092m	1.34 m/s	6.34 m/s

Determination of the initial velocity of a ball with Time-distance method

Mass of the Ball m Kg	Distance between photogates d M	Time of flight t S	Initial velocity of ball from eq V=d/t m/s	Average velocity of the ball V, m/s
0.0651kg	0.1 m	.0153 s	6.536 m/s	6.351 m/s
	0.1 m	.0166 s	6.024 m/s	6.351 m/s
	0.1 m	.0154 s	6.493 m/s	6.351 m/s
0.0698kg	0.1 m	.0164 s	6.098 m/s	6.190m/s
	0.1 m	.0165 s	6.061 m/s	6.190m/s
	0.1 m	.0156 s	6.410 m/s	6.190m/s

% difference for velocity of the ball 1= 3.1%
% difference for velocity of the ball 2= 5.5%

There may have been several reasons for error in this experiment due to the difficulty of accurate measurement of distances as the photogates are thicker the approximation can be wrong. When measuring the distance between the photogate, I measured the distance from middle of the photogate. Friction plays a huge role in this experiment as it might slow down the catch mechanism and we might have a lower value for it. Catch mechanism is basically a way to stop the pendulum at it's highest position when the pendulum along with the ball is fired from the spring loaded gun. There might have been energy loss in the swing. The position of the center of mass of the pendulum might be different before and after the collision.

Conclusion

Ballistic pendulum is used to measure the velocity of projectiles through the conservation of linear momentum and mechanical energy. The spring loaded gun shoots a metal ball , the hollow pendulum bob is suspended at its heights which as a result the pendulum and the projectile swing upward and a catch mechanisms stops the pendulum at its height of the position of swing.

References

Computer-Based College Physics Laboratory Experiments, Roman Kezerashvili, Gurami Publishing.

Operating Instructions: 75425 CENCO Ballistic Pendulum

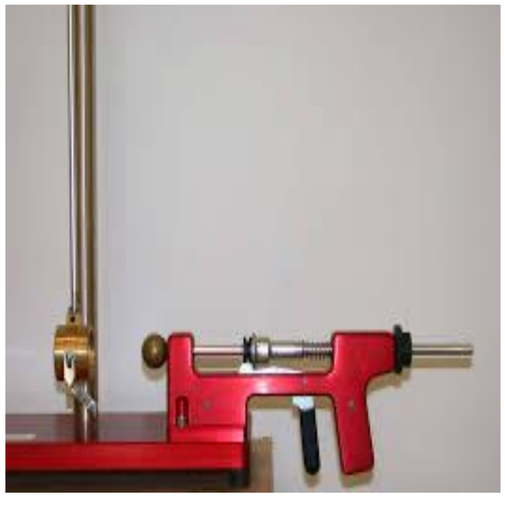

Design and Manufacturing of a Walking Machine

Author: Aneita Lucille Torres, **Mentor:** Prof. Angran Xiao
Department of Mechanical Engineering Technology

Abstract

Technology is influenced by many different sources. One of said sources is nature. In this project, regular vehicles with wheels can not travel through specific terrain or obstacles, a solution could be to design a robot that can walk like an animal such as a dog. This is useful for tasks like carrying supplies through areas too dangerous for people to go through. Our group's objective is to design, construct, and program a quadruped robot that can walk.

Introduction

Our goal is to build a small version of the 4-legged robot that can support the weight of items it would carry. This required creating a design that does not put strain on the robot's limbs and motor due to its own weight. In addition, the robot will also need custom-made parts such as segments of the leg as well as coding to tell the motors how to move each part of the leg. The robot will be controlled via remote to tell it where to go.

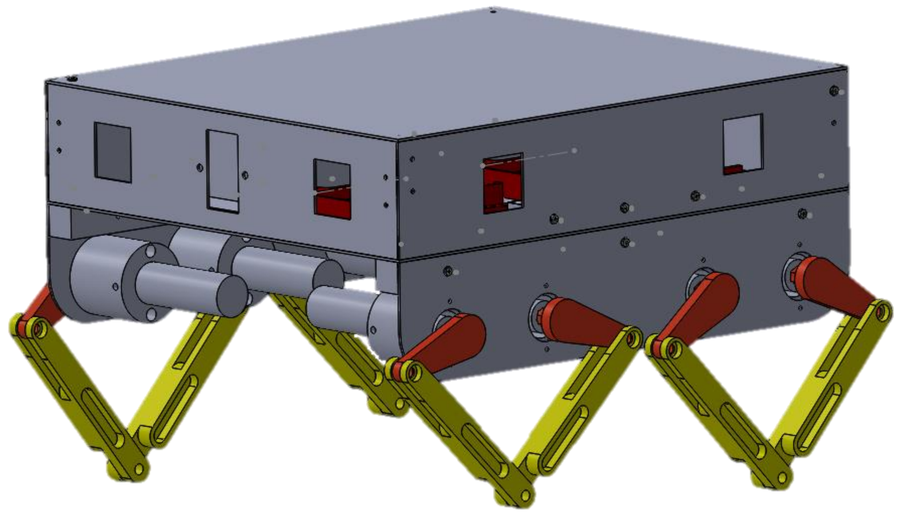

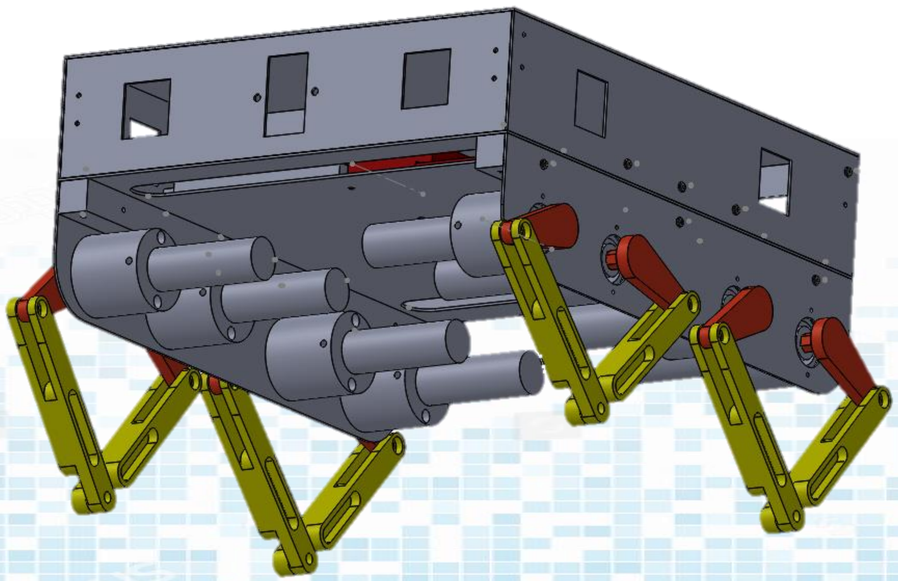

Tools

Solidworks- A program used to make 3D models. It is a Computer-Aided Design(CAD) and Computer-Aided Engineering(CAE) Software.
3D Printer- A machine that takes 3D virtual models saved as .STL files, and constructs the physical 3D form.
Arduino- An open source electronics platform that anyone can modify and share. It includes its own microcontrollers and programming software which uses C++.

Methods

During the brainstorming phase, we looked up examples of quadruped robots through google images to see how they were designed. From there, we design the robot based on the designs observed. Using the 3D modeling program, Solidworks, we created a 3D virtual model of our robot. Next, we used the 3D printer to create custom parts of our robot such as the legs and torso. Any other needed parts, such as the motors, are bought. Then, we create the code that will make the motors move the legs in a specific way that will make it walk. Putting the robot together, we test the robot to see if our robot functions as we intended. The coding process also extends to the remote controlling the robot tell it where to walk to. Finally, during the development of our robot, we reiterate previous steps taken to build our robot to refine on it. This includes redesigning the robot, reprograming it, creating new custom parts, and more testing.

Conclusion

Through examining quadruped animals and other quadruped robots, designing our robot, programing, testing, and refining, we were able to create and build our robot. Though different from other designs of 4-legged robots, it achieves our needs for our robot to do. Using a remote control, we can make our robot carry items and walk from one location to another.

Green Roof System Integrated Soil Methods

Jude Rene Vallon, Faculty Mentor: Ivan L. Guzman, PhD

Department of Construction Management & Civil Engineering Technology
New York City College of Technology, The City University of New York (CUNY)

Abstract

If existing buildings are to be considered for the addition of a green roof on their building, owners must factor in the cost of engineering the roof to support increased dead and live loads due green roof infrastructure, growing media, vegetation and foot traffic. By engineering green roof installations to be lighter, it can become more inclusive of existing buildings. The project consists of assessing the impact of an array of re-purposed textiles (cotton, polyester and linen) integrated into lightweight engineered soil from the Brooklyn Navy Yard - Brooklyn Grange (BG) soil in order to observe its effects on the reduction in load, hydraulic conductivity and water retention capacity. In integrating textile fabrics into the soil material at different percentages, it would result in textile replacing soil grains by volume and thus reducing the weight of the soil; and moreover, potentially modifying the hydrogeological properties of the soil. The engineering students of Fall 2019 (CMCE 2456 sect. D050) conducted the testing.

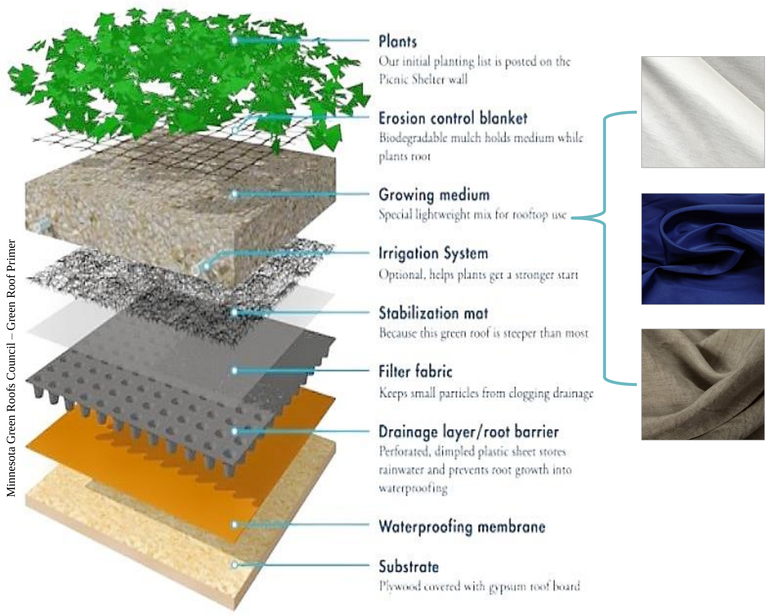

Green Roof System Layers

Alterations from 1st Round of Experiment

In keeping with ASTM E2399 standard and building on previous work presented during GeoCongress 2019, sieve bases were modified to reduce systematic errors.


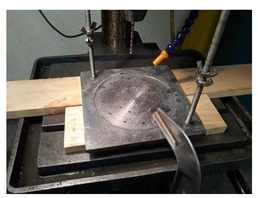
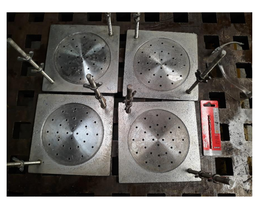

Materials and Methods


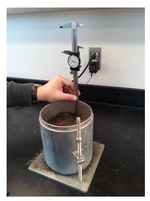
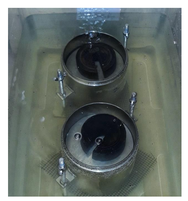

Day 1

- Soil was conditioned by adding percent textile by weight (0%, 0.5%, 1.0%, 2.0%, and 3.0%)
- Soil was compacted by using a Modified proctor hammer.
- Soil specimens were submerged in a bath for 24-hours with weighted steel plates to prevent soil from swelling.



Day 2

- After 24-hours soil specimens were placed on wood stands to drain for 120mins. At which time, the Maximum Media Density (MMD) can be recorded. MMD is the weight of the soil used to account for dead loads in a structural analysis.
- A falling head hydraulic conductivity test (permeability test) was then conducted in the specimens.


Day 3

- Soil was then transferred into aluminum pans to dry at 220-250° F for 24-hours (or until completely dry) and obtain dry weight of soil sample.
- In accordance with ASTM E2399, the entire process is repeated a 2nd time for each soil specimen.

References

- ASTM International. (2015). *Standard test method for maximum media density for dead load analysis of vegetative (green) roof systems*. West Conshohocken, PA. Retrieved from www.astm.org
- Guzman, I. L., & Torres, S. (2018) Repurposed Fibers to Decrease Hydraulic Conductivity without Compromising Load Restrictions in Urban Roof Farms Geo Congress 2019
- UofTDaniels (2014) Green Roof Gurus Panel https://youtu.be/4Hz85VR6rPE Published on Oct 31, 2014.

Acknowledgments

First acknowledge ESP sponsors providing this research opportunity. Thanks to the Brooklyn Grange Farm for supplying their soil. Thank you to Benny Santiago and Chris Guzman with technical modifications. And special appreciation to the student leaders Frandy Rubio, Ilana Berger and Kendall McLaughlin (and their teams) of the Fall 2019 CMCE 2456 (sect. C050) class for conducting tests and supplying the raw data.

Results

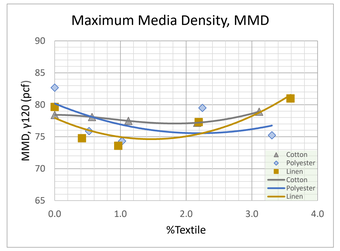

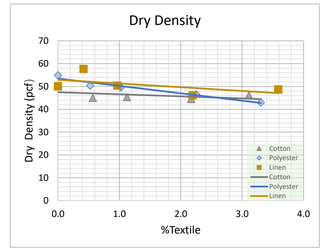

- The maximum media density (MMD) and the dry density of the soil decreases with additional textiles.

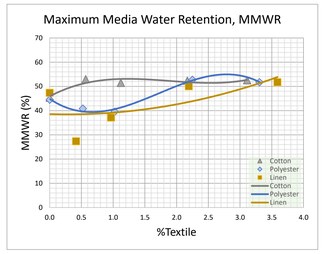

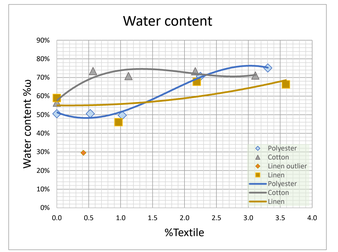

- Adding textile increases water retention in the cotton and polyester specimens, increasing the availability of water for plant growth.

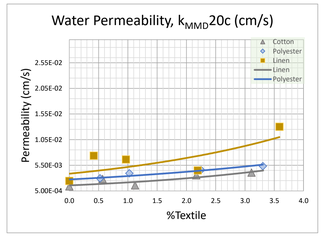

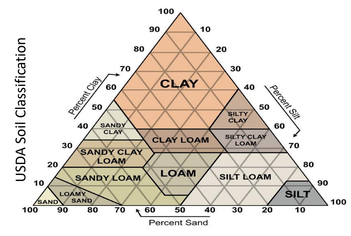

- The water permeability increases with the addition of percent textile, slightly shifting specimens towards another classification.

*All graphs depict data from the repeat-2nd trials only of each specimen for more accuracy.

Discussion and Implications

- The textile effectively reduces the dead load of the soil specimens.
- The water retention (MMWR) thresholds will help in calculating the capacities in stormwater mitigation of a green roof design.
- Water (moisture) content of the different integrated soil specimens can assist gardeners in matching suitable vegetation for successful growth.
- Rescue worn textile from landfills and repurposes as a structural medium.

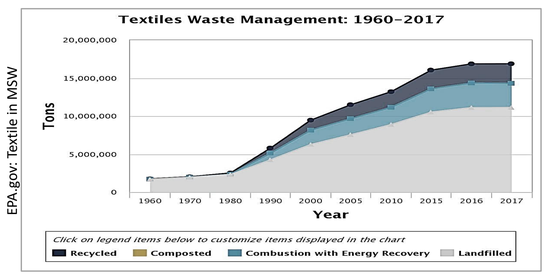

Peer-Assisted Learning in Calculus II: Examining Gender Differences

Xiaoqing Wu, Dr. Janet Liou-Mark

Department of Mathematics, New York City College of Technology

Abstract

Mathematics is a topic in which undergraduate students find challenging, particularly for females. By providing a peer-assisted workshop during the semester, undergraduates are offered academic support throughout the course. New York City College of Technology, though a Department of Education Minority Science and Engineering Improvement Program (DOE MSEIP) grant, has adopted the Peer-Led Team Learning (PLTL) instructional model in a few Calculus II sections. Peer Leaders engage the students one-hour a week in working on selected problems sets in a collaborative setting. This project examines if there are gender differences in Calculus II class in 1) PLTL workshop attendance, 2) departmental final grade, and 3) Calculus II course grade. Results showed that there were no statistically significant gender differences in all three areas. Hence, the PLTL workshops may be an intervention that may help females succeed in higher-level mathematics courses if they persist in the course.

Peer-Led Team Learning (PLTL)

- Peer-Led Team Learning (PLTL) is an instructional model where students work collaboratively in groups.
- In the PLTL workshop eight to ten students are assigned to a group with a designated pear leader. The workshop is held one hour each week after the respective lecture class.
- In addition, faculty members are closely involved in the PLTL session, thus peer leaders can discuss what topics to cover during the PLTL workshop and ask the professor questions.
- The six critical components of the PLTL model are displayed on the right.

Literature Review

- According to the recent reports, while more women are getting STEM (Science, Technology, Engineering, and Mathematics) degrees, they still lag behind men. (Liou-Mark, Ghosh-Dastidar , Samaroo , and Villatoro 2018; Osikominu, Pfeifer 2018).
- Women are less likely to pursue math-intensive fields due to their relatively lower math and science expectancies and values in comparison with men. (Wang and Degol 2013).
- In Sweden, the Supplemental Instruction (SI) is a method of improving student performance by using collaborative activities under the guidance of a 'senior' student. (Malm, Bryngfors and Mörner 2014). All students who attended SI meetings performed better on average than those students who did not attend. More importantly, female SI students are more frequent visitors to SI meetings than male students. And, those female SI students earned higher average score in their math class in the first school year.
- The Peer-Assisted Learning program in the United States is a similar program to Supplemental Instruction (SI) in Sweden. In medical school, Peer-Assisted Learning (PAL) leaders can provide guidance to students to improve their academic performance and help struggling students improve their critical thinking and problem-solving skills. The Peer-Assisted learning program also encourages students form study groups, which help make the study experience more enjoyable with their peers (Usman and Jamil 2019).
- In addition, both female and male students were satisfied with the contents covered in PAL. They felt easy to communicate with a peer as compared to their teacher, and the peer tutors also performed well in their respective sessions (Usman and Jamil, 2019).

Acknowledgements

The authors would like to thank the DOE MSEIP grant (P120A150063) for proving funds to support the PLTL workshop model and City Tech's Emerging Scholars program, under the leadership of Prof. Hamidreza Norouzi, for supporting this research.

Methodology

- This research study used data collected from the Peer-Led Team Learning (PLTL) workshops sections of MAT 1575: Calculus II between Fall 2016 to Fall 2018 academic years (five semesters) at New York City College of Technology.
- Attendance was taken every workshop session by the peer leaders. There were a total of 13 workshop sessions every semester.
- At the end of the semester, the department final grade and the course grade were collected. Gender of the participants were also recorded.
- Independent z-tests at the $p<.05$ level were conducted to determine if there were statistically significant mean differences between mean and female in their workshop attendance, department final grade, and course grade.

Participants

- There were a total of 217 undergraduates who enrolled in the PLTL workshop section of Calculus II from Fall 2016 to Fall 2018 (five semesters)
- Seventy-seven students were excluded from the study because they either did not state their gender (27), received an absent grade (ABS) as their departmental final grade (6), a grade over 100 percent (14), W grade (19), WU grade (6). Thus, the total valid participants for the study was 140.
- There were 28 females and 112 males who qualified for this study.

Results

- Based on the z-test, there were no statistically significant mean difference in the departmental final grade between males and female undergraduates taking Calculus II. Results showed males scored slightly higher than females on the departmental exam. A summary is shown in Table 1.
- Based on the analysis of the research on total workshop attendance and course grade, there were no statistically significant mean difference between female participants and male participants in the MAT 1575 Course. The result is shown in Tables 2 and 3.

Table 1. Summary Results of Departmental Final Grade

	Female(n=28)	Male(n=112)	Z-test
Mean	65.89	71.58	
Standard Deviation	17.63	16.88	Z= -1.5169 P=0.06463

Table 2. Summary Results of Total Workshop Attendance

	Female(n=28)	Male(n=112)	Z-test
Mean	11.18	11.02	
Standard Deviation	2.21	2.75	Z= 0.3264, P=0.3720

Table 3. Summary Results of Course Grade

	Female(n=28)	Male(n=112)	Z-test
Mean	2.04	2.20	
Standard Deviation	1.25	1.24	Z= -0.5779, P=0.2816

Limitation of the Study

- A small sample size of females. The gender imbalance can be seen in the participation of higher-level math courses.
- Students with W/WU grades were excluded from the study. It may be interesting to examine the reason for withdrawal from the course.

Conclusions

- The PLTL workshop in Calculus II may be beneficial if students attend it every week.
- If females were supported in a problem-solving session, they can perform just as well as males in higher level courses.

References

Liou-Mark, J., Ghosh-Dastidar, U., Samaroo, D., & Villatoro, M. (2018). The Peer-Led Team Learning Leadership Program for First Year Minority Science, Technology, Engineering, and Mathematics Students. Journal of Peer Learning, 11, 65-75.

Malm, J., Bryngfors, L., & Mörner, L.-L. (2014). The potential of Supplemental Instruction in engineering education – helping new students to adjust to and succeed in University studies. European Journal of Engineering Education, 40(4), 347–365. doi.org/10.1080/03043797.2014.967179

Osikominu, A., & Pfeifer, G. (2018). Perceived Wages and the Gender Gap in STEM Fields. IDEAS Working Paper Series from RePEc, IDEAS Working Paper Series from RePEc, 2018.

Usman, R., & Jamil, B. (2019). Perceptions of undergraduate medical students about peer assisted learning. The Professional Medical Journal, 26(08), 1283–1288. doi.org/10.29309/tpmj/2019.26.08.3870

Wang, M.-T., & Degol, J. (2013). Motivational pathways to STEM career choices: Using expectancy–value perspective to understand individual and gender differences in STEM fields. Developmental Review, 33(4), 304–340. doi: 10.1016/j.dr.2013.08.001

Sleep-Wake Disturbances in Mild Traumatic Brain Injury: Meta analysis of Literature and Modeling of Cerebral Tissue Vulnerability

XiangFu Zhang, Subhendra Sarkar, Mary Alice Browne

New York City College of Technology Department of Radiologic Technology & Medical Imaging

Introduction

Mild traumatic brain injury (mTBI) is defined by the Management of Concussion/mTBI Working Group as Normal imagining; a brief period of loss of consciousness (LOC) less than 30 minutes; post traumatic-amnesia (PTA) less than a day; and with Glasgow Coma Scale (GSC)of 13-15. The injury is usually as a result of the head being struck by an object or undergo a whiplash motion.

Despite the prevalence of Mild TBI, an estimation of 42 million people worldwide suffer from mTBI or concussion every year, the exact damage it has on the brain is largely a mystery due to its lack of reliable diagnosis tool. Especially, sleep disorder, it is one of the most complaints by patients with mTBI, the exact cause of this disorder is yet to be uncovered.

The objective of this work is to suggest possible etiologies of sleep disturbances as a result of mTBI. Based on the previous research works suggest, the pineal gland region and thalamic regions are vulnerable to mechanical damage and perfusion damage as a result of mTBI, tissue damage in the occipital lobe and alteration of cerebrospinal fluid might also plays a role in causing the sleep disturbances .

Fig 1. Anatomy and location of pineal gland making it vulnerable to CSF pressure spikes during mTBI

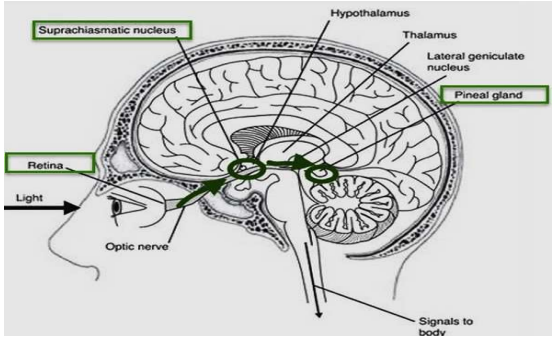

Acknowledgements

- Thanks to Emerging Scholar Program of New York City College of Technology for this opportunity.

Methods

We have evaluated multiples published works containing keywords such as mild traumatic brain injury, sleep disorders/issues, and cerebrospinal fluid and have identified a few articles that have conclusively observed or discussed at least one dominant damages due to mTBI. The endpoint is to summarize a few possible contributory factors of sleep disturbance as a result of mTBI.

Result and Discussion

Our model emphasizes the following four main effects due to tissue connectivity or functional dependence describe below:
Mild traumatic brain injury causes mechanical and perfusion damage in the brain which lead functional defects in different regions of the brain.

1) The direct impact between the tentorium and the pineal gland which causes pineal gland injury and disruption of melatonin production that regulates sleep-wake cycle. [1]

2) We hypothesize that during mild TBI, ventricles may undergo a dynamic pressure loading from the CSF, particularly the 4th ventricle, that could have a direct effect on the pineal gland. There seems to be no other significant mechanical injury in mild TBI (common to all kinds of mTBI) that affects acutely the sleep patterns of a large number of mTBI patients, starting as early as the day of trauma. This alteration might also have an impact on the flow of CSF and obstruct it's critical role in transporting sleep-wake regulating chemical compounds such as melatonin, oleamide, and orexin-A.

3) Perfusion deficit in the occipital region [2] contributes to visual problem that could potentially lead to visual impairments and potentially affect sleep. Another evidence was noted by using MR spectroscopy, it showed a reduction of NAA in the occipital lobe, which reflect diffuse axonal injury [3].

4) The thalamus is another site of injury for mTBI[4], which is an important region of the brain that helps promote sleep and maintain wakefulness.

Although, most researchers have not observed any MR spectroscopic abnormalities in mTBI, it contradict with our experience (Sarkar et al, unpublished results). The MR spectroscopic abnormalities do not appear acutely and are limited to frontal and temporal regions. Hence, one may propose neuro metabolite production to alter over time when mTBI progresses in certain patient groups without predictability and seems to get repaired with time. However, it is not clear why these abnormalities are affected only in frontal and temporal regions [2] in mTBI.

Results (Contd …)

Fig 2. lack of sensitivity in mTBI for MR spectroscopy [4]

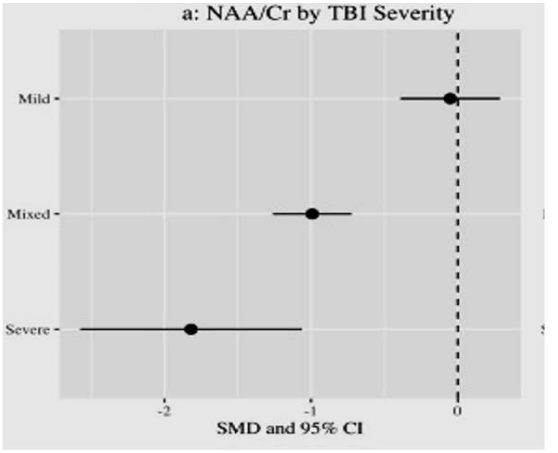

(SMD: Std Mean Dev) NAA, Cr metabolites, from M. Brown et al. Magnetic resonance spectroscopy abnormalities in traumatic brain injury: A meta-analysis. Journal of Neuroradiology. 45:2018, Pg. 123-29.

References

1. Yaeger, K., Alhilali, L., & Fakhran, S. (2014). Evaluation of Tentorial Length and Angle in Sleep-Wake Disturbances After Mild Traumatic Brain Injury. American Journal of Roentgenology, 202(3), 614-618.
2. Crider, T., Eng, D., Sarkar, P. R., Cordero, J., Krusz, J. C., & Sarkar, S. N. (2018). Microvascular and large vein abnormalities in young patients after mild head trauma and associated fatigue: A brain SPECT evaluation and posture dependence modeling. Clin Neurol Neurosurg, 170, 159-164.
3. Kubas, B., Lebkowski, W., Lebkowska, U., Kułak, W., Tarasow, E., & Walecki, J. (2010). Proton MR spectroscopy in mild traumatic brain injury. Polish journal of radiology, 75(4), 7–10.
4. P. Narayana. White matter changes in patients with mild traumatic brain injury: MRI perspective Concussion (2017)
5. Brown et al. Magnetic resonance spectroscopic abnormalities in traumatic brain injury: A meta-analysis. (2018) J Neuroradiology, 45, 123-29.

Kinetic Study of Amine Cured Epoxy Resins

Xiaona Zhou[1], Xiaolan Wu[2], Nadia Rodriguez[1], Santoshi Mohanta[3]
Swati Neogi[3], Diana Samaroo[2], Urmi Ghosh-Dastidar[1]
[1]Department of Mathematics, [2]Department of Chemistry, [3]Department of Chemical Engineering,
[1,2]New York City College of Technology, and [3]Indian Institute of Technology, Kharagpur

Abstract

The epoxy resin is a class of polymer containing more than one epoxy group (or cyclic ether) and featuring a broad range of applications in the field of paints and coatings, adhesives, electronics. With utilization of different curing agents including amines and anhydrides, epoxy resins can be hardened via curing reactions[1,2]. Owing to their excellent mechanical, electrical properties, chemical stability and extensively industrial applications, many chemists have been interested in studying the curing kinetics of epoxy resins. However, one of the major challenges towards the kinetic studies of epoxy resins curing is the high-cost of laboratory simulation of epoxy resins formations. The construction of computer-simulating kinetic models is not only significant to overcome this challenge but also to optimize a better chemical environment and experimental parameters, which ultimately contribute to the success in formation of desired epoxy resin products. Our research focuses on establishing a suitable kinetic model to better study the curing reaction of epoxy resins. Presently, we are working on investigating potential proposed kinetic models based on mathematical analysis on experimental data. Future work will focus on using the functionality and accuracy of our proposed kinetics model to predict and further to establish better reaction conditions for epoxy curing.

Introduction

Epoxy resin contains more than one epoxide group within its chemical structure[1]. During the general curing process (figure 1) with an amine, the epoxy group reacts with a primary amine via a S_N2-type of nucleophilic reaction and produce a secondary amine, which then facilitates the product formation of a tertiary amine. However, the curing products vary depending on the use of different curing agents. In our research project, anhydride-type curing agent is used.

The kinetic study of cured epoxy resins can be examined by various techniques, such as Differential Scanning Calorimetry (DSC), which was used to investigate the kinetics of the epoxy resin cured under isothermal conditions in our research. The DSC technique can measure the heat flow from the reacting system, and is a very convenient tool to study the overall epoxy-amine cure[1]. After mathematically analyzing the DCS data, unknown kinetic parameters of epoxy curing can be obtained based on the most fundamental cure kinetic rate equation (Equation1) and proposed kinetic models (Equation 2).

The goal of this research was to use experimental data to fit into a proposed kinetic model for curing of epoxy resin.

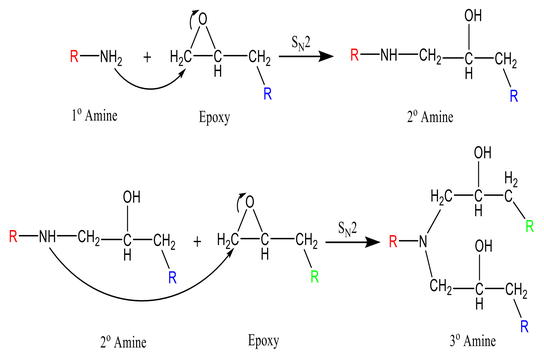

Figure 1: General Curing Mechanism for Epoxy-Amine Curing

$$\frac{d\alpha}{dt} = k\,(1-\alpha)^n$$

Equation 1: Most fundamental cure kinetic rate equation

$$\frac{d\alpha}{dt} = (k_1 + k_2\alpha)\, e^{-m\alpha^n}$$

Equation 2: Proposed kinetics model[2].

Experimental Methods

All experimental data was collected at the Indian Institute of Technology, Kharagpur, India (April 2018) by N. Rodriguez.

Sample was prepared by mixing commercially available medium reactive UP resin (containing maleic anhydride), cobalt nitrate, and methyl ethyl ketone peroxide (100:1:1).

- Styrene was added to adjust the final product viscosity to 250.25 cP.

To investigate the resin cure kinetics, experiments were carried out using Diamond Differential Scanning Calorimetry (DSC) (figure 2) under isothermal conditions at 105°C, 110°C, 115°C, 120°C, and 125°C.

- Heat flow was recorded to reaction completion (within 180 minutes).

Exotherm data was converted to degree of cure (α), and rate of cure ($d\alpha/dt$).

Figure 2: Differential Scanning Calorimeter

Experimental Data and Results

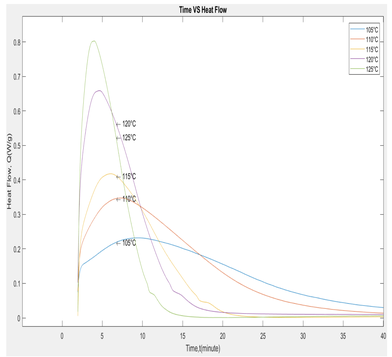

Figure 3: Normalized heat flow curves of epoxy resin at five different temperatures with respect to time in minutes. The total heat flow is computed by calculating the area under the curve of time verses heat flow function.

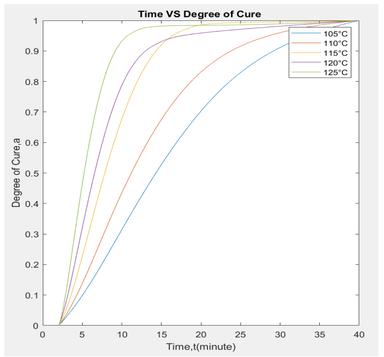

Figure 4: Degree of cure of epoxy resin at five different temperatures with respect to cure time in minutes. It is equal to the instantaneous heat flow divided by the total heat of reaction.

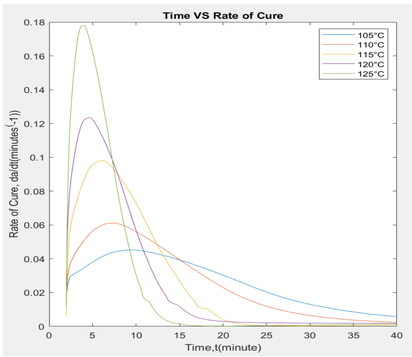

Figure 5: Rate of cure of epoxy resin at five different temperatures with respect to cure time in minutes. It is the derivative of the function of the instantaneous degree of cure.

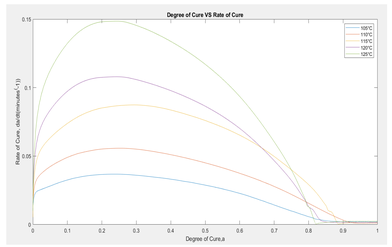

Figure 6: Degree of cure versus rate of cure

```
%Calculate the Total Heat Flow
Int_105 = trapz(data.Time(2:18806), data.Heatflow105(2:18806));
B=[];
%Calculate the instantaneous heat flow of reaction
for i=3:18806
    A=trapz(data.Time(2:i),data.Heatflow105(2:i));
    B(i-2)=A/Int_105;
end
subplot(1,2,1);
plot(data.Time(2:18805),B)
title('Time VS Degree of Cure at 105°C ');
xlabel('Time,t(minute)')
ylabel('Degree of Cure,a')
dy=gradient(B,data.Time(3:18806));%Calculate the rate of cure
subplot(1,2,2);
plot(data.Time(2:18805),dy)
title('Time VS Rate of Cure at 105°C');
xlabel('Time,t(minute)')
ylabel('Rate of Cure, da/dt(minutes^(-1))')
```

Figure 7: the MATLAB codes used to calculate the total heat flow and instantaneous heat flow of curing reaction.

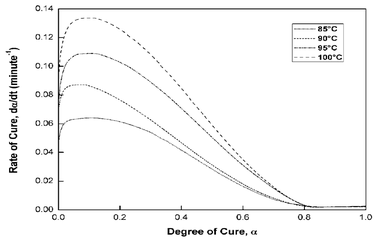

Figure 8: Graph of degree of cure versus rate of cure from previously published results[2] using similar material without UP resin.

Isothermal Temperature °C	Total heat of reaction ΔH_T, (W-min/g)	Empirical rate constant, k_1 (min^{-1})	Order of reaction, n	Coefficient of determination, R^2
105	6.899	0.0335	3.46	0.9481
110	6.677	0.0753	4.87	0.9857
115	5.321	0.1718	6.02	0.9868
120	6.685	0.3024	6.60	0.9883
125	6.200	0.5624	7.67	0.9174

Table 1. Summary of the values of total heat of reaction, kinetic rate for amine cured epoxy resin and the data fitted to the simplest resin cure kinetic model (equation 1)

Isothermal Temperature °C	Total heat of reaction ΔH_T, (W-min/g)	Empirical rate constant, k_1 (min^{-1})	Empirical rate constant, k_2 (min^{-1})	Order of reaction, m	Order of reaction, n	Coefficient of determination, R^2
105	6.899	0.02261	0.06438	5.749	2.725	0.9869
110	6.677	0.03833	0.04471	6.178	4.182	0.9844
115	5.321	0.05702	0.05111	15.6	6.692	0.965
120	6.685	0.07347	0.07245	13.08	5.315	0.9759
125	6.200	0.09412	0.08735	33.44	6.609	0.9569

Table 2. Summary of the values of total heat of reaction, kinetic rate for amine cured epoxy resin and the data fitted to resin cure kinetic model using equation 2.

Discussion and Conclusion

- Using the kinetic model in equation 1 and 2, kinetics parameters (e.g. the total heat flow, degree of cure, rate of cure etc.) were determined.
- Based on the data collected, using nonlinear regression analysis, we concluded that the data fit to kinetic model in equation 2 was acceptable, based on the coefficient of determination.
- We are currently working on publishing a paper based on this project.

References

1. Vyazovkin, S., & Sbirrazzuoli, N. (1996). Mechanism and Kinetics of Epoxy−Amine Cure Studied by Differential Scanning Calorimetry. Macromolecules, 29(6), 1867-1873. doi:10.1021/ma951162w.
2. Bhunia, S., Niyogi, D., Marru, P., & Neogi, S. (2013). Modelling of curing kinetics of amine cured epoxy resins for vacuum assisted resin infusion molding. The Canadian Journal of Chemical Engineering, 92(4), 703-711. doi:10.1002/cjce.21862.

Acknowledgements: We are grateful to Hafijul Sardar (Lab In-charge), Arnab Roy (Lab Assistant), Vijay Sharma (Lab Assistant) and students Sangeeta Sankhla (M. Tech Joint), Sai Sankar Chokkapu (M. Tech), Victor Avisek Chatterjee (Research Scholar) for their assistance in data collection. This work is partially supported by Emerging Scholar program, CUNY Research Scholar Program, and NSF Grant #1458714 .

An enticing study of prime numbers of the shape $p = x^2 + y^2$

Xiaona Zhou
Emerging Scholars Program
Mentor: Professor Satyanand Singh

Abstract

We will study and prove important results on primes of the shape $x^2 + y^2$ using number theoretic techniques. Our analysis involves maps, actions over sets, fixed points and involutions. This presentation is readily accessible to an advanced undergraduate student and lay the groundwork for future studies.

Background

Theorem:
Let $p > 2$ be a prime integer. Then p can be written as $p = a^2 + b^2 \Leftrightarrow p$ is of the form $p = 4k + 1$.

The theorem was posited by Albert Girard in 1625 and again by Fermat in 1640. Euler was the first one to proof this theorem. Many mathematicians have proved this theorem using different methods. This project is taken from a book called "An Open Door to Number Theory.". The whole project consists of 13 exercises, and when we proved all the exercises, we would have proved the theorem. This project is an extension of Zagier's one sentence proof.

A One-Sentence Proof That Every Prime $p \equiv 1 \pmod 4$ Is a Sum of Two Squares

D. Zagier
Department of Mathematics, University of Maryland, College Park, MD 20742

The involution on the finite set $S = \{(x,y,z) \in \mathbb{N}^3 : x^2 + 4yz = p\}$ defined by

$$(x,y,z) \mapsto \begin{cases} (x+2z,\ z,\ y-x-z) & \text{if } x < y-z \\ (2y-x,\ y,\ x-y+z) & \text{if } y-z < x < 2y \\ (x-2y,\ x-y+z,\ y) & \text{if } x > 2y \end{cases}$$

has exactly one fixed point, so $|S|$ is odd and the involution defined by $(x,y,z) \mapsto (x,z,y)$ also has a fixed point. □

Prove the Forward Implication

Theorem 0.1. *Let $p > 2$ be a prime integer. If p can be written as $p = a^2 + b^2$, then p is of form $p = 4k + 1$.*

1 Proof of the forward implication.

Proof. $p > 2$ is a prime integer, which means p is odd. $p = a^2 + b^2$; a^2 and b^2 must be one odd integer and one even integer. Let a^2 be an odd integer. Therefore, a is odd, and $a = 2x + 1$, where $x \in \mathbb{N}$. Let b^2 be an even integer. Therefore, b is even, and $b = 2m$, where $m \in \mathbb{N}$.
$p = a^2 + b^2 = (2x+1)^2 + (2m)^2 = 4x^2 + 4x + 1 + 4m^2 = 4(x^2 + x + m^2) + 1$
Since $x, m \in \mathbb{N}$, $(x^2 + x + m^2) \in \mathbb{N}$. Therefore, $p = a^2 + b^2 = 4k + 1$, where $k = (x^2 + x + m^2) \in \mathbb{N}$. □

More Proofs

2 Proof that if p is of the form $p = 1+4k$, then the point (1,1,k) is a fixed point for f. Conclude that $p = 4k + 1 \Leftrightarrow$ the function $f : S \to S$ has a fixed point.

define a map $f : \mathbb{N}^3 \to \mathbb{N}^3$ by

$$f(x,y,z) = \begin{cases} (x+2z, z, y-x-z) & \text{if } x < y-z \\ (2y-x, y, x-y+z) & \text{if } y-z < x < 2y \\ (x-2y, x-y+z, y) & \text{if } 2y < x \end{cases} \quad (1)$$

(1). Proof that $p = 4k + 1 \to$ the function $f : S \to S$ has a fixed point.
(2). Proof that $f : S \to S$ has a fixed point $\to p = 4k + 1$

Proof.

Case 1. When $x < y - z$, $f(x,y,z) = (x+2z, z, y-x-z) = (x,y,z)$. That is

$$\begin{cases} x + 2z = x \\ z = y \\ y - x - z = z \end{cases}$$

solve the system of equations:

$$\begin{cases} x = 0 \\ y = 0 \\ z = 0 \end{cases}$$

Since $x, y, z \in \mathbb{N}$, and $p = x^2 + 4yz$, this is not a solution. Therefore, f does not has a fixed point when $x < y - z$.

Case 2. When $y - z < x < 2y$, $f(x,y,z) = (2y-x, y, x-y+z) = (x,y,z)$. That is

$$\begin{cases} 2y - x = x \\ y = y \\ x - y + z = z \end{cases}$$

solve the system of equations:

$$\begin{cases} x = y \\ \text{z is free} \end{cases}$$

Since $x, y, z \in \mathbb{N}$, and $p = x^2 + 4yz$. $p = x^2 + 4xz = x(x + 4z)$. Therefore,

$$\begin{cases} x = p, x + 4z = 1 \\ x = 1, x + 4z = p, \end{cases}$$

Since $x \neq p$, we further define the solution as

$$\begin{cases} x = 1 \\ y = 1 \\ z = \frac{p-1}{4} \end{cases}$$

That is, $(1, 1, \frac{p-1}{4})$ is a fixed point for f. Therefore, $p = 4k + 1$, where $k \in \mathbb{N}$

Case 3. When $2y < x$, $f(x,y,z) = (x-2y, x-y+z, y) = (x,y,z)$. That is

$$\begin{cases} x - 2y = x \\ x - y + z = y \\ y = z \end{cases}$$

solve the system of equation:

$$\begin{cases} x = 0 \\ y = 0 \\ z = 0 \end{cases}$$

Since $x, y, z \in \mathbb{N}$, and $p = x^2 + 4yz$, this is not a solution. Therefore, f does not has a fixed point when $x < y - z$.

□

3 We now define $g : \mathbb{N}^3 \to \mathbb{N}^3$ by $g(x,y,z) = (x,z,y)$. Proof that g also maps S to itself, and that it is an involution on S. Conclude that S has a fixed point under g, which must be the form of (a,c,c). Show that this gives the desired solution: $p = a^2 + (2c)^2$. In fact you have shown the stronger statement that a prime p is of the form $p = 4k + 1 \implies p$ can be written uniquely as $p = a^2 + b^2$.

(1). Proof that g also maps S to S.

Proof. Since $g(x,y,z) = (x,z,y)$ and $S = \{(x,y,z) \in \mathbb{N}^3 : x^2 + 4yz = p\}$

$$\begin{aligned} g(x,y,z) &= (x,z,y) \\ g(S) &= g(x,y,z) \\ &= x^2 + 4zy \\ &= x^2 + 4yz = p \end{aligned}$$

That is $g(S) = S$. Therefore, g maps S to itself, and it is an involution on S. □

(2). Proof that if S has a fixed point under g, then it must be of the form (a,c,c).

Proof. S has a fixed point under g when $g(x,y,z) = (x,z,y) = (x,y,z)$. Solved the equation, we have

$$\begin{cases} x = x \\ y = z \\ z = y \end{cases}$$

Therefore, a fixed point must be of the form (a,c,c). That is $S_1 = \{(a,c,c) : a^2 + (2c)^2 = p\}$ where $S_1 \in S$.
From Exercise 8, we know that

$$p = 4k + 1 \Leftrightarrow the function f : S \to S has a fixed point.$$

From this exercise we know that when S has a fixed point, $p = a^2 + (2c)^2$. That is the same as $p = a^2 + b^2$, where $b = 2c$. Therefore, we have proved that $p = 4k + 1 \implies p$ can be written uniquely as $p = a^2 + b^2$ □

Selected preferences

- Campbell, Duff. An Open Door to Number Theory. MAA Press, an Imprint of the American Mathematical Society, 2018.
- "Leonhard Euler." *Wikipedia*, Wikimedia Foundation, 18 Oct. 2019, en.wikipedia.org/wiki/Leonhard_Euler.
- Zagier, Don. *A One-Sentence Proof That Every Prime $p\Equiv 1(\Mod 4)$ Is a Sum of Two Squares Author(s): D. Zagier*. 2011, A One-Sentence Proof That Every Prime $p\equiv 1(\mod 4)$ Is a Sum of Two Squares Author(s): D. Zagier.